EVALUATING THE JPCP CRACKING MODEL OF THE MECHANISTIC-EMPIRICAL PAVEMENT DESIGN GUIDE

by

Juan José Gutiérrez Puertas

Ingeniero Civil, Universidad de los Andes, Colombia, 2003

Submitted to the Graduate Faculty of

Swanson School of Engineering in partial fulfillment

of the requirements for the degree of

Master of Science

University of Pittsburgh

2008

UNIVERSITY OF PITTSBURGH

SWANSON SCHOOL OF ENGINEERING

This thesis was presented

by

Juan José Gutiérrez Puertas

It was defended on

March 28, 2008

and approved by

Luis Vallejo, Ph.D., Professor, Civil and Environmental Engineering Department

Jeen-Shang Lin, Sc.D., Associate Professor, Civil and Environmental Engineering Department

Thesis Advisor: Julie M. Vandenbossche, Ph.D., Assistant Professor, Civil and Environmental Engineering Department

EVALUATING THE JPCP CRACKING MODEL OF THE MECHANISTIC-EMPIRICAL PAVEMENT DESIGN GUIDE

Juan José Gutiérrez Puertas, M.S.

University of Pittsburgh, 2008

The Mechanistic-Empirical Pavement Design Guide (MEPDG) cracking model is a performance-based component of the new pavement design guide developed as a result of Project R1-37A of the National Cooperative Highway Research Program of the National Research Council, Transportation Research Board, which exists in the form of a software tool. The pavement academic community has been lately involved in analysis aimed at the evaluation of reasonableness and accuracy of the tool, given that it introduces several inputs that had been ignored in traditional design tools. Among these studies, the most notorious have implemented sensitivity analysis approaches. This research work introduces the potential uses of several sensitivity analysis approaches in the context of evaluation of the MEPDG cracking model. It also addresses important issues regarding failure mechanisms and newly introduced inputs that lack understanding, such as the permanent built-in temperature gradient in concrete slabs; the research concludes that anomalies are present in the prediction of fatigue damage that causes top-down cracking and demonstrates how the results contradict the current engineering understanding of this failure mechanism and the MEPDG literature. It also addresses, from a qualitative stand, the nature and treatment the permanent built-in temperature gradient has received in the design of the algorithm and suggests that the empirical model should be revised. In regard to sensitivity analysis of the MEPDG cracking model, this research recommends some

potential uses of 2^k screening methods and points in the direction of Response Surface Methodology (RSM) for further non-linear analysis in order to arrive at more exhaustive sensitivity analysis tools that cover wide input ranges. A case-study is also explored in order to show, qualitatively and quantitatively, what the discrepancies are in the predictions of the MEPDG cracking model.

TABLE OF CONTENTS

LIST OF TABLES

LIST OF FIGURES

ACKNOWLEDGEMENTS

The author would like to thank Dr. Julie M. Vandenbossche for her valuable comments, guidance and financial support; Mr. Jagannath Mallela, of Applied Research Associates, Inc., for his valuable clarifications in regard to the MEPDG 1.0 software; Mr. Thomas Burnham and Mr. Timothy Cline, of the Minnesota Department of Transportation, for sharing valuable survey data used in the last chapter of this work; Dr. Mainak Mazumdar, for his inspiring orientation in the topic of sensitivity analysis and model regression; Dr. Luis Vallejo and Dr. Jeen-Shang Lin for their support and for having accepted to join the examination committee.

This work is dedicated to my wife Jennifer, Mom, Dad and my sister Ana. You are my greatest source of energy and motivation.

1.0 INTRODUCTION

1.1 BACKGROUND

The Jointed Plain Concrete Pavement (JPCP) Cracking Model of the Mechanistic-Empirical Pavement Design Guide (MEPDG) is a complex modeling tool in the field of pavement engineering that incorporates many variables, the influence of which had been ignored in previous design and analysis approaches (10).

The inputs required in the new procedure can be classified under five main groups: geometrical/general, structural, traffic, environmental and material properties. Each input contributes as part of complex explicit and implicit (e.g. FEA) mathematical models that ultimately lead to the estimation of cracking, faulting, and roughness as standard performance parameters. The focus of this research will be on the cracking prediction.

As opposed to traditional approaches to pavement design and analysis (e.g. AASHTO Guide for Design of Pavement Structures, 1993), the MEPDG incorporates many additional inputs for characterizing material properties, structural properties, traffic loads and environmental loads.

Among current analysis and design tools the MEPDG is intended to replace, the AASHTO 1993 design procedure is a tool that relies on traffic (ESALs), foundation characteristics (modulus of subgrade reaction k), PCC mechanic properties (modulus of rupture

of PCC), load transfer coefficient, drainage coefficient and reliability to produce slab thickness as the output of the system; the thickness design is obtained through one single empirical implicit equation.

On the other hand, the MEPDG performance approach not only includes the inputs considered in the old AASHTO procedure but it also attempts to account, in a more comprehensive manner, for the phenomena that affect pavement performance. The output of the new procedure is the predicted quantity of distress (i.e. cracking) present at a given time.

Within the MEPDG models, of which the cracking model is part, raw inputs are processed and produce the so-called processed inputs. Figure 1.1 shows the methodology of the MEPDG, where the difference between raw inputs and processed inputs is illustrated.

One of the most important improvements of the new procedure is the inclusion of environmental loads, which are incorporated into the MEPDG through the EICM (Enhanced Integrated Climatic Model), a model capable of predicting temperature and moisture conditions across the depth (i.e. one-dimensional model) of the pavement structure on an hourly basis. Environmental loads affect constitutive material properties of the pavement layers and PCC slab. The complexity involved in the new procedure can be understood as the result of the search for more mechanistic and less empirical approaches.

The mechanistic response of the pavement structure to the interaction between traffic (actual axle loads as opposed to ESALs) and actual material and structural properties of the pavement materials is managed by a huge neural network (NN) incorporated into the MEPDG. This neural network is based on FEM analyses. As a result of the coupling of the NN and the EICM, the MEPDG is capable of analyzing the performance of pavements on an incremental basis, taking the date of construction, design life, and the time-based evolution of cracking into account.

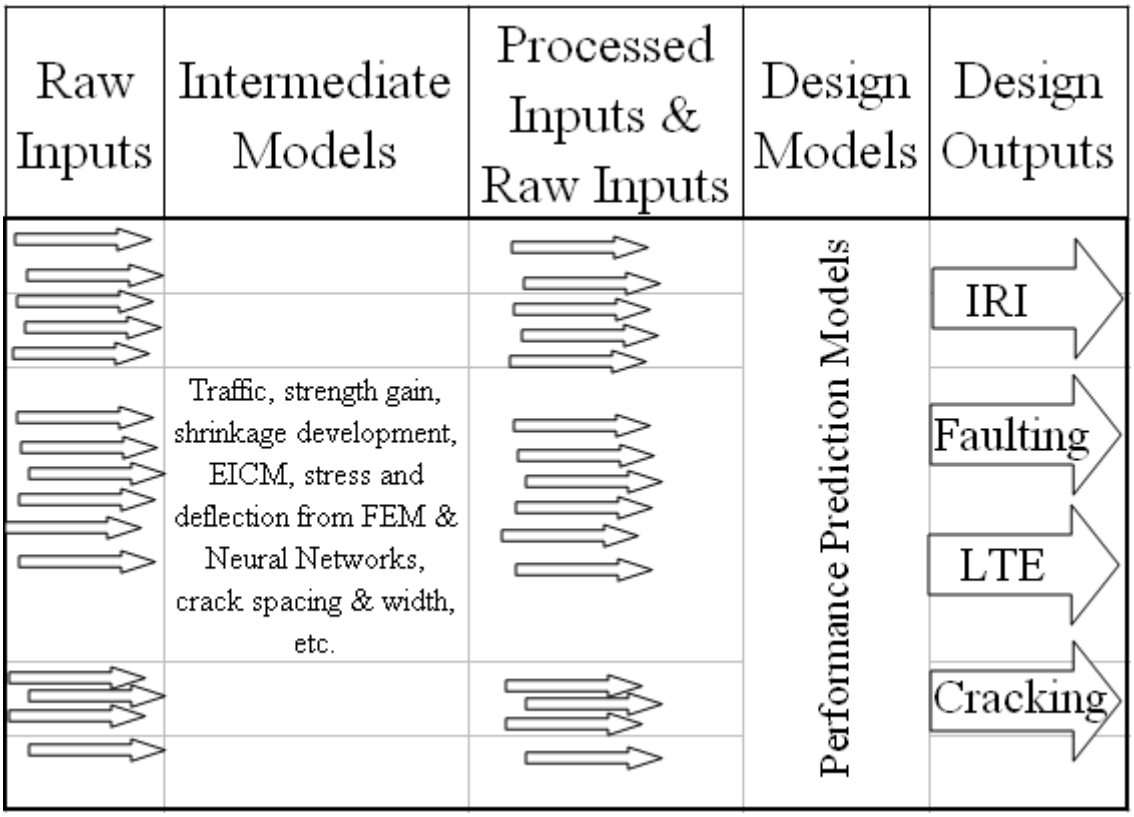

Figure 1.1 Methodology of the MEPDG software for rigid pavements (10)

An important feature contributed by the cracking model of the MEPDG is its robustness. Each input is capable of withstanding a relatively large range of values so that the process of design can be flexible and adaptable to, among other things, varying climatic conditions, available construction materials, and type of trucks that constitute the large portions of traffic load spectra at a certain site. Robustness of the cracking model is possible because it has been calibrated by using a large set of Long Term Pavement Performance (LTPP) data that include all representative regions across the United States.

Given the high complexity of the model, the pavement community is currently involved in analyzing the tool at a deep level of detail. Studies have been published that attempt to assess the degree of accuracy of the model, its reasonableness, and the sensitivity of its output to different inputs (sensitivity analysis). The present research intends to contribute to this search through qualitative and quantitative results.

1.2 RESEARCH OBJECTIVES

The present research has three main objectives. The first objective is to test the MEPDG cracking model at different input sets in order to determine if the model produces a reasonable output. The second objective is to determine if the current sensitivity analysis approaches are suitable for the MEPDG cracking model, specifically, whether linear regression methods are sufficient for sensitivity analysis. The third objective is to compare the results obtained through the MEPDG to a real case, the inputs and performance of which are very well known.

1.3 GENERAL RESEARCH APPROACH

The core of this research work will be performed through runs of the MEPDG Version 1.0 software. A critical step of this research is to decide which variables need to be investigated. A strategy that yields this information is thus needed. The experiments designed will be separated into two kinds. The first set of experiments will be dedicated to investigate the reasonableness of the model at various inputs of diverse nature. The second set of experiments will be dedicated to sensitivity analysis.

The first source of information for sensitivity analysis is a one-at-a-time (OAT) analysis performed at the University of Pittsburgh, which yielded valuable general information on a large set of inputs of the MEPDG. A total of twenty one inputs were examined. The findings of the California experiment (8), which will be briefly described in 2.3.4, are a further source of information although caution must be used when considering the results of that study since it was performed using an earlier version of the software.

Taking the available findings as a start basis, a set of inputs is proposed for screening methods of the 2^k type. The set should contain variables that are already known to be important in the sensitivity of the response, as well as variables whose role is suspected to be fundamental.

It is critical that the importance of correlations and interactions between variables in the context of a sensitivity analysis on the MEPDG are not neglected. In this research, these two concepts are carefully addressed.

In the case of correlated variables, which are common within the MEPDG, a search for all possible correlations will need to be performed. An example of typical correlations in the MEPDG are the various mechanical properties of Portland cement concrete, in which the change

in magnitude of one specific property is tied to change in magnitude of the other properties, due to their interdependency (e.g. modulus of elasticity and modulus of rupture of PCC).

Along with correlations between variables, there are also interactions. However, information about interactions is an output of the system rather than an input. Reference 15 presents an illustrative example of interactions in the joint effect of traffic, climate and foundation support. It seems that these three inputs are independent from each other. However, the action of two traffic loads of the same magnitude varies with varying climate and/or foundation support conditions.

1.4 SIGNIFICANCE OF THE RESEARCH

Comprehensive models in engineering resemble black box systems, the components and algorithms of which are intended to represent real processes of high complexity. The MEPDG cracking model is an example of such models. The MEPDG cracking model contains explicit and implicit models (e.g. FEA neural networks) that make it difficult to determine the relative importance of the various inputs and the reasonableness of the outputs. Though more mechanistic than previous approaches, some degree of empiricism has needed to remain in the system of the MEPDG because exhaustive mechanistic knowledge is far from being available. For this reason, the cracking model relies heavily on available data from LTPP, thus leading to the "mechanistic-empirical" terminology. It is imperative to find out whether the cracking model, in its high complexity, is capable of producing correct and accurate outputs that mark a step forward with respect to traditional approaches.

As one of the techniques included in the present work, a sensitivity analysis is useful in identifying the variables that are most influential on the final output. This is useful in optimizing the resources (both monetary and time) necessary in defining the inputs. From a research point of view, finding the most influential inputs is very important as it leads researchers to focus on the important factors that control the response of models. It can also serve as a very useful guidance in the process of analyzing and judging reasonableness of models. In the particular case of pavement performance models, a sensitivity analysis can allow focus to concentrate on factors that are influential to specific models and to eliminate factors, the contribution of which is negligible on the side of the response. From a practical point of view, project budgets often require that resources be optimized, which is the case in the field of pavement design and construction.

A sensitivity analysis can reveal the inputs on which further investigation should be made; more resources can be spent in the determination of the magnitudes of the most influential factors, contributing to the optimization of the design process.

2.0 LITERATURE REVIEW

2.1 RELEVANT ENVIRONMENTAL LOADS IN THE MEPDG

A major feature of the cracking model is the incorporation of environmental loads in the form of temperature and moisture gradients, which cause curling and warping respectively. The temperature related mechanism is treated in this work.

The bottom cells of Figure 2.1 and Figure 2.2 illustrate the convention to define positive and negative equivalent temperature differences. It is important at this point to differentiate between temperature gradients and equivalent temperature differences. Temperature gradients are actual temperature distributions across the slab depth that can be nonlinear. On the other hand, equivalent temperature differences are linear gradients. The stresses and deformations induced by nonlinear and linear gradients are assumed to be the same based on equivalent temperature moments. This method was proposed by Snyder and Janssen in 2000 and substantially simplifies calculations as any complex nonlinear temperature gradient can be transformed to an equivalent linear gradient. In this work the term equivalent temperature difference is used.

After concrete is cast in the construction of slabs, it takes several hours to set depending on the cement type, the mixture design, and the external temperature conditions present. At set time, complex non-linear temperature gradients are present across the depth of the slab, mainly

due to the combination of two factors. The first factor is the difference in temperature generated by the curing process; the second factor is the difference in temperature generated by the different rates at which temperature magnitude caused by sun radiation dissipates across the depth of the slab. If, for example, concrete is cast in the early morning of a sunny summer day and is exposed to high temperatures throughout the day, by the time it sets, a positive gradient is present at the slab (case 3 in Figure 2.1 and Figure 2.2). For a future flat condition (such as that of set time), the slab must experience the same magnitude and sign of gradient it experienced at set time. Therefore, the slab is said to have a negative built-in temperature difference present when the gradient is equal to zero. As a result, the slab will be deformed as if it were under the influence of a negative gradient when the gradient is equal to zero. In the future life of a pavement constructed under such conditions, which are frequent in the United States due to the fact that the summer is the construction season, daily or positive gradients acting on the slabs will be safe. However, during the night time, when negative gradients are present, the effect is that observed in the third case, right side of Figure 2.2. Under these conditions, a traffic loading configuration that exert loading at the two extremes of the slab is critical as it induces tensile stresses to develop on the top of the slab. The eventual failure after many applications of this configuration is said to be due to top-down cracking (10).

Opposite construction conditions to those described in the previous paragraph would lead to opposite critical conditions and failure mechanisms. In this case, bottom-up cracking would be the failure mechanism. Details of the wheelbase configurations that induce critical loading conditions are discussed in 4.1.1.

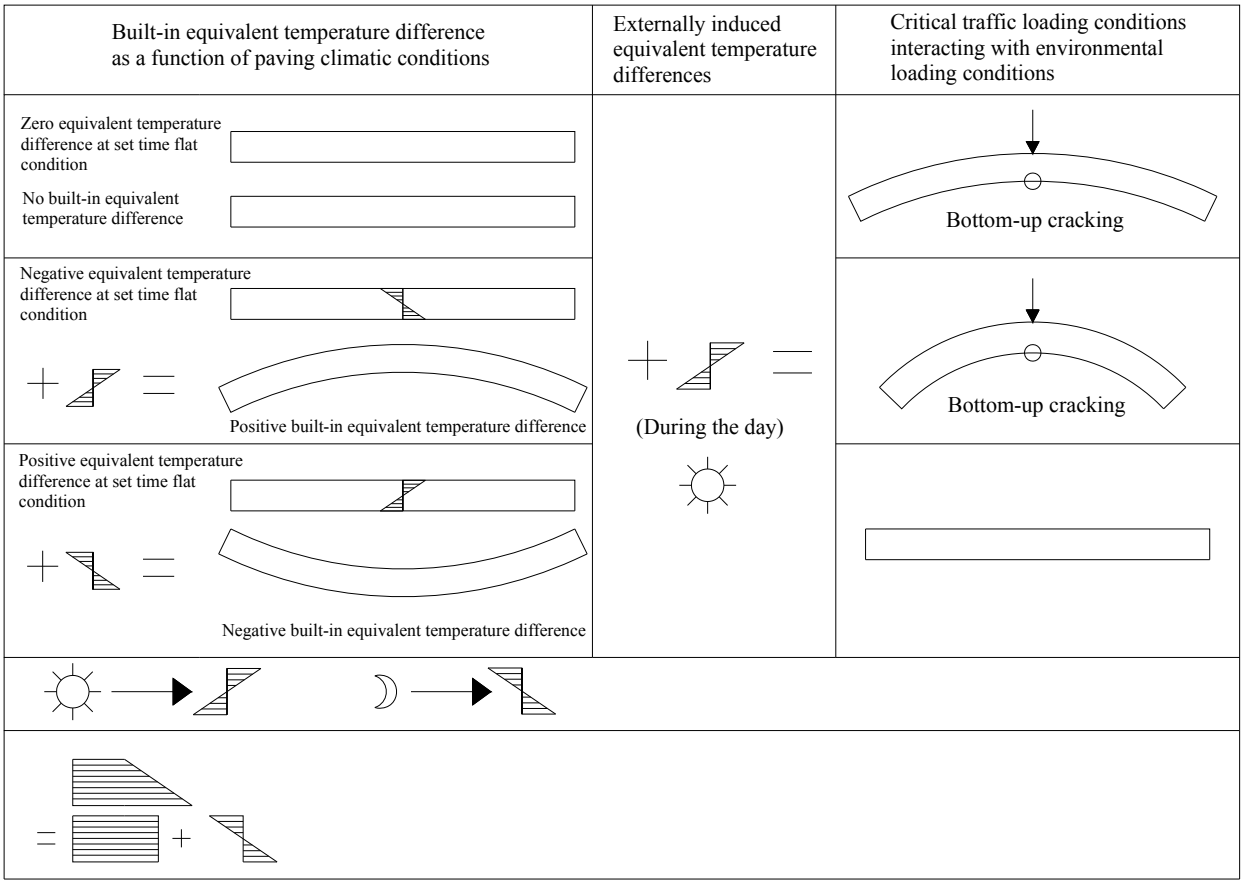

Figure 2.1 Interaction of environmental and traffic loads in the presence of positive gradients

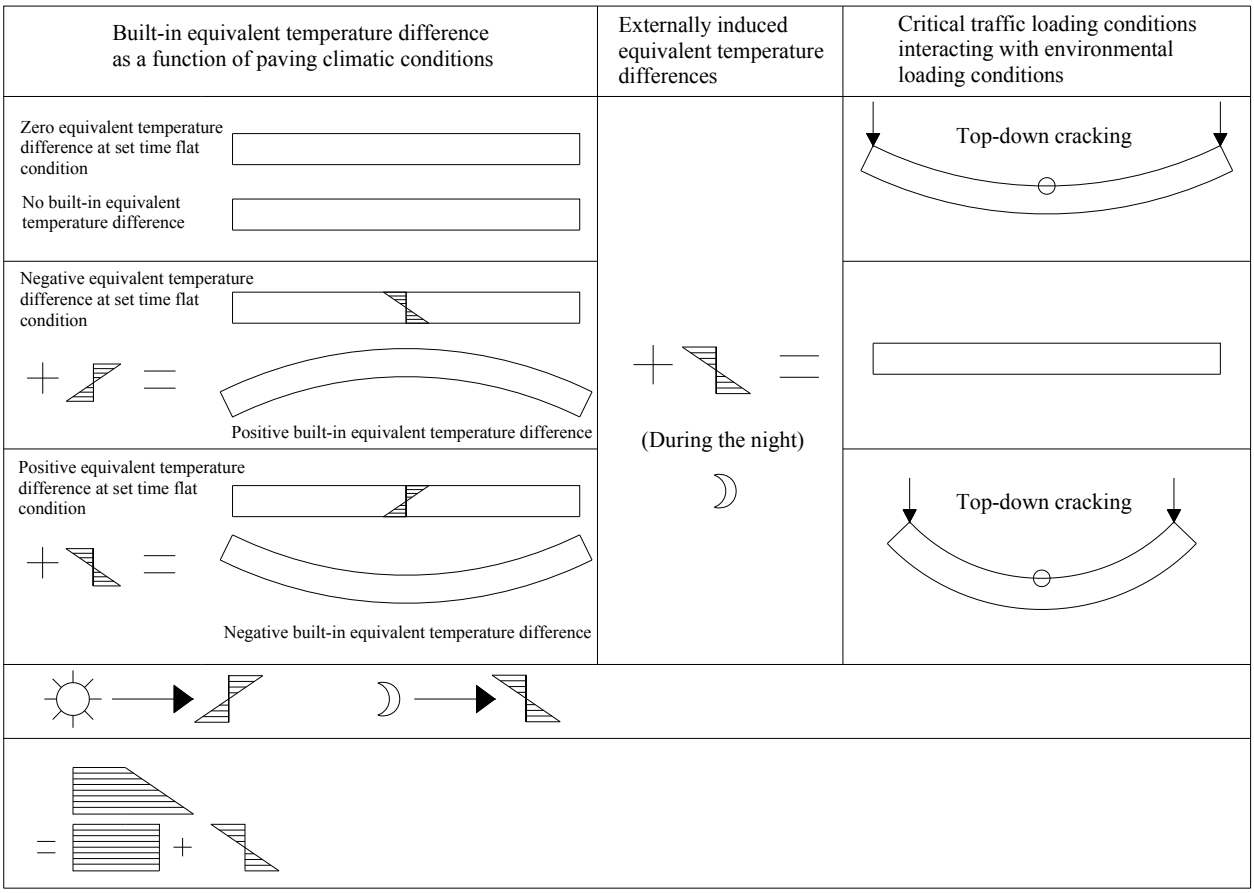

Figure 2.2 Interaction of environmental and traffic loads in the presence of negative gradients

2.2 REVIEW OF THE MEPDG CRACKING MODEL

Within the MEPDG theory, cracking is expected to occur due to fatigue as a consequence of the loading conditions depicted in Figure 4.1, parts a and b, following Miner's fatigue assumption.

Basically, the mechanistic tool of the cracking model, represented by the output of the neural networks, estimates fatigue damage FD (10):

$$FD = \sum \frac{n_{ijklmn}}{N_{ijklmn}} \qquad (1)$$

Where:

n: Number of load applications

N: Number of allowable load applications

i: Age

j: Month

k: Axle type

l: Load level

m: Temperature difference

n: Traffic path

The allowable number of load applications is determined by a field-calibrated model (10):

$$\log\left(N_{ijklmn}\right) = C_1\left(\frac{MR_i}{\sigma_{ijklmn}}\right)^{C_2} + 0.4371 \qquad (2)$$

In equation 2, *MR* refers to the modulus of rupture (i.e. strength) and σ is the acting stress; C_1 and C_2 are calibration constants. Finally, the empirical nature of the MEPDG cracking model comes through the correlation found between FD and total cracking of 196 field sections and a total of 516 observations (10):

$$CRK = \frac{1}{1 + FD^{-1.98}} \qquad (3)$$

$$R^2 = 0.75$$

$$TCRACK = (CRK_{B-U} + CRK_{T-D} - CRK_{B-U} * CRK_{T-D}) * 100\% \qquad (4)$$

Equation 4 shows how total cracking is obtained by adding bottom-up and top-down cracking and subtracting the probability that both occur.

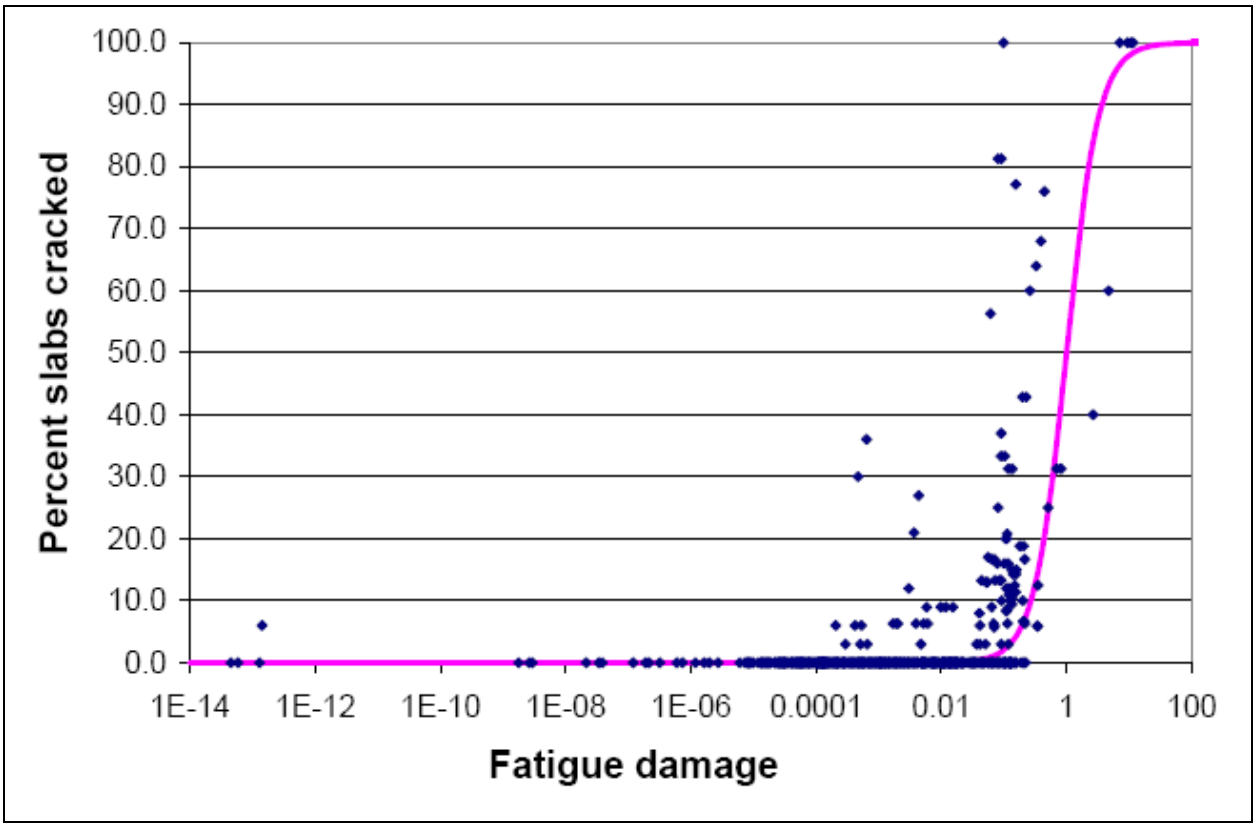

Figure 2.3 Empirical model described by equation 3 (10)

2.3 SENSITIVITY ANALYSIS

The academic pavement community involved in research on the MEPDG has begun to perform sensitivity analyses on the performance models. Sensitivity analyses have yielded valuable information regarding the impact of variables in the final output of the different models. The knowledge gained through these approaches is expected to be useful to judge the reasonableness of the internal models building the MEPDG. Also, objective measurements of importance can be assessed to each input through appropriate sensitivity analysis tools.

Some analyses have been carried out in the last few years on earlier versions of the MEPDG, which have contributed to gaining general knowledge regarding the relative importance of the various newly introduced variables. Among these studies, some analyses have been made on a one-at-a-time basis (OAT), for example the study performed by Hall and Beam (9). OAT is a rather rudimentary sensitivity analysis technique that yields rough results, the interpretation of which might lead to misleading conclusions if OAT analyses are carried out without the help of more sophisticated complementary techniques. OAT approaches, however, can be of great interest in an initial phase of the analysis and can be introduced as part of more elaborate studies.

Sensitivity analysis is a very actively growing area of mathematics with important applications in economy, business, science and engineering. The term sensitivity analysis is variously interpreted in different technical communities and problem settings (6). Higher reliability demands and more involved processes, mostly in the hi-tech areas of engineering design, have been lately pushing the development of very complex mathematical techniques that are used to solve sensitivity analysis problems whose solutions would otherwise be unthinkable (1, 2, 3, 6, 7).

In the engineering design field, it is remarkable that most of the available literature on sensitivity analysis is recent; this suggests that research is progressing significantly. In civil engineering, pioneering treatments of the problem are related mostly to structural analysis.

There are various approaches towards performing a sensitivity analysis, each of which is based on specific mathematical and statistical techniques. Three types of sensitivity analyses may be implemented in the sensitivity analysis of the MEPDG. The first type, referred to as one-at-a-time (OAT), has been the traditional approach and certainly one that should be interpreted in a more careful way than the current practice does. The second type is referred to as probabilistic sensitivity analysis (PSA). Under PSA, some state of the art techniques have facilitated the solution of certain sensitivity analysis problems that otherwise would be extremely expensive problems to solve in terms of time and computational capacity. The third approach is deterministic in nature and consists of model regression techniques.

2.3.1 One-at-a-time (OAT) sensitivity analysis

The most intuitive approach towards a sensitivity analysis is to compute partial derivatives of a function with respect to each of its independent variables. Let a response variable Y (e.g. the output value of a performance prediction model) be $Y = f(X)$, where X is a vector of inputs. An intuitive means to ascertain the sensitivity of Y with respect to a single input X_i is to compute $\partial Y/\partial X_i$ and then compare the derivative values between the inputs under analysis so that a ranking can be established.

Among some sensitivity analysis approaches, the partial derivative has been represented by the change of the output due to the change in one of the inputs. Even though this technique

accounts for the main effect of a given input, it completely ignores the interaction of the given input with other inputs. This method is called a one at a time (OAT) method. Provided that interactions in a given system are small with respect to the main effects of its variables, this method often yields valuable information regarding which inputs are important in the model. However, conclusions on the extent to which one given variable is more influential than another, should not be made solely on the basis of this approach. Ranking of importance is not possible either.

2.3.2 Probabilistic Sensitivity Analysis

Even though the nature of the model under study is not probabilistic but deterministic, probabilistic approaches would eventually be of interest to the pavement community. Many inputs of the MEPDG could consist of probability density functions rather than mere expected values. Material properties, differences between designed and constructed thicknesses, traffic trends and vehicle types, climate predictions, all should be treated with a degree of uncertainty. Probably one of the most fruitful products of probabilistic sensitivity analysis would be a sophisticated reliability model.

In an attempt to briefly address probabilistic sensitivity analysis, it can be noticed that the effect of the interaction between the uncertainties of each input or the joint dispersion effect on the global response cannot be taken into account in a deterministic approach. This can be expressed mathematically by the expression for total variance.

As quoted by Liu et al (3), "…with variance-based methods, the total variance of an output $Y = f(X)$ is decomposed into items contributed by various sources of input variations $X = [X_1, X_2, ..., X_n]$ in an ANOVA-like way:

$$V = \sum_i V_i + \sum_{i<j} V_{ij} + ... + V_{1,2,3,...,n} \qquad (5)$$

In the above expression, V is the total variance of the model output. The first order term V_i represents the partial variance in Y due to the individual (main) effect of a random variable X_i, while higher order terms indicate interaction effects between two or more random inputs."

As expressed above, from the standpoint of probability, it is reasonable to expect that all inputs have their own dispersion or uncertainty. The interactions between inputs have additional effects to the main effects of each input. Therefore the magnitude of the dispersion of each input affects not only the main effect of that variable but also that of the interaction with other variables.

In contrast to the OAT or deterministic approaches, probabilistic sensitivity analysis (PSA) makes it possible to deal with the joint dispersion of all inputs and its effect on the response variable. Also, some other powerful uses can be made of PSA, for example the answers to the following questions (2):

In a prior-design context:

Which variable(s) could be safely eliminated without bringing much influence on the uncertainty in the response?

In a post-design context:

Which random uncertainties should be further controlled (eliminated) to gain the largest improvement on the probabilistic performance of a response?

If the interest is to study the effects of input variance on the output variance, variance-based methods can be used to quantify the importance of inputs to an output (1).

Within variance-based analysis, it is possible to establish a quantitative ranking of inputs, as this would be very helpful towards the evaluation of a model in terms of reasonableness. Considering this situation, Sudjianto et al (1) employ the Kolmogorov-Smirnov (KS) distance to quantify the importance of an input.

2.3.3 Response Surface Methodology and Sensitivity Analysis

In a deterministic context, just like the nature of the MEPDG, a sensitivity analysis can simply be treated as a model regression, in which coefficients are direct measurements of the sensitivity of the different inputs and their interactions. Techniques for multi-variable model regression are treated in the field of Response Surface Methodology (RSM).

In the process of fitting a multi-variable model through RSM, the first step is generally the screening of the model. One of the most widely used screening techniques is that of two-level factorial designs or 2^k experiments. Myers and Montgomery (2002) stress the importance of 2^k designs in three different applications:

- They are used as screening experiments to identify the important process or system inputs.

- They are used to fit a first-order response surface model and to generate the factor effect estimates required to perform the method of steepest ascent.
- They are essential in the process of central composite designs, which are the most important designs for fitting second-order response surface models.

2.3.4 The California Study as a choice in MEPDG sensitivity analysis

Kannekanti and Harvey at the University of California, Berkeley and Davis (2005) conducted sensitivity analyses on the design of JPCP as part of a greater effort to evaluate the MEPDG suitability for the state of California. Their main concern was that very few LTPP California zones had been part of the calibration dataset for the MEPDG.

The California analysis has a different philosophy than the one behind OAT analysis and illustrates, in a general way, what the current approach towards sensitivity analysis is in the pavement community. Different values of several inputs were combined in a global factorial experiment and then basic statistics of the performance response were computed after 8,640 cases were run with the MEPDG software.

The study captures the global effect of the role each variable contributes to the response of the model and the interactions between variables, though no differentiation can be identified between the two. Basic statistics of the output (maximum value, minimum value, 75^{th}, 50^{th}, 25^{th} percentile values) were computed on the output at each input at their different levels (see Table 2-1). These statistics were compared between the different values of the variable under study as a means to assess a sensitivity degree to each variable, even though no explicit quantitative ranking was defined. The main drawback of this type of analysis is its computational cost. As a

consequence, the California study was limited to a small number of variables and a small number of levels. However, the approach is neat from a practical point of view, and further research can be made in the same direction by including further inputs, for example inputs whose influence is suspected to be important on the response of the system, which were not included in the California study.

Table 2-1 California experiment for JPCP sensitivity analysis of MEPDG

Input	Values taken by inputs	Number of values taken by inputs
Axle Load Spectra	Rural Urban	**2**
Traffic Volume (Traffic Index)	12 13 16	**3**
Climate Regions	LA Sacramento Reno	**3**
Slab thickness	7 8 9 12 13	**5**
Base	ATB CTB	**2**
Subgrade	High plasticity clay Poorly graded sand	**2**
Dowels	Dowels No dowels	**2**
Shoulder type	Asphalt shoulders Tied shoulders Widened truck lane	**3**
Joint spacing	15ft 19ft	**2**
PCC flexural strength	626psi 700psi	**2**
Number of cases		**8640**

2.3.4.1 Comparison between two different approaches

Rankings of inputs by order of importance for two different approaches are summarized in Table 2-2. The California experiment yields results that clearly differ from the results an OAT yields. The OAT in the case of Table 2-2 was performed as part of a course in advanced pavement design at the University of Pittsburgh. The underlined italic-styled inputs were common to both approaches. It can be appreciated that unequal rankings result from the two approaches. It is important to emphasize that the ranges of inputs used are not the same for the two approaches, so it is expected that this explains, to some extent, the difference found.

Table 2-2 Comparison of rankings between OAT and the California experiment

	Cracking Model		Faulting Model		Smoothness Model	
Rank	**California experiment**	**OAT analysis**	**California experiment**	**OAT analysis**	**California experiment**	**OAT analysis**
1	*Joint spacing*	*PCC modulus of rupture*	Dowels / no dowels	Curl / warp effective temperature difference	Traffic index	*PCC modulus of rupture*
2	*Climate*	*Joint spacing*	Traffic index	Dowel diameter	Dowels / no dowels	*Joint spacing*
3	*Slab thickness*	*Slab thickness*	*Slab thickness*	Design lane width	*Slab thickness*	Curl / warp effective temperature difference
4	Traffic index	Curl / warp effective temperature difference	Shoulder type	Traffic wander	*Climate*	*Slab thickness*
5	Shoulder type	Design lane width	*Climate*	PCC coefficient of thermal expansion	Shoulder type	Design lane width
6	Base type	*Climate*	*Joint spacing*	*Climate*	*Joint spacing*	*Climate*
7	*PCC modulus of rupture*	Traffic wander	Load spectra	*Slab thickness*	Base type	Traffic wander
8	Subgrade type	PCC coefficient of thermal expansion	Base type	Shortwave absorptivity	Load spectra	Dowel diameter
9	Load spectra	Shortwave absorptivity	*Subgrade type*	*Subgrade type*	*PCC modulus of rupture*	PCC of thermal expansion
10		Subgrade type	*PCC modulus of rupture*	*PCC modulus of rupture*	Subgrade type	Shortwave absorptivity
11		Time after which friction is lost		*Joint spacing*		Thermal conductivity
12		Thermal conductivity		Thermal conductivity		Erodability

3.0 EXPERIMENTS ON THE REASONABLENESS OF THE MODEL

3.1 TRAFFIC INFLUENCE ON PERFORMANCE

Section 4.1.1 introduces a simplification of traffic as an input for sensitivity analysis. In this process, general research was conducted in order to compare the influence of several different vehicle types on performance. The details of that analysis are provided below.

3.1.1 Design of experiment for vehicle type analysis

The cases that were analyzed in the process of simplifying traffic characterization, as depicted in 4.1.1, are contained in Table 3-1. The objective of this analysis was to select a single vehicle type that best represents the bulk of traffic that ultimately determines the performance of the pavement in order to simplify the role of traffic in sensitivity analysis. The influence of vehicle types for different wheelbase configurations and joint spacing distances is analyzed, especially in regard to the amount of top-down fatigue damage they produce at different conditions. In order to isolate the top-down modus of failure, traffic was applied to the pavement only during night hours from 8:00 PM to 8:00 AM.

Table 3-1 Design of experiment for vehicle type analysis

Vehicle type	5, 6, 7, 8, 9, 10, 11, 12, 13
Joint Spacing [ft]	12, 20
Wheelbase 12-15-18 [%]	100-0-0, 0-100-0, 0-0-100, 33.3-33.3-33.3
Total number of cases	72

3.1.1.1 Pavement structure and other inputs for traffic analysis

Detailed information about all inputs for this analysis can be found in Appendix A. Table 3-2 presents a summary of the pavement structure, traffic, climate and other inputs common to all cases.

Table 3-2 Summary of inputs for vehicle type analysis

Design Life	20	years
Performance Criteria	Limit	Reliability
Transverse Cracking (% slabs cracked)	15	90
Traffic		
Initial two-way AADTT:	10000	
Number of lanes in design direction:	2	
Percent of trucks in design direction (%):	50	
Percent of trucks in design lane (%):	100	

Growth Rate	Growth Function
6.0%	Compound

Structure--Design Features	
Permanent curl/warp (°F):	-10
Structure--Layers	
Layer 1 – JPCP	
General Properties	
PCC material	JPCP
Layer thickness (in):	8
Unit weight (pcf):	150
Poisson's ratio	0.2
Strength Properties	
Input level:	Level 3
28-day PCC modulus of rupture (psi):	600
28-day PCC compressive strength (psi):	n/a
Layer 2 -- Asphalt permeable base	
Material type:	Asphalt permeable base
Layer thickness (in):	5
Layer 3 -- Crushed stone	
Unbound Material:	Crushed stone
Thickness(in):	10
Layer 4 -- A-6	
Unbound Material:	A-6
Thickness(in):	Semi-infinite

3.1.1.2 Anomalies with wheelbase and top-down fatigue

Figure 3.1 through Figure 3.9 show the predicted fatigue damage for the different wheelbase configurations in combination with different vehicle types and joint spacing.

Figure 3.1 shows that the top-down fatigue damage for Class 5 vehicles is zero. On the other hand, Class 6 and 7 vehicles (Figure 3.2 and Figure 3.3) produced large top-down fatigue damage for all wheelbase configurations when the joint spacing is equal to 20 ft. It is remarkable that the fatigue damage produced by these two types is substantially higher than that produced by heavier vehicle types.

The magnitude of fatigue damage caused by vehicle Classes 8 through 13 is very similar for both joint spacing and all wheelbase configurations. In general, for all vehicle classes no top-down fatigue was estimated for a joint spacing of 12 ft.

Higher top-down fatigue damage occurred at a joint spacing of 20 ft, which was expected. However, the relative magnitude of fatigue damage for different wheelbase configurations did not result as expected. In all vehicle classes, higher top-down fatigue damage appears to correspond to shorter wheelbase distances. This contradicts the general understanding of the failure mechanism depicted in section 2.2.

With a joint spacing of 20 ft, the highest expected top-down fatigue damage should be a wheelbase of 18 ft as it would yield the highest tensile stresses on top of slabs. However, according to the MEPDG, the highest top-down fatigue damage was produced by a wheelbase of only 12 ft.

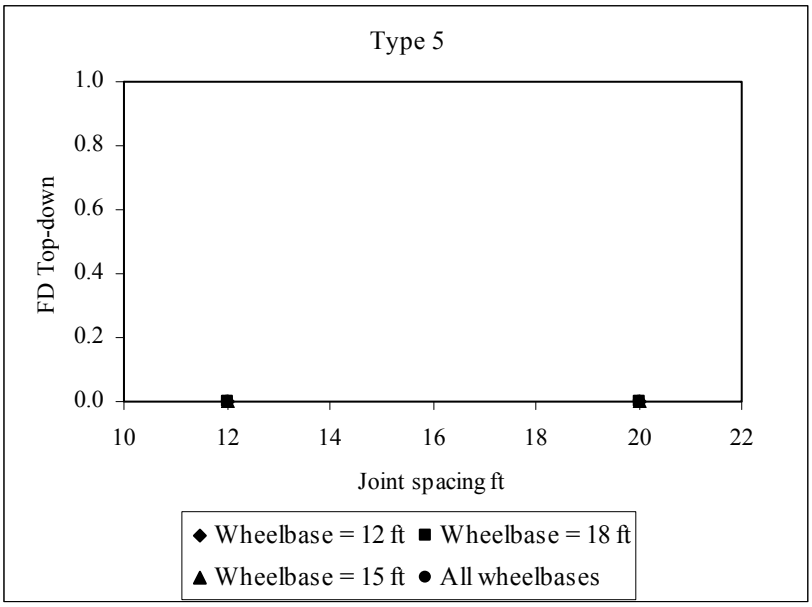

Figure 3.1 Top-down fatigue damage for vehicle type 5

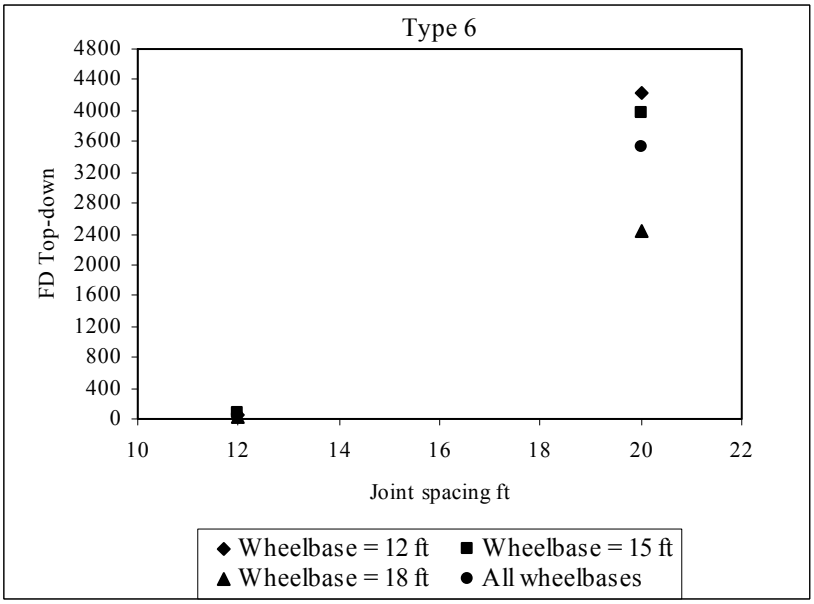

Figure 3.2 Top-down fatigue damage for vehicle type 6

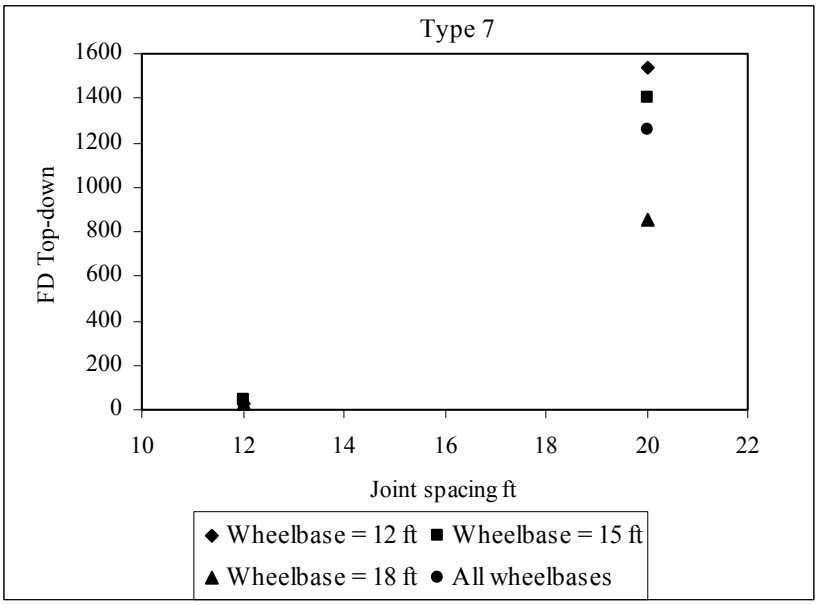

Figure 3.3 Top-down fatigue damage for vehicle type 7

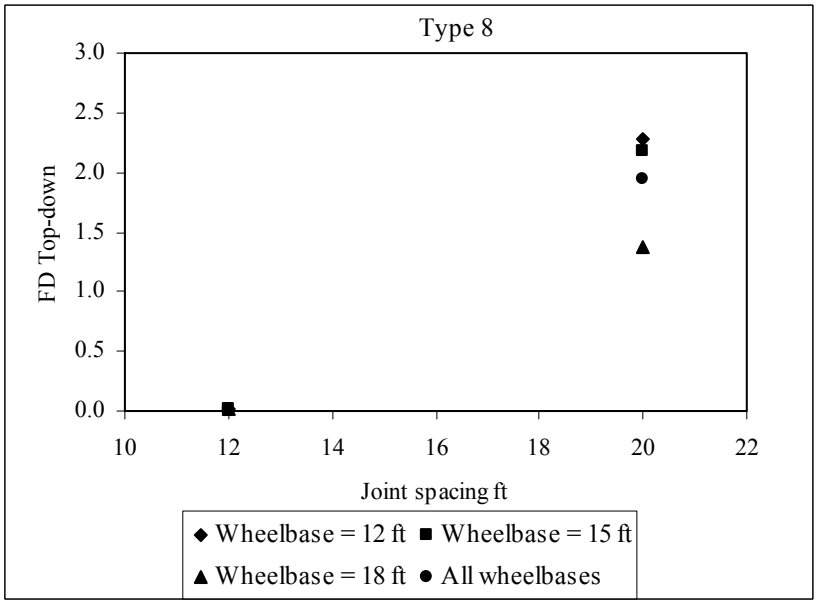

Figure 3.4 Top-down fatigue damage for vehicle type 8

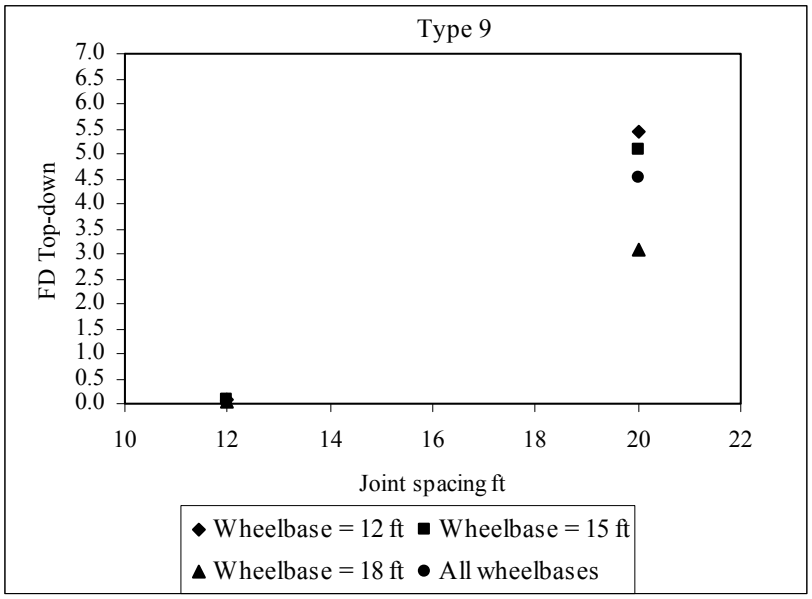

Figure 3.5 Top-down fatigue damage for vehicle type 9

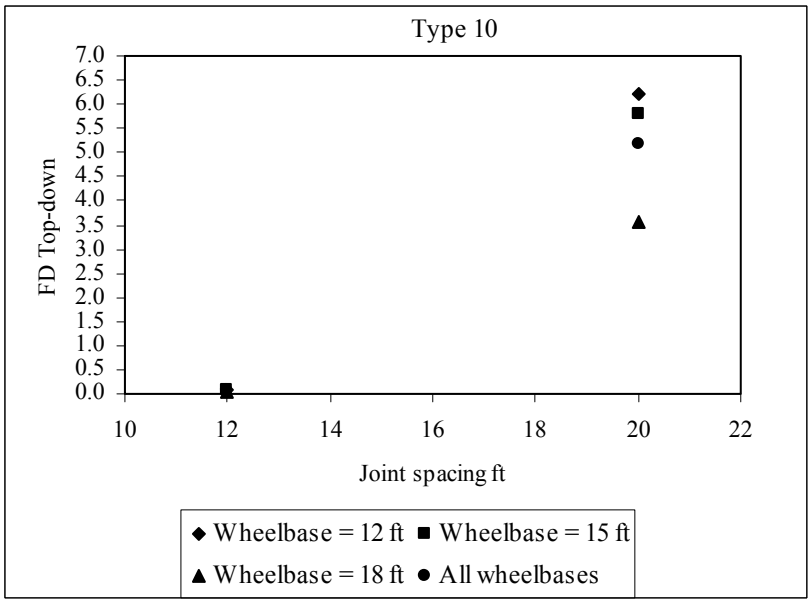

Figure 3.6 Top-down fatigue damage for vehicle type 10

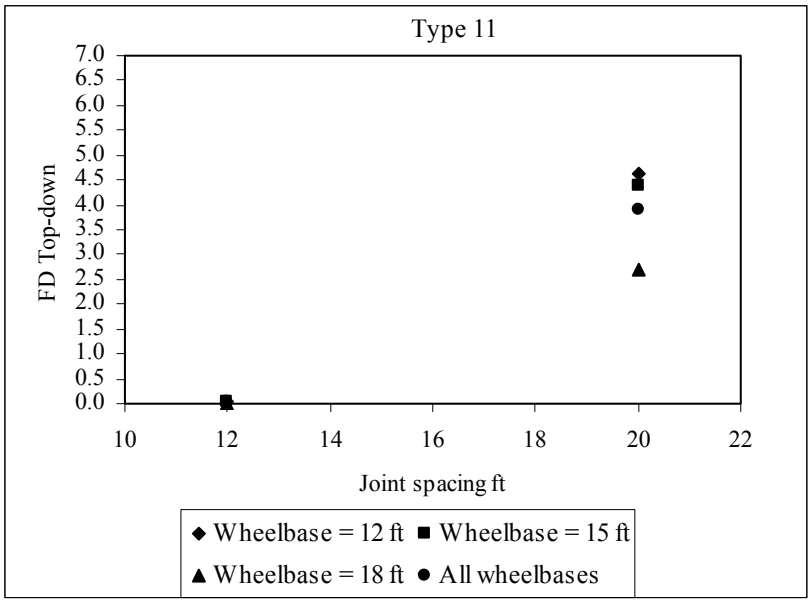

Figure 3.7 Top-down fatigue damage for vehicle type 11

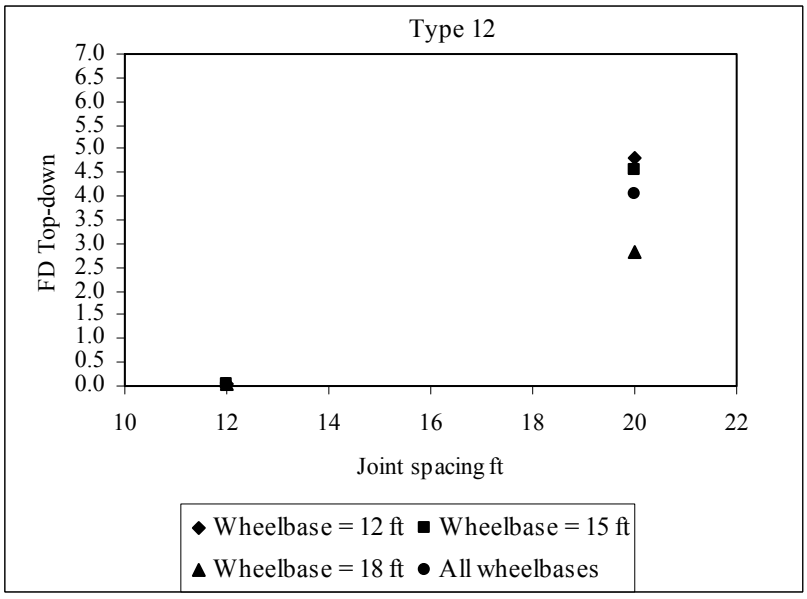

Figure 3.8 Top-down fatigue damage for vehicle type 12

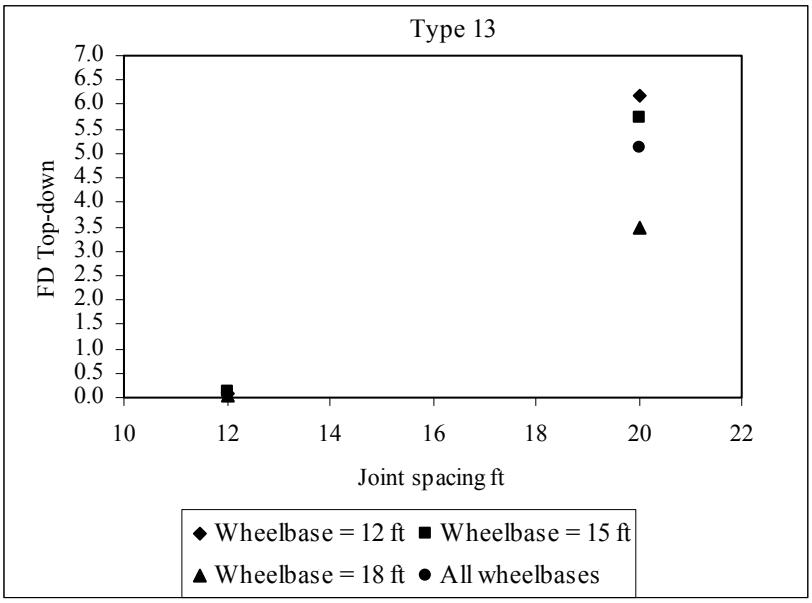

Figure 3.9 Top-down fatigue damage for vehicle type 13

3.2 ON THE BUILT-IN EQUIVALENT TEMPERATURE DIFFERENCE

The MEPDG (10) defines the built-in permanent temperature gradient as follows:

"PCC paving is often performed during the mornings of hot sunny days, a condition that tends to expose the newly paved PCC slabs to a high positive temperature difference from intense solar radiation plus the heat of hydration. The PCC slabs are flat when they harden, but depending on the exposure conditions a significant amount of positive temperature gradient (upper portion of the slab is much warmer than bottom) may be present at the time of hardening. This temperature has been termed the 'built-in temperature gradient' or in this guide it is called the 'zero-stress temperature gradient.' Whenever the temperature gradient in the slabs fall below the amount locked into the slab at the time of construction (the zero-stress gradient), the slabs will attempt to curl upward causing tensile stress at the top of the slab which can lead to top-down cracking of JPCP. Thus, an effective negative temperature gradient is permanently built into the slabs…..If the PCC paving is performed in the morning, the maximum heat of hydration and the maximum solar radiation coincides at about the same time resulting in a large

built-in temperature gradient when the slab solidifies. If PCC paving is performed later in the afternoon or at night so that the highest temperature from the heat of hydration does not correspond with the most intense solar radiation, the amount of permanent temperature gradient 'built' into the slab will be much lower and could potentially even be negative (thus locking in a positive built-in)."

For the effects of positive and negative built-in gradients refer to section 2.2. In the process developed to relate FD to cracking (see equation 3), sites were included that were very well documented regarding materials, date of construction, development of distress with time, and actual climate present during the period of time studied, among others. Only one characteristic of each site was unknown, namely the so-called permanent effective curl/warp temperature difference or zero-stress effective gradient.

Among the inputs of the cracking model, the permanent effective curl/warp temperature difference is assumed to be a very influential input. This input corresponds to the effective temperature difference between top and bottom a concrete slab present at set time, as previously described. The nature of this input in the MEPDG cracking model deserves attention because of two reasons:

1. In the process of fitting the model to correlate fatigue damage and cracking, the "permanent built-in" was treated as a constant (equal to -10) that yielded the best fit for the given set of available points. However, the current state of the model allows the user to input a different value, whenever it is available. This dual nature of the built-in seems somewhat contradictory as it leads to the following situation:

Let Charleston, WV be a site used in the regression analysis (equation 3, Figure 2.3). The Charleston site is thus run with all known inputs and a built-in gradient equal

to -10. Let MEPDG-CRACK$_{-10}$ be the output of the system, which is also a data point for the regression.

Now suppose the site is re-designed using the tool, with built-in temperature difference taking a value other than -10, say equal to x (which engineers claim to have measured on the day of construction), producing MEPDG-CRACK$_x$. ***Question 1.*** *What result should be regarded to be true for Charleston?*

a) MEPDG-CRACK$_{-10}$

b) MEPDG-CRACK$_x$ ≠ MEPDG-CRACK$_{-10}$

In the MEPDG, both are regarded true, which is a contradiction. The first result is regarded true because it is assumed to be a valid point for the model regression. The second point is also regarded true because it is an output of the MEPDG. Unfortunately the answer to question 1 should be "none".

The above described contradiction may be the consequence of treating the built-in temperature difference in an ambiguous manner, first as a "universal" constant and then as an independent (and random) variable.

Question 2. *If the actual built-in temperature difference is different than -10 by such an amount that MEPDG-CRACK$_x$ and MEPDG-CRACK$_{-10}$ differ by a large magnitude, how can MEPDG-CRACK$_{-10}$ be claimed as a valid point of the regression model? If it were concluded that MEPDG-CRACK$_{-10}$ is not a valid point, can MEPDG-CRACKx be correct?* Unfortunately the answers are no, no.

2. The second reason is that due to the uncertainty that surrounds this input and the unknown magnitude of its range for a given site, this input is suspected to have a significant impact in the performance of a pavement structure. To what extent this is true is intended to be clarified through a sensitivity analysis.

3.2.1 Design of experiment for built-in effective temperature difference

Table 3-3 contains the different values of built-in effective temperature difference and the various sites analyzed.

Table 3-3 Design of experiment for built-in effective temperature difference

Built-in effective temperature difference	-30, -25, -20, -15, -10, -5, 0, 5, 10
Site	Pittsburgh, Phoenix, Miami, Wichita, Aspen

3.2.1.1 Pavement structure for built-in effective temperature difference

Table 3-4 presents a summary of the pavement structure, traffic, climate and other inputs common to all cases for this analysis. Appendix A contains full data information.

Table 3-4 Summary of inputs for vehicle type analysis

Design Life	20 years	
Performance Criteria	Limit	Reliability
Transverse Cracking (% slabs cracked)	15	50
Traffic		
Initial two-way AADTT:	2000	
Number of lanes in design direction:	2	
Percent of trucks in design direction (%):	50	
Percent of trucks in design lane (%):	95	

Growth Rate	Growth Function
	No growth

Structure--Design Features		
Permanent curl/warp (°F):	Variable	
Structure--Layers		
Layer 1 – JPCP		
General Properties		
PCC material	JPCP	
Layer thickness (in):	10	
Unit weight (pcf):	150	
Poisson's ratio	0.2	
Strength Properties		
Input level:	Level 3	
28-day PCC modulus of rupture (psi):	600	
28-day PCC compressive strength (psi):	n/a	
Layer 2 -- Unbound material		
Material type:	A-3	
Layer thickness (in):	5	
Layer 3 -- Unbound material		
Unbound Material:	A-3	
Thickness(in):	Semi-infinite	

3.2.1.2 Anomalies with the built-in effective temperature difference

As previously mentioned, one of the most important inputs in the MEPDG is the built-in effective temperature difference. An important objective of this research is to evaluate how this particularly interesting component of the MEPDG is performing in the current version. The main motivation for this part of the research is the fact that actual data for defining this input is practically nonexistent. Also, the dual nature with which this input has been handled in the process of model calibration, as depicted in 3.2, suggests that the reasonableness of the general behavior of the model in response to this input should be carefully checked.

The most intuitive approach to check the model output in response to built-in effective temperature difference is to evaluate a single design for sites across the United States, the climatic characteristics of which are known to vary from each other. Figure 3.10 shows maximum daily air temperature differences for several sites across the country. This is based on data sets that have a minimum of seven years of climatic data. The data necessary to produce this figure was obtained from NOAA (12). From Figure 3.10, it seems apparent that the maximum daily temperature difference varies considerably from site to site. For example, Miami exhibits the least temperature variations, while Aspen exhibits the greatest differences.

Figure 3.11 shows the actual effective temperature differences acting on various sites for the proposed pavement design, obtained directly from the output files of the MEPDG. In accordance with Figure 3.11, it can be seen that effective temperature differences in the pavement slabs are higher in sites with higher daily temperature swings, as expected (e.g. Aspen, Phoenix).

Based on the evidence that temperature differences acting on the pavement vary substantially from site to site, one of the main objectives conceived in the philosophy of the MEPDG is to account for the variability in environmental loads, which is basically a function of geographic location (climate). In this sense, a value or range of values for the built-in effective temperature difference for a given site could be thought to exist, such that the performance of the pavement structure in response to temperature loads falls within a certain value or range of values, correspondingly. Furthermore, if a safe value or range of values of built-in effective temperature difference exists, then the magnitude of this value or range of values should equal the magnitude of the actual gradients acting on the pavement structure. This equality stands for the situation where concrete slabs remain flat, thus avoiding the conditions depicted in section 2.2 from taking place. Following this line of thought, the range of values for which the performance of the pavement structure is safest should be a site property, because it is the climate of the site that ultimately determines the magnitude of the safe range, according to its frequency distribution of temperature differences.

The intuitive thought depicted in the previous paragraph leads to expect variations in the performance of a given pavement structure constructed in different climatic regions. However, for the basic design presented in Table 3-4 evaluated for different climatic regions, there appears to be a single value of built-in effective temperature difference for which total cracking is minimized. This singular value is equal to or close to -12, this exact value being common to sites of distinct climates. This finding is depicted in Figure 3.12. Figure 3.11 includes the value of -12 as a reference value. It can be appreciated in this figure that most mean values of effective temperature difference distributions clearly differ from this magnitude.

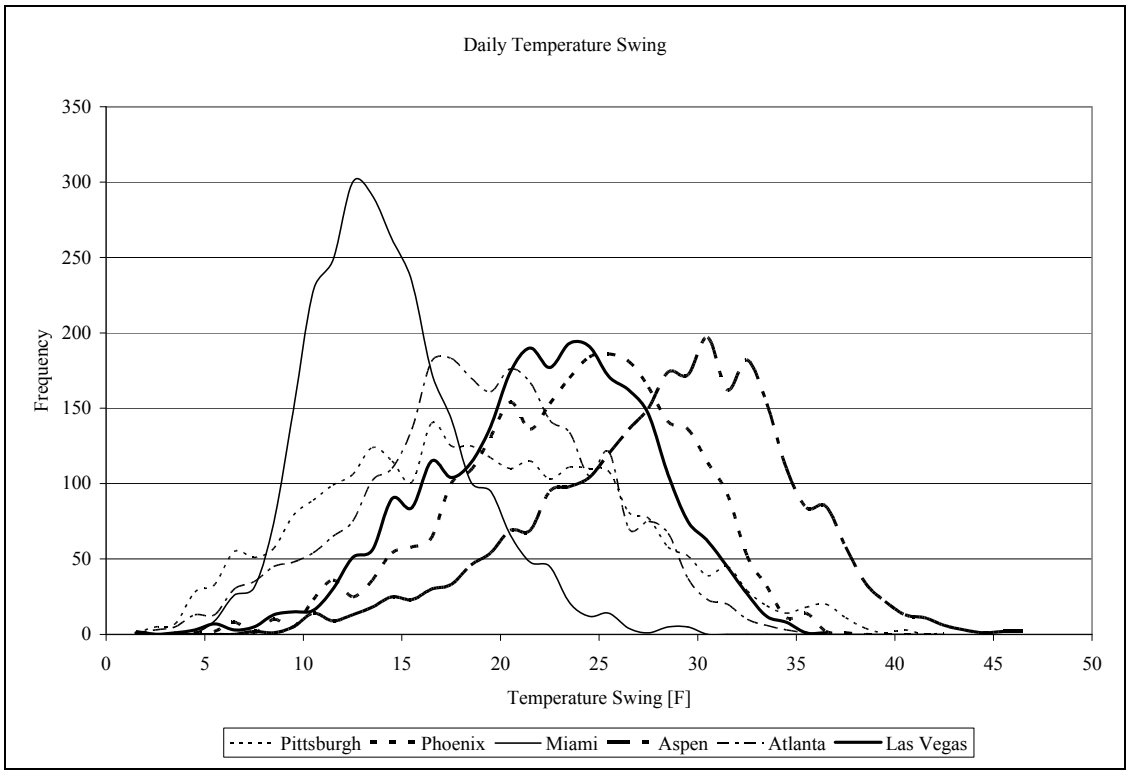

Figure 3.10 Frequency distribution of daily maximum ambient temperature difference

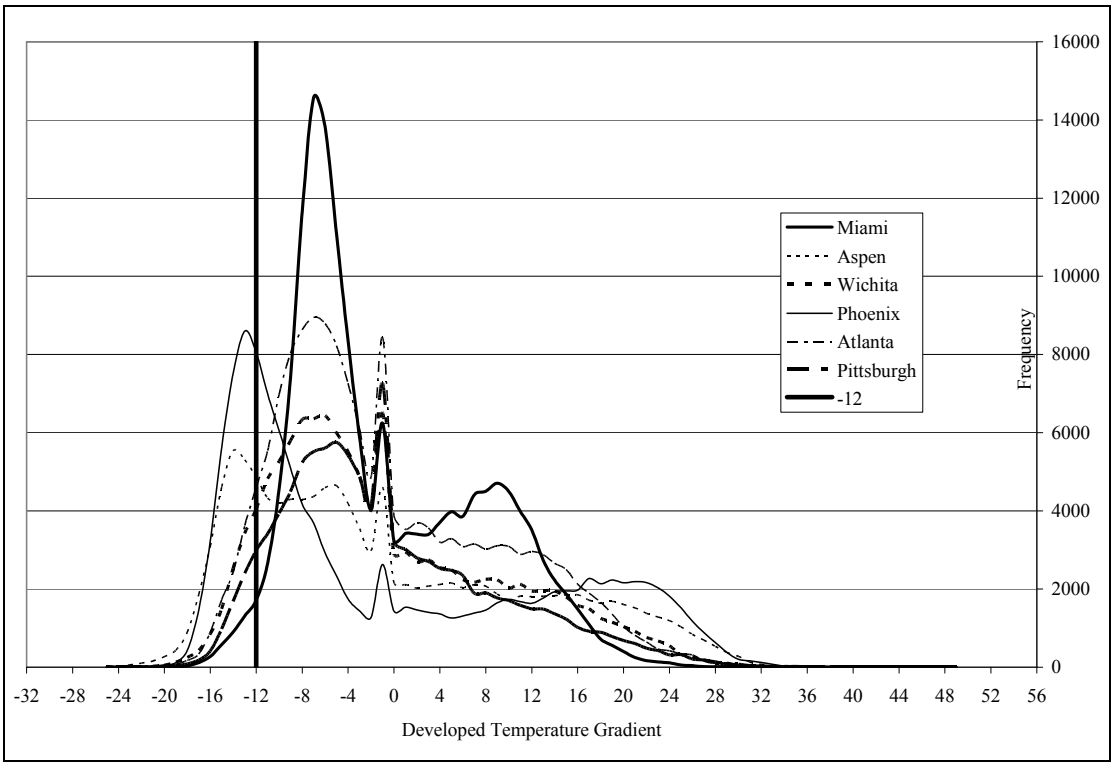

Figure 3.11 Frequency distribution of temperature gradients for different sites

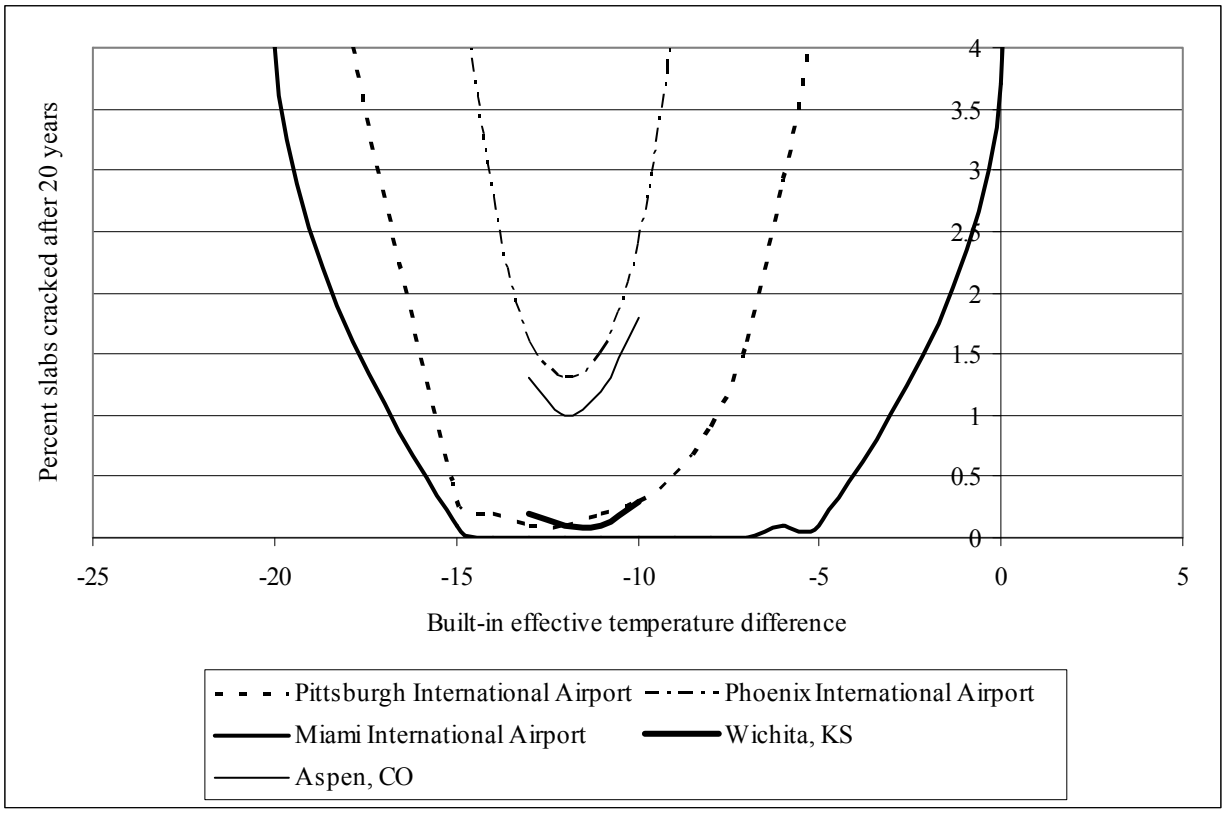

Figure 3.12 Cracking as a function of built-in effective temperature difference

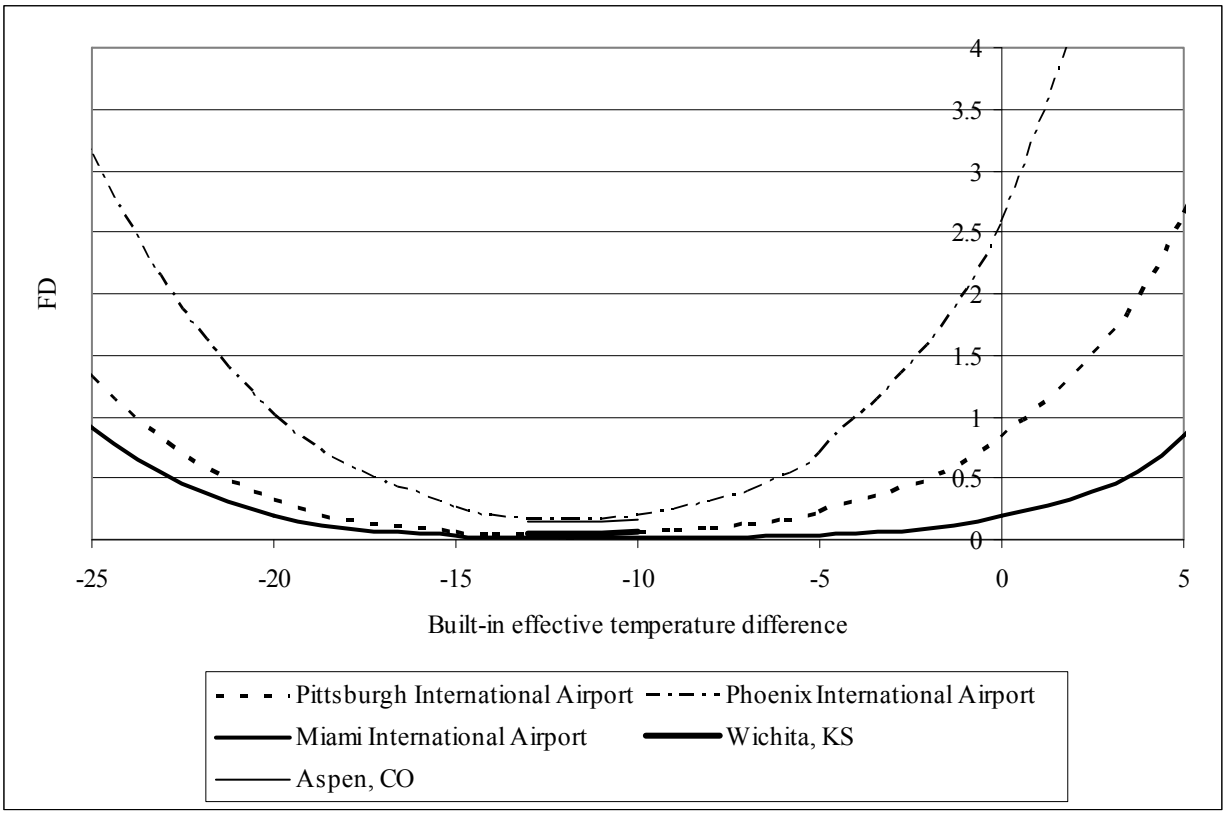

Figure 3.13 Fatigue damage as a function of built-in effective temperature difference

Table 3-5 Data for built-in temperature difference analysis

		Built-in temperature difference								
Site		-15	-14	-13	-12	-11	-10	-9	-8	-7
Pittsburgh, PA	FDb-u	0.01	0.014	0.02		0.037	0.051	0.069	0.094	0.126
	FDt-d	0.053	0.036	0.023	0.015	0.01	0.007	0.005	0.003	0.002
	FD_{total}	0.063	0.049	0.043	0.015	0.047	0.058	0.074	0.097	0.128
	TCRACK	0.3	0.2	0.1	0.1	0.2	0.3	0.5	0.9	1.6
Phoenix, AZ	FDb-u	0.027	0.039	0.054	0.077	0.107	0.148	0.205	0.28	0.382
	FDt-d	0.231	0.163	0.114	0.078	0.058	0.043	0.031	0.022	0.016
	FD_{total}	0.258	0.202	0.168	0.155	0.166	0.191	0.237	0.302	0.398
	TCRACK	5.3	2.8	1.6	1.3	1.5	2.4	4.3	7.5	13
Miami, FL	FDb-u	0.0007	0.001	0.002	0.003	0.004	0.006	0.009	0.012	0.018
	FDt-d	0.03	0.019	0.012	0.008	0.005	0.003	0.002	0.001	9E-04
	FD_{total}	0.031	0.02	0.014	0.01	0.009	0.009	0.011	0.014	0.019
	TCRACK	0.1	0	0	0	0	0	0	0	0
Wichita, KS	FDb-u			0.017	0.024	0.034	0.047			
	FDt-d			0.035	0.022	0.016	0.011			
	FD_{total}			0.051	0.047	0.049	0.058			
	TCRACK			0.2	0.1	0.1	0.3			
Aspen, CO	FDb-u			0.047	0.067	0.092	0.125			
	FDt-d			0.102	0.073	0.057	0.043			
	FD_{total}			0.149	0.139	0.149	0.168			
	TCRACK			1.3	1	1.2	1.8			
Atlanta, GA	FDb-u			0.013	0.018	0.025	0.035			
	FDt-d			0.026	0.016	0.012	0.008			
	FD_{total}			0.039	0.034	0.037	0.043			
	TCRACK			0.1	0.1	0.1	0.1			

3.3 CONCLUSIONS (I)

The MEPDG fatigue damage predictions seem to be opposite to the current understanding and to the way the literature of the MEPDG (10) describes the critical load conditions. The experiment was aimed at top-down fatigue damage, for which only night hours were considered. As expected, the bottom-up fatigue damage was zero and the top-down fatigue damage was higher than zero. However, short wheelbase distances produced higher fatigue damage than longer wheelbase distances, contradicting the nature of the cracking mechanism that is used to explain top-down cracking. If the drawing 1b of Figure 4.1 is conceived as the general qualitative condition for top-down cracking to occur, then the most probable loading condition to cause the highest cracking would be one in which the wheelbase distance is close to the joint spacing. Actually, this is supposed to be the condition the MEPDG considers when estimating T-D FD. The wheelbase distance being close to joint spacing would cause the highest critical tensile stresses, and it is therefore considered the most critical. Consistently, the configuration depicted in drawing 2a would be expected to be more damaging than that depicted in drawing 2c. From the results, the opposite holds. Furthermore, according to the MEPDG literature, a configuration like the one depicted in drawing 2c would not even be accounted for in the top-down fatigue damage calculations, as it would not correspond to the critical loading condition. The results, however, show that the shorter the wheelbase, the higher the top-down fatigue damage.

It is difficult to judge what type of programming error is producing these results as the software code is not available. A conclusion can only be drawn in terms of reasonableness by comparing the results with engineering judgment. The results obtained through these runs suggest that the wheelbase is being considered inside the software in an anomalous way. The results for top-down fatigue damage should clearly represent the engineering judgment

associated with them in a qualitative manner. For the specific case of Class 5 trucks, no damage is accumulated. This may also be subjected to revision in the improvement of the software.

The treatment given to the permanent built-in temperature difference in the MEPDG is confusing since it is used as a constant first, and then left as a modifiable input, introducing fundamental contradiction. A regression like that illustrated in Figure 2.3 should be carefully implemented since it is based on data points that do not strictly correspond to reality. The permanent built-in proves (as will be appreciated in 4.4) a very important input, suggesting that its characterization must be accomplished in a very careful way. Searching for a value (i.e. -10 as it turned out) that produces the best model fit simplifies the procedure by producing a model with an acceptable coefficient of determination. However, it might introduce error as the actual built-in temperature difference is arbitrarily set, constituting a drawback of the procedure from the mechanistic point of view.

An explanation regarding the singularity found at a permanent built-in of -12 (or around -12) is out of sight. It is important to emphasize that fatigue damage follows the same trend as the cracking. That is, for a value of -12 or very close to this value the summation of bottom-up and top-down fatigue damage is minimized. Recalling that fatigue damage is a fully mechanistic output inside the MEPDG, it is very confusing to find that the least fatigue damage corresponds to a singular value of permanent built-in without dependence of climate. In order to complement this analysis, Figure 3.13 needs to be considered. If fatigue damage is a mechanistic result on which real properties, temperatures and loads are considered and processed by FEM within the NN, then dependence on climate would be expected. It is not thinkable that the least fatigue damage corresponds to a universal value of permanent built-in, because gradient distributions change from site to site, as demonstrated through Figure 3.11.

4.0 SCREENING EXPERIMENTS FOR SENSITIVITY ANALYSIS

4.1 INPUTS FOR ANALYSIS

The Mechanistic-Empirical Design Guide considers three hierarchical input levels depending on the quality of sources of data available to the designer. The quality of data source refers to the degree of objectivity and accuracy of the various possible sources. The more objective and possibly accurate the data is, the higher it is ranked within the levels 1 through 3, with level 1 being the highest. Level differentiation will not be attempted in this research. Instead, inputs will be defined on the basis of universally accepted ranges for each input.

It was previously discussed that earlier studies provided valuable information regarding the most influential inputs for the MEPDG. Also, knowledge and understanding of the performance models involved as well as engineering judgment serve as tools to focus on a target set of inputs for a sensitivity analysis. The size of the target set is a function of the computational effort, which in turn is a function of time and resources available. Ultimately, a sensitivity analysis of the type proposed for this research focuses on a rather small set of inputs that are suspected to be most influential. As part of this approach, a general knowledge of the complete set of variables is required, so as to illustrate the nature and relatively low impact of variables that are not included in the analysis. The present section includes a general presentation of all inputs of the MEPDG following the flow of Figure 1.1.

Among all inputs of the MEPDG, traffic inputs need to be discussed in an isolated manner in order to point out the complexity of all possible variations involved. A simplification that can be made in order to consistently address the role of traffic in sensitivity analysis is discussed. Simplifying traffic input characterization serves well in achieving repeatability and comparability of sensitivity analyses. Also, load magnitude differentiation can be addressed in a more flexible manner if traffic input characterization is simplified.

4.1.1 Traffic input characterization

The present subsection provides a complete list of traffic inputs involved in the MEPDG and a discussion on how traffic inputs can be simplified in the sensitivity analysis. In terms of the frame of Figure 1.1, traffic inputs can be classified as raw inputs, the magnitudes of which need to be determined by the designer. The traffic output is a direct function of all traffic inputs, and consists of the hourly number of axles per axle type and per load group that are applied to the pavement in critical conditions, as depicted in Figure 4.1.

Raw traffic inputs are included in Table 4-1. In a theoretical sense, each raw traffic input can make part of the target set of analysis inputs. However, there is an infinite number of possible combinations of traffic inputs that can yield different magnitudes of traffic output (e.g. increasing or decreasing the AADTT, increasing or decreasing axle loads, etc.). Furthermore, in the interaction between traffic and structural response, several inputs among raw traffic values could be modified to influence the structural response of the pavement, the critical stress build-up and ultimately the magnitude of distress predicted by the performance models (e.g. modifying mean wheel location would ultimately modify critical stresses at critical zones).

The discussion of the previous paragraph leads to the need to characterize traffic in a unified manner, so that traffic can be treated as a single factor rather than a large and complex set of inputs. This can be done through a standardized vehicle type.

Table 4-1 Traffic raw inputs

Input	Description	Relevance to SA
Initial 2-way AADTT	Designer-determined from traffic data	Critical to the amount of damage. Relevant and pertinent to sensitivity analysis
Number of lanes in design direction	Designer-determined from geometric design	N/A
Number of trucks in design direction	Designer-determined from traffic data	May be set equal to AADTT
Number of trucks in design lane	Designer-determined from traffic data	May be set equal to AADTT
Operational speed	Designer-determined from geometric design	N/A
Monthly adjustment factors	Designer-determined from traffic data	For the present research it is set at default values
Vehicle class distribution	Designer-determined from traffic data	May be simplified to a unique test vehicle class
Hourly distribution	Designer-determined from traffic data	For the present research it is set at default values
Growth function	Designer-determined from traffic data	N/A
Axle load distribution	Designer-determined from traffic data	For the present research it is set at default values
Number of axles per vehicle class	Designer-determined from traffic data	For the present research it is set at default values
Mean wheel location	Designer-determined from traffic data and geometric design	For the present research it is set at default values
Traffic wander standard deviation	Designer-determined from traffic data and geometric design	For the present research it is set at default values
Design lane width	Designer-determined from geometric design	For the present research it is set at default values
Average axle width	Designer-determined from traffic data	For the present research it is set at default values
Dual tire spacing	Designer-determined from traffic data	For the present research it is set at default values
Tire pressure	Designer-determined from traffic data	For the present research it is set at default values
Axle spacing	Spacing between adjacent axles within tandem, tridem, quad unit	For the present research it is set at default values
Average axle spacing	Spacing between adjacent axle units (e.g. between single and tandem, single and tridem, tandem and tridem, etc.)	Critical interaction with joint spacing. Relevant and pertinent to sensitivity analysis

Table 4-1 (continued)

Percent trucks per axle spacing	Refers to the proportion of trucks for each average axle spacing	Critical interaction with joint spacing. Relevant and pertinent to sensitivity analysis

Information on raw traffic inputs and their pertinence to the sensitivity analysis are contained in Table 4-1. It has been previously said that an effort in simplifying traffic characterization needs to be made for the sake of clarity, reproducibility and comparability. Most inputs have been labeled as non-applicable in terms of pertinence to the sensitivity analysis. An effort has been made to isolate the traffic inputs that would characterize traffic impact in terms of critical maximum and minimum.

The best way to simplify traffic characterization is to establish a unique test vehicle classification. A Class 9 vehicle may be chosen as it contributes a large proportion of traffic volume on a nation-wide basis. Part 1 of Figure 4.1 shows a scheme of the critical loading conditions that produce critical tensile stresses in the concrete slab when interacting with temperature and moisture gradients. Situation 1a is critical for bottom-up (BU) cracking in interaction with positive temperature and moisture gradients and 1b is critical for top-down (TD) cracking when in interaction with negative gradients.

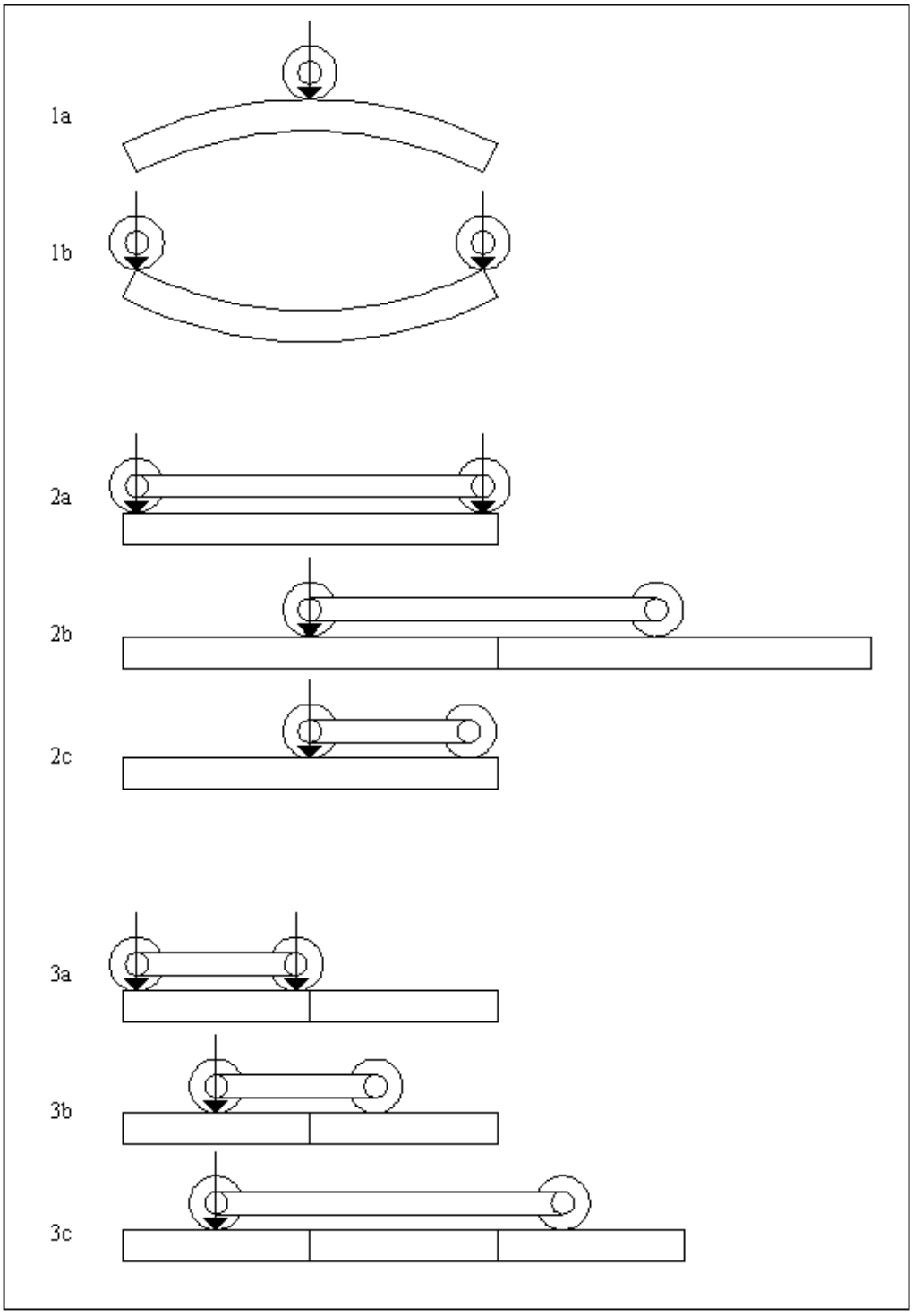

Figure 4.1 Critical loading conditions

There is an important interaction between joint spacing and average axle spacing. The second and third sets of critical loading conditions in Figure 4.1 illustrate the fact that an average axle spacing similar to the joint spacing can actually exert the two possible critical loading conditions on the slab (BU, TD). Axles with a spacing different than that of the joint spacing can only exert BU cracking. This feature is important since joint spacing may be modified within the sensitive analysis. If only one average axle spacing is employed, then the model response in terms of damage would be misleadingly higher for the joint spacing closest to the axle spacing. This confounding effect would make it difficult to isolate the effect of joint spacing in the sensitivity analysis.

The test vehicle class should be a Class 9 vehicle with two different axle spacing in equal proportions (50% each) and in accordance to the joint spacing being analyzed. The axle load spectra of vehicle class 9 can be set at default values. The number of trucks in the design lane may be assumed to correspond to 100% of the AADTT (Annual Average Daily Truck Traffic). As a consequence, the manipulation of traffic can be made entirely by modification of the AADTT. This approach is sound in the sense that varying AADTT is consistent with the incremental nature of damage in the performance models. There are two main reasons to model traffic through a Class 9 vehicle. The first reason is that wheelbase modifications can only be made to vehicle Classes 8 through 13, which includes Class 9. The second reason is that Class 9 vehicles, according to the default vehicle distribution of the MEPDG, correspond to more than 1/3 of the total traffic on a nation-wide basis.

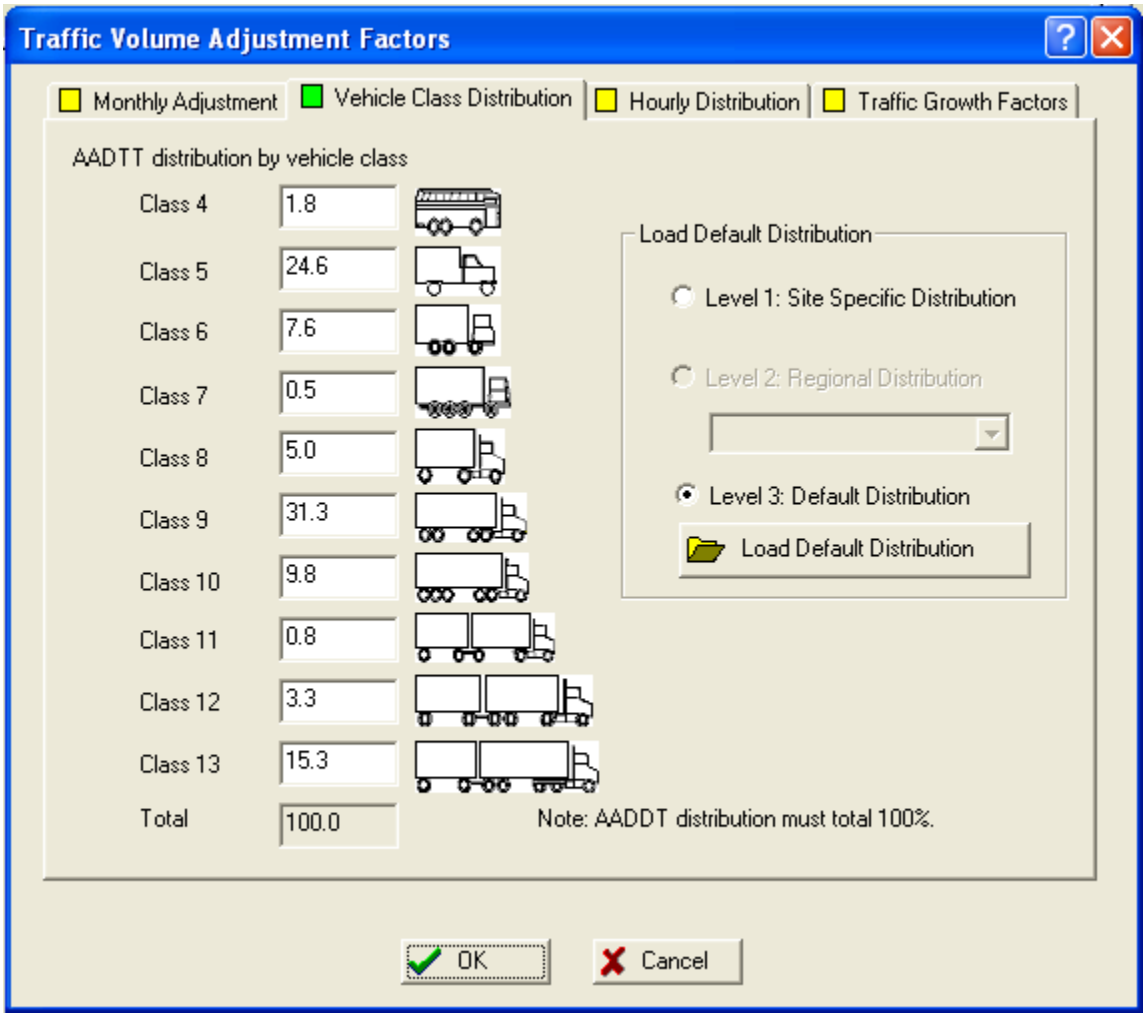

Figure 4.2 MEPDG 1.0 interface showing vehicle class input (from MEPDG 1.0)

4.1.2 Environmental input characterization

According to the flow of Figure 1.1, environmental inputs can be divided into raw inputs and processed inputs. The computational model in charge of transforming raw inputs into processed inputs is the Enhanced Integrated Climate Model (EICM), which is embedded in the MEPDG software. The EICM is a one-dimensional model that predicts the temperatures and moisture

conditions in the pavement structure based on input data from weather stations and material properties of each layer. The EICM predicts the dynamic modulus of all asphalt layers as a function of the mixture design, the predicted temperature, and the resilient modulus of all granular layers as a function of the material properties and the moisture content. The temperature of the granular layers is also considered but only when temperatures drop below freezing. In the process of calibration of the MEPDG, a total of 800 weather stations were used across the United States. For specific sites, virtual weather stations can be generated based on interpolations between up to the six weather stations closest to the construction site.

The inputs supplied by weather stations to be used within the EICM are:

- Hourly air temperature
- Hourly precipitation
- Hourly wind speed
- Hourly percentage sunshine
- Hourly relative humidity

The EICM processed inputs are:

- Hourly temperature profiles defined at eleven points across the depth of the PCC slab
- Hourly temperature and moisture profiles through other pavement layers, including frost depth
- Monthly predictions of modulus of resilience for layers of stabilized and unstabilized layers below the pavement surface
- Annual freezing index values
- Mean annual number of wet days

- Number of freeze-thaw cycles
- Monthly relative humidity values in the PCC

The previous mentioned raw and processed inputs are of significant importance in the performance of pavements. Most of these inputs are imposed by nature in the form of a particular climate. Relatively little can be done by the designer in terms of modification to the processed inputs. However, those processed inputs can vary substantially if different materials are used.

Even though in the context of the MEPDG some inputs are regarded as environmental inputs, these can also be classified under material inputs. Therefore, the only true environmental input is climate. In this sense, climate becomes a single input factor on its own. Climate can be modified (i.e. by choosing a specific location within the United States) and the resulting performance of pavements is expected to be highly dependent on such modifications.

4.1.3 Material input characterization

Materials forming the pavement structure need to be defined to characterize the structural behaviour and the heat and moisture flow through the pavement structure using the EICM.

4.1.3.1 Material inputs for unbound layers

Material properties of unbound layers are based on mass and volume parameters that ultimately define the mechanical behaviour (modulus of resilience) as a result of changes in moisture and temperature (e.g. frozen layers have higher modulus) throughout the life of a pavement. The Fredlund and Xing soil-water curves that relate degree of saturation and suction are also functions of those mass and volume parameters (10). There are three basic inputs that form the

basis for mass and volume parameter estimation. The three basic input variables are the maximum dry density ($\gamma_{d\ max}$), the specific gravity (G_s) and the optimum gravimetric water content (w_{opt}). Further processed inputs, which are internally computed by the EICM, include the initial degree of saturation (S_{opt}), optimum volumetric water content (θ_{opt}), and saturated volumetric water content (θ_{sat}).

The determination of the basic parameters $\gamma_{d\ max}$, G_s, and w_{opt} can be performed on a level 2 basis through correlations, in which case these basic parameters can also be seen as processed inputs, since their magnitudes are dependent on the magnitudes of other available inputs. The level 2 inputs are based on the availability of two of the basic soil characterization laboratory procedures, namely the sieve analysis for particle size distribution, and the Atterberg Limits for plasticity characterization. The basic index-type inputs needed to characterize particle size and plasticity, used in turn to estimate values of $\gamma_{d\ max}$, G_s, and w_{opt} and the Fredlund and Xing parameters are:

- P_{200}: percentage of material by weight passing the #200 sieve
- D_{60}: the particle size of which 60% of the material, by weight, is smaller.
- PI: plasticity index, from the Atterberg Limits tests.

From a sensitivity analysis point of view, the fact that the complete behaviour of granular layers can be defined based on only three inputs is very convenient.

Other important variables of the unbound layers are:

- Thickness of the layer
- Poisson's ratio (assumed constant for different materials)
- Coefficient of lateral pressure (assumed constant for different materials)
- Modulus of resilience (also a function of P_{200}, PI)

4.1.3.2 Material properties of Portland Cement Concrete (PCC)

PCC material characterization is critical in the sense that the pavement distress associated with cracking used in defining performance occurs in this material. PCC material properties influence the response of the pavement to both traffic and environmental loads. Many concrete properties must be defined to characterize these responses. Some of them play an exclusive role on specific correlations, in the same way as was described for the unbound material properties. For example, drying shrinkage and PCC zero stress temperature are estimated through correlations based on:

- Cement type
- Cementitious material content
- Water to cementitious materials ratio
- Aggregate type

Drying shrinkage and PCC zero stress temperature however, can also be directly input by the designer. Even though a more local analysis could be carried out to try to assess the degree of sensitivity of the above listed inputs, it is important to make as many simplifications as possible to improve the efficiency of the sensitivity analysis. Furthermore, these sub-inputs do not affect any other properties within the performance models of the MEPDG. Therefore, it is more convenient to directly experiment with the magnitudes of drying shrinkage and PCC zero stress temperature, rather than with their correlating sub-inputs.

Other variables of the PCC material characterization are:

- Thickness of the slab
- Modulus of elasticity

- Modulus of rupture
- Coefficient of thermal expansion
- Thermal conductivity
- Specific heat
- Unit weight of concrete
- Poisson's ratio
- Reversible shrinkage
- Time to develop 50% of ultimate shrinkage
- Curing method

4.1.3.3 Material inputs for asphalt-stabilized layers

The performance of asphalt stabilized layers depends on the following inputs:

- Thickness of the layer
- Gradation
- Asphalt binder
- Reference temperature
- Effective binder content
- Air voids
- Unit weight
- Poisson's ratio
- Thermal conductivity
- Specific heat

In accordance with the general presentation of inputs of the MEPDG, it can be seen from Table 4-5 that the sensitivity analysis of the present research includes most relevant inputs.

4.2 CORRELATIONS AND INTERACTIONS OF VARIABLES

The quality of the design of experiment relies heavily on the concepts of correlations and interactions. Correlations between variables refer to the interdependency between them, whereas interactions can occur between independent variables and play a role on the variability of the response. A description of these concepts is presented in the following subsections, together with specific considerations that need to be made on the variables under study. In the specific case of correlations, a conceptual matrix can be produced to define all possible variable correlations in an exhaustive way.

4.2.1 Correlations among PCC input

There are many correlations between concrete material properties. Modulus of elasticity, compressive strength and modulus of rupture fall into this group. In the design of the experiment, it is important to keep consistency among these correlations. If one of these variables is studied, changing its value necessarily requires the consistent change in the values of its correlated variables. Failing to account for correlations between variables may lead to unrealistic results.

Other correlated variables include variables related to the thermal behavior of PCC. It is known that the thermal behavior of PCC is primarily controlled by the aggregate, which constitutes the larger volume proportion among PCC components. Thermal properties of concrete include the coefficient of thermal expansion, specific heat and thermal conductivity. Specific magnitudes of these properties are related to a specific type of aggregate. Therefore, changing one of these magnitudes means changing the type of aggregate. If the type of aggregate

is changed, then the other properties also change. For this reason, modifying the value of one of these properties requires the modification of the values of the other two. In this sense, these variables can also be said to be correlated. Furthermore, the PCC coefficient of thermal expansion is a function of the volumetric components of PCC and the coefficients of thermal expansion of these individual components.

The MEPDG literature also correlates ultimate shrinkage strain with cement type, curing characteristics, water content in the mix by weight and the 28-day compressive strength. If one of these factors is to be considered in the analysis, then ultimate shrinkage strain needs to be modified accordingly.

4.2.1.1 PCC strength parameters

One of the characteristics of PCC material properties are the correlations existing between modulus of elasticity, compressive strength, and modulus of rupture. This feature is very useful in the context of the MEPDG, as it allows the designer to perform a limited number of tests and avoid performing others, the results of which may be estimated based upon the available information. If the requirements of a project regarding PCC properties allow for approximations, compressive strength tests can be performed, upon which the modulus of elasticity and modulus of rupture can be estimated. The MEPDG (10) suggests the use of equations 6 and 7 (English units) to estimate PCC material properties.

$$E_c = 33\rho^{3/2} f'_c{}^{1/2} \qquad (6)$$

E_c = PCC static modulus of elasticity

ρ = PCC unit weight

f'_c = PCC compressive strength

$$MR = 9.5 f'^{1/2}_c \quad (7)$$

MR = Modulus of rupture

4.2.1.2 PCC mix proportions and coefficient of thermal expansion

In general, the estimation of the PCC coefficient of thermal expansion involves the volumetric proportions of the PCC mix, which are considered through the following equation (10):

$$\alpha_{PCC} = \alpha_{AGG} V_{AGG} + \alpha_{PASTE} V_{PASTE} \quad (8)$$

The MEPDG literature suggests a cement paste coefficient of thermal expansion within the range between $10x10^{-6}$/°F and $11x10^{-6}$/°F corresponding to a range of w/c of 0.4 to 0.6. A value of $10.5x10^{-6}$/°F may be chosen for the paste. Therefore, if the sensitivity analysis attempts to study the impact of the variation in mix proportions, the coefficient of thermal expansion is to be affected.

4.2.1.3 PCC thermal properties

Table 4-2 shows three PCC thermal properties for different types of aggregates. If one of the three properties needs to be modified, the other two should be modified accordingly.

Table 4-2 Typical thermal properties of concrete, adapted (13)

Aggregate type	PCC Coefficient of thermal expansion [microstrain per ºC]	PCC Thermal conductivity [Btu / h ft ºF]	PCC Specific heat [Btu / lb ºF]
Quartzite	12	2.00	0.23
Limestone	6	1.71	0.23
Granite	8	1.54	0.24
Basalt	7	1.17	0.24

4.2.1.4 Other correlated inputs

Equation 9 shows a correlation of the list of variables used in the estimation of ultimate shrinkage strain of PCC.

$$\varepsilon_{su} = C_1 \cdot C_2 \cdot \left[26w^{2.1}\left(f'_c\right)^{-0.28} + 270\right] \qquad (9)$$

Where:

ε_{su} = Ultimate shrinkage strain $\left(x10^{-6}\right)$

C_1 = Cement type factor

1.0 for type I cement

0.85 for type II cement

1.1 for type III cement

C_2 = Type of curing factor

0.75 if steam cured

1.0 if cured in water or 100% relative humidity

1.2 if sealed during curing (curing compound)

w = Water content of the mix under consideration, in lb/ft^3

f'_c = 28-day PCC compressive strength, in psi

For the sake of consistency in the sensitivity analysis, modifying one of the inputs in equation 9 requires modifying the ultimate shrinkage strain. Furthermore, if a modification is made on strength inputs of PCC (i.e. implying a modification of f'c), the effect on ultimate shrinkage strain must be accounted for.

4.2.2 Correlations between inputs of the unbound layers

Under level 2 (based on estimations or correlations), the MEPDG considers several estimation models of the mechanical, thermodynamic and hydraulic behavior of unbound layers. These models are almost exhaustively based on two parameters, the percentage of material that passes sieve # 200, P_{200}, and the plasticity index of the material, PI.

4.2.2.1 Resilient Modulus, particle size distribution and Atterberg limits

P_{200} and PI ultimately determine the resilient modulus of the unbound material, the most important factor in the mechanical behavior of the unbound layers. The indirect correlation is through correlations between P_{200}, PI and CBR first, and then through correlations between CBR and MR. On the other hand, P_{200} and PI also affect the hydraulic and thermodynamic behavior of unbound layers, as these are important inputs of the EICM. Therefore, directly modifying the magnitude of the resilient modulus requires adjusting these parameters, and vice versa.

$$CBR = \frac{75}{1 + 0.728(wPI)} \qquad (10)$$

Where:

$$wPI = P_{200} \cdot PI$$

P_{200} = Percent passing #200 sieve size

PI = Plasticity index, %

$$M_R = 2555(CBR)^{0.64} \qquad (11)$$

M_R = Modulus of resilience, psi

Equations 10 and 11 show two independent models considered in the MEPDG literature. Upon these two, a third estimation can be worked out, that relates MR, P_{200} and PI. The result is equation 12.

$$MR = 2555\left[\frac{75}{1+0.728(P_{200}PI)}\right]^{0.64} \qquad (12)$$

4.2.2.2 Coefficient of lateral expansion and Poisson's ratio

The coefficient of lateral pressure and the Poisson's ratio are correlated through the following expression:

$$k_0 = \frac{\mu}{1-\mu} \qquad (13)$$

k_0 = Coefficient of lateral expansion

μ = Poisson's ratio

Table 4-3 summarizes the correlations between inputs that need to be accounted for in a sensitivity analysis. There is a large number of additional correlations that are contained in the MEPDG internally (e.g. the dependence of the Fredlund and Xing model on P_{200} and PI). However, most internal correlations are considered in the algorithms inside the MEPDG and do not depend on any inputs that the user can control.

On the other hand, the inputs contained in Table 4-3 are directly controlled by the user, so that if one variable is modified, all correlated variables must be modified manually by the user.

Table 4-3 MEPDG input correlations

	E_{PCC}	MR_{PCC}*	$f'c_{PCC}$	α_{PCC}	K	C	MR_{unb}*	P_{200}	PI	k_0	μ	ε_{su}
E_{PCC}		● Eq. 5, 6	● Eq. 5									● Eq. 8, 5
MR_{PCC}*	● Eq. 5, 6		● Eq. 6									● Eq. 8, 6
$f'c_{PCC}$	● Eq. 5	● Eq. 6										● Eq. 8
α_{PCC}					● T 4.2	● T 4.2						
K				● T 4.2		● T 4.2						
C				● T 4.2	● T 4.2							
MR_{unb}*								● Eq. 11	● Eq. 11			
P_{200}							● Eq. 11					
PI							● Eq. 11					
k_0											● Eq. 12	
μ										● Eq. 12		
ε_{su}	● Eq. 8, 5	● Eq. 8, 6	● Eq. 8									

*In PCC, MR refers to modulus of rupture. In unbound materials, MR refers to modulus of resilience

4.2.3 Interactions

Interactions may occur between independent variables. In the context of the MEPDG there are interactions that can influence the response of the system. Interactions often lead to confounding. In experimental design, the influence or effect of a single factor on the response of the system is often required. This is called the main effect of the factor. If the main effect of the factor is to be analyzed, it is important to keep all other factors constant at their mean values throughout the experiment, so that the variation in the response can be explained solely by the variation in that particular factor. However, it is common among experiments, that beside the factor under analysis, one or more factors cannot be kept constant throughout the different runs, due to their nature. If interactions exist between the factor under analysis and one or more factors that are not kept constant throughout the various runs, then the variability in the response cannot be explained solely by the variation in the factor under analysis. In other words, the main effect of the factor under analysis cannot be isolated. In such a case, factors are said to be confounded.

In the context of the MEPDG, there are interactions between some variables. In the analysis of such variables, care must be taken in the interpretation of the results. Vandenbossche et al (15) propose an example involving the effects of traffic volume, climate and foundation support on slab cracking. These three variables are independent of each other; the variation of one of them holding the other two constant can increase or decrease the rate of slab cracking (e.g. increasing traffic leads to higher cracking). However, the structural response of the slabs to traffic also depends on the foundation conditions and the support conditions of the slabs due to temperature and moisture gradients and support conditions. The response to the same amount of traffic distribution and traffic loads may be dramatically different in a cold winter day (frozen foundation, i.e. high modulus of resilience in the foundation) at a time when the slabs are flat

(zero-gradient, i.e. good support conditions) than it would be on a spring day with a very deformed slab due to peak temperature gradients (e.g. at the time of positive peak) and poor foundation conditions (low modulus of resilience). Even though in nature the three variables are independent, their interaction can be influential on the response of the system.

4.2.3.1 Sorting main effects and interactions

In the present research, it is desirable to assess the main effect of each variable and the interaction effects with other variables when exploring the sensitivity of the system to its inputs. As stated in the objectives of this research, it is desirable to show that first order regressions are not adequate to describe the model. This task can be performed through 2^k factorial experiments. In a 2^k factorial experiment, it is assumed that each of the k factors occurs at two levels, a high level and a low level (Hogg, Ledolter, 5). A table can be constructed with all the possible (factorial) combinations of high and low values of each variable. Then, the main effects and interaction effects can be quantified. This is very useful as it yields information regarding which interactions are stronger.

The procedure to assess main effects and interactions is based on specific definitions that are presented below for the case of the 2^3 experiment. It will be illustrated that the same process can be carried out for any k.

A 2^3 experiment consists of running combinations involving three inputs at their maximum and minimum values. The resulting number of runs is $2^3 = 8$ and the correct organization of the table for this experiment is shown below.

Table 4-4 The 2^3 factorial experiment (5)

	Inputs			Interactions				Output
Run	x_1	x_2	x_3	x_1x_2	x_1x_3	x_2x_3	$x_1x_2x_3$	
1	-	-	-	+	+	+	-	Y_1
2	+	-	-	-	-	+	+	Y_2
3	-	+	-	-	+	-	+	Y_3
4	+	+	-	+	-	-	-	Y_4
5	-	-	+	+	-	-	+	Y_5
6	+	-	+	-	+	-	-	Y_6
7	-	+	+	-	-	+	-	Y_7
8	+	+	+	+	+	+	+	Y_8

The patterns that need to be kept for consistency in the application of this method are shown in Table 4-4. -1 stands for the low coded input, whereas +1 stands for the high coded input under analysis.

A coded input X_{CODED} can be defined as (11):

$$X_{CODED} = \frac{X - (X_{LOW} + X_{HIGH})/2}{(X_{HIGH} - X_{LOW})/2} \qquad (14)$$

If $X = X_{LOW}$, $X_{CODED} = -1$; if $X = X_{HIGH}$, $X_{CODED} = +1$.

The pattern for the first input is the alternation of low and high values beginning with the low value. In other words, it is a 1 x low, 1 x high pattern. The second input is organized in a 2 x low, 2 x high pattern. The third input is organized in a 4 x low, 4 x high pattern. An easy way to

illustrate this is to associate it with 2^0, 2^1, 2^2 repetitions of the low value followed by the same number of repetitions of the high value, repeating the same pattern down to the last run.

i Definition of the main effect of an input

Hogg and Ledolter (5) define the main effect of an input to be one half of the difference between the averages of the responses at the high and low levels of the input. Following this definition and recalling Table 4-4, the following are the mathematical expressions of the main effect of each input:

$$Main(x_1) = \frac{1}{2}\left(\frac{Y_2 + Y_4 + Y_6 + Y_8}{4} - \frac{Y_1 + Y_3 + Y_5 + Y_7}{4}\right) = \frac{-Y_1 + Y_2 - Y_3 + Y_4 - Y_5 + Y_6 - Y_7 + Y_8}{8} \quad (15)$$

At this point, it is important to note that the resulting expression for the main effect of x_1 involves all outputs of the experiment organized from Y_1 to Y_8, the denominator is 2^3 and the sign pattern is exactly that of the x_1 column. Likewise, the main effects of inputs x_2 and x_3 are shown below.

$$Main(x_2) = \frac{1}{2}\left(\frac{Y_3 + Y_4 + Y_7 + Y_8}{4} - \frac{Y_1 + Y_2 + Y_5 + Y_6}{4}\right) = \frac{-Y_1 - Y_2 + Y_3 + Y_4 - Y_5 - Y_6 + Y_7 + Y_8}{8} \quad (16)$$

$$Main(x_3) = \frac{1}{2}\left(\frac{Y_5 + Y_6 + Y_7 + Y_8}{4} - \frac{Y_1 + Y_2 + Y_3 + Y_4}{4}\right) = \frac{-Y_1 - Y_2 - Y_3 - Y_4 + Y_5 + Y_6 + Y_7 + Y_8}{8} \quad (17)$$

The final expression of the main effect of x_2 contains the same sign (level) pattern as the column of x_2. The same is true for x_3.

ii Definition of interactions between 2 inputs

The interaction between inputs i and j, where i ≠ j is one half of the difference between the main effect of factor i at the high level of factor j and that at the low level of factor j.

$$Inter(x_1, x_2) = \frac{1}{2}\left[\frac{1}{2}\left(\frac{Y_4 + Y_8}{2} - \frac{Y_3 + Y_7}{2}\right) - \frac{1}{2}\left(\frac{Y_2 + Y_6}{2} - \frac{Y_1 + Y_5}{2}\right)\right]$$
$$= \frac{Y_1 - Y_2 - Y_3 + Y_4 + Y_5 - Y_6 - Y_7 + Y_8}{8} \quad (18)$$

$$Inter(x_1, x_3) = \frac{1}{2}\left[\frac{1}{2}\left(\frac{Y_6 + Y_8}{2} - \frac{Y_5 + Y_7}{2}\right) - \frac{1}{2}\left(\frac{Y_2 + Y_4}{2} - \frac{Y_1 + Y_3}{2}\right)\right]$$
$$= \frac{Y_1 - Y_2 + Y_3 - Y_4 - Y_5 + Y_6 - Y_7 + Y_8}{8} \quad (19)$$

$$Inter(x_2, x_3) = \frac{1}{2}\left[\frac{1}{2}\left(\frac{Y_7 + Y_8}{2} - \frac{Y_5 + Y_6}{2}\right) - \frac{1}{2}\left(\frac{Y_3 + Y_4}{2} - \frac{Y_1 + Y_2}{2}\right)\right]$$
$$= \frac{Y_1 + Y_2 - Y_3 - Y_4 - Y_5 - Y_6 + Y_7 + Y_8}{8} \quad (20)$$

iii Definition of interactions between 3 inputs

The interaction between three inputs x_1, x_2 and x_3 is equal to one half of the difference between the interaction (x_1, x_2) at the high and low levels of x_3.

$$Inter(x_1, x_2, x_3) = \frac{1}{2}\left[\frac{1}{2}\left(\frac{Y_8 - Y_7}{2} - \frac{Y_6 - Y_5}{2}\right) - \frac{1}{2}\left(\frac{Y_4 - Y_3}{2} - \frac{Y_2 - Y_1}{2}\right)\right]$$
$$= \frac{-Y_1 + Y_2 + Y_3 - Y_4 + Y_5 - Y_6 - Y_7 + Y_8}{8} \quad (21)$$

This interaction is equal to one half of the difference between the interaction (x_1, x_3) at the high and low levels of x_2 or one half of the difference between the interaction (x_2, x_3) at the high and low levels of x_1.

4.2.3.2 Interpreting the physical meaning of the numerical assessment

In consistency with the definitions of the main effects and interaction effects, the interpretation of the numerical result can be made after multiplying the result by 2. For the case of x_1, Main(x_1) is the increase (or decrease depending on the sign) in the output due to raising x_1 from x_1^- to x_1^+. Likewise, Inter(x_1, x_2) is the increase difference (or decrease depending on the sign) in the output due to raising x_1 from x_1^- to x_1^+at x_2^+ and x_2^-. It is equivalent to say that Inter(x_1, x_2) is the difference:

$$Inter(x_1, x_2) = Main(x_1)\Big|_{x_2^+} - Main(x_1)\Big|_{x_2^-} \qquad (22)$$

The above equation may be read as follows: If the main effect of $x_1$is the same at x_2^+ and x_2^-, the interaction between x_1 and x_2 is zero.

4.3 FIRST SCREENING 2^K EXPERIMENT

Two general experiments involving six variables were designed, in which only two levels (max. and min. values) were taken by each input, totaling $2^6 = 64$ runs (see Table 4-5) each. As a general estimation tool, 2^k type experiments yield input main effects and interactions between inputs, under the assumption that the regression is of first order.

Table 4-5 contains the first 2^k experiment carried out. Six inputs were chosen, which were expected to be influential in the cracking model. The ranges used are within reasonable universal ranges. The main objective of this research regarding sensitivity analysis is to show that linear regression based sensitivity analysis can lead to large errors. 2^k analyses constitute a very versatile tool to check whether linear assumptions are realistic.

Table 4-5 2^k screening experiment input ranges

Input Number	Input	Units	Low value	Mean Value	High Value		Extremes ("Universal" range)	
1	Joint Spacing	ft	16	17	18		10	24
2	Slab Thickness	in	10.5	11	11.5		6.5	15
3	PCC Modulus of Rupture	psi	618	650	678		450	850
4	Set Temperature	°F	100	105	110		70	140
5	PCC Coefficient of Thermal Expansion	in/in/°F (x10-6)	5.7	6.0	6.3		4.1	7.3
6	Traffic	AADTT (Annual Average Daily Truck Traffic)	3613	3800	3966			

The actual runs that were performed for the first 2^k experiment are contained in Table 4-6. The output obtained by the MEPDG and the estimation made by a first degree regression based on the coefficients shown in Table 4-8, are presented in Table 4-7. As can be appreciated in Table 4-7, the residuals for the regression of Table 4-8 turn out to be zero. This simply means that a first degree model could be perfectly fitted through the (min, max) values chosen for the six inputs. This result was expected because the minimum and maximum values are actually very

close to each other. However, this result does not particularly lead to any conclusion about how well the model would describe the output for varying inputs. In order to do a quick check, it was observed that the interaction between the joint spacing and the slab thickness turned out to be large (Table 4-8, row 3) Based on this fact, it was thought that a quick check of the model could be done by varying these two inputs simultaneously, in opposite directions (one from high to low and the other one from low to high), and within the 2^k extremes used for fitting the model. As an additional and easy check, all other inputs were kept at their mean values within their ranges (coded variables equal to zero). The result of this check can be observed in Figure 4.3, the data being contained in Table 4-9.

The result illustrated in Figure 4.3 immediately suggests that care should be exercised while fitting complex models through first order functions. Even though the trend of the regression follows to some extent the actual model response, it is evident that the interaction coefficients, though responsible for the slight curvature of the regression, are not capable of describing the real phenomenon to a more satisfactory extent. Furthermore, it is disturbing that this discrepancy was found fully within the regression ranges, for which a linear assumption would be deemed reasonable, especially since the values chosen were very close to each other. The MEPDG cracking model appears to be so non-linear that even small interval linear analysis fails to represent the actual data in a satisfactory way. This suggests that linear modeling should only be practiced as first-phase or reconnaissance approaches, but not to draw final conclusions.

Even though accurate numerical sensitivity assessments should not be understood as conclusive, one positive aspect of 2^k approaches is that it yields very useful information as to the general influence of variables and interactions between variables. In the specific case of this first experiment, it turned out that set temperature was not influential. It also provides information regarding interactions between inputs. The strong interaction between joint spacing and slab thickness, which was expected, was third in the general ranking.

Table 4-6 2^k First experiment design

	Inputs							
	x1	x2	x3			x4	x5	x6
Run	Joint Spacing [ft]	Slab Thickness [in]	PCC MR*	w/c	cem [lb/yd3]	Set Temperature [F]	CTE [F^{-1}]	AADTT
1	16	10.5	618	0.56	577	100	5.70E-06	3613
2	18	10.5	618	0.56	577	100	5.70E-06	3613
3	16	11.5	618	0.56	577	100	5.70E-06	3613
4	18	11.5	618	0.56	577	100	5.70E-06	3613
5	16	10.5	678	0.47	683	100	5.70E-06	3613
6	18	10.5	678	0.47	683	100	5.70E-06	3613
7	16	11.5	678	0.47	683	100	5.70E-06	3613
8	18	11.5	678	0.47	683	100	5.70E-06	3613
9	16	10.5	618	0.56	577	110	5.70E-06	3613
10	18	10.5	618	0.56	577	110	5.70E-06	3613
11	16	11.5	618	0.56	577	110	5.70E-06	3613
12	18	11.5	618	0.56	577	110	5.70E-06	3613
13	16	10.5	678	0.47	683	110	5.70E-06	3613
14	18	10.5	678	0.47	683	110	5.70E-06	3613
15	16	11.5	678	0.47	683	110	5.70E-06	3613
16	18	11.5	678	0.47	683	110	5.70E-06	3613
17	16	10.5	618	0.56	577	100	6.30E-06	3613
18	18	10.5	618	0.56	577	100	6.30E-06	3613
19	16	11.5	618	0.56	577	100	6.30E-06	3613
20	18	11.5	618	0.56	577	100	6.30E-06	3613
21	16	10.5	678	0.47	683	100	6.30E-06	3613
22	18	10.5	678	0.47	683	100	6.30E-06	3613
23	16	11.5	678	0.47	683	100	6.30E-06	3613
24	18	11.5	678	0.47	683	100	6.30E-06	3613
25	16	10.5	618	0.56	577	110	6.30E-06	3613
26	18	10.5	618	0.56	577	110	6.30E-06	3613
27	16	11.5	618	0.56	577	110	6.30E-06	3613
28	18	11.5	618	0.56	577	110	6.30E-06	3613
29	16	10.5	678	0.47	683	110	6.30E-06	3613
30	18	10.5	678	0.47	683	110	6.30E-06	3613
31	16	11.5	678	0.47	683	110	6.30E-06	3613
32	18	11.5	678	0.47	683	110	6.30E-06	3613
33	16	10.5	618	0.56	577	100	5.70E-06	3966

Table 4-6 (continued)

34	18	10.5	618	0.56	577	100	5.70E-06	3966
35	16	11.5	618	0.56	577	100	5.70E-06	3966
36	18	11.5	618	0.56	577	100	5.70E-06	3966
37	16	10.5	678	0.47	683	100	5.70E-06	3966
38	18	10.5	678	0.47	683	100	5.70E-06	3966
39	16	11.5	678	0.47	683	100	5.70E-06	3966
40	18	11.5	678	0.47	683	100	5.70E-06	3966
41	16	10.5	618	0.56	577	110	5.70E-06	3966
42	18	10.5	618	0.56	577	110	5.70E-06	3966
43	16	11.5	618	0.56	577	110	5.70E-06	3966
44	18	11.5	618	0.56	577	110	5.70E-06	3966
45	16	10.5	678	0.47	683	110	5.70E-06	3966
46	18	10.5	678	0.47	683	110	5.70E-06	3966
47	16	11.5	678	0.47	683	110	5.70E-06	3966
48	18	11.5	678	0.47	683	110	5.70E-06	3966
49	16	10.5	618	0.56	577	100	6.30E-06	3966
50	18	10.5	618	0.56	577	100	6.30E-06	3966
51	16	11.5	618	0.56	577	100	6.30E-06	3966
52	18	11.5	618	0.56	577	100	6.30E-06	3966
53	16	10.5	678	0.47	683	100	6.30E-06	3966
54	18	10.5	678	0.47	683	100	6.30E-06	3966
55	16	11.5	678	0.47	683	100	6.30E-06	3966
56	18	11.5	678	0.47	683	100	6.30E-06	3966
57	16	10.5	618	0.56	577	110	6.30E-06	3966
58	18	10.5	618	0.56	577	110	6.30E-06	3966
59	16	11.5	618	0.56	577	110	6.30E-06	3966
60	18	11.5	618	0.56	577	110	6.30E-06	3966
61	16	10.5	678	0.47	683	110	6.30E-06	3966
62	18	10.5	678	0.47	683	110	6.30E-06	3966
63	16	11.5	678	0.47	683	110	6.30E-06	3966
64	18	11.5	678	0.47	683	110	6.30E-06	3966

Table 4-7 2^k First experiment output

	Outputs				
Run	FDb-u	FDt-d	Slabs cracked [%]	Regression Model [%]	Residuals
1	0.5077	0.0187	20.8	20.8	0.000
2	2.4305	0.0712	85.4	85.4	0.000
3	0.0724	0.0122	0.6	0.6	0.000
4	0.4761	0.0554	19	19	0.000
5	0.2268	0.0097	5	5	0.000
6	1.2433	0.042	60.7	60.7	0.000
7	0.0283	0.0059	0.1	0.1	0.000
8	0.2108	0.0296	4.5	4.5	0.000
9	0.5077	0.0187	20.8	20.8	0.000
10	2.4305	0.0712	85.4	85.4	0.000
11	0.0724	0.0122	0.6	0.6	0.000
12	0.4761	0.0554	19	19	0.000
13	0.2268	0.0097	5	5	0.000
14	1.2433	0.042	60.7	60.7	0.000
15	0.0283	0.0059	0.1	0.1	0.000
16	0.2108	0.0296	4.5	4.5	0.000
17	0.9242	0.0571	46.3	46.3	0.000
18	4.5356	0.2153	95.5	95.5	0.000
19	0.1335	0.0373	2	2	0.000
20	0.8998	0.1651	46.3	46.3	0.000
21	0.4195	0.0295	15.3	15.3	0.000
22	2.3541	0.124	84.7	84.7	0.000
23	0.0531	0.0185	0.3	0.3	0.000
24	0.407	0.09	15.2	15.2	0.000
25	0.9242	0.0571	46.3	46.3	0.000
26	4.5356	0.2153	95.5	95.5	0.000
27	0.1335	0.0373	2	2	0.000
28	0.8998	0.1651	46.3	46.3	0.000
29	0.4195	0.0295	15.3	15.3	0.000
30	2.3541	0.124	84.7	84.7	0.000
31	0.0531	0.0185	0.3	0.3	0.000
32	0.407	0.09	15.2	15.2	0.000
33	0.5574	0.0205	23.9	23.9	0.000
34	2.668	0.0782	87.5	87.5	0.000
35	0.0794	0.0134	0.7	0.7	0.000
36	0.5226	0.0609	22	22	0.000
37	0.249	0.0107	6	6	0.000
38	1.3648	0.0461	65	65	0.000
39	0.0311	0.0065	0.1	0.1	0.000

Table 4-7 (continued)

40	0.2314	0.0325	5.3	5.3	0.000
41	0.5574	0.0205	23.9	23.9	0.000
42	2.668	0.0782	87.5	87.5	0.000
43	0.0794	0.0134	0.7	0.7	0.000
44	0.5226	0.0609	22	22	0.000
45	0.249	0.0107	6	6	0.000
46	1.3648	0.0461	65	65	0.000
47	0.0311	0.0065	0.1	0.1	0.000
48	0.2314	0.0325	5.3	5.3	0.000
49	1.0145	0.0627	50.9	50.9	0.000
50	4.9788	0.2363	96.2	96.2	0.000
51	0.1466	0.0409	2.4	2.4	0.000
52	0.9877	0.1812	51	51	0.000
53	0.4605	0.0323	17.8	17.8	0.000
54	2.5841	0.1361	87	87	0.000
55	0.0583	0.0203	0.4	0.4	0.000
56	0.4468	0.0988	17.7	17.7	0.000
57	1.0145	0.0627	50.9	50.9	0.000
58	4.9788	0.2363	96.2	96.2	0.000
59	0.1466	0.0409	2.4	2.4	0.000
60	0.9877	0.1812	51	51	0.000
61	0.4605	0.0323	17.8	17.8	0.000
62	2.5841	0.1361	87	87	0.000
63	0.0583	0.0203	0.4	0.4	0.000
64	0.4468	0.0988	17.7	17.7	0.000

Table 4-8 2^k sensitivity analysis ranking

Rank	Main Effect / Interaction	Coefficients	Absolute Value	SIGN (nature)
1	x2	-20.638	20.6375	negative
2	x1	20.325	20.325	positive
3	x1x2	-9.425	9.425	negative
4	x3	-8.294	8.29375	negative
5	x5	6.950	6.95	positive
6	x1x2x3	-3.794	3.79375	negative
7	x1x2x3x5	-2.756	2.75625	negative
8	x1x2x5	2.675	2.675	positive
9	x1x5	2.063	2.0625	positive
10	x2x3	2.019	2.01875	positive
11	x1x3	-1.881	1.88125	negative
12	x2x5	-1.763	1.7625	negative
13	x3x5	-1.219	1.21875	negative
14	x2x3x5	-1.019	1.01875	negative
15	x6	1.006	1.00625	positive
16	x1x3x5	0.844	0.84375	positive
17	x1x2x6	0.381	0.38125	positive
18	x1x2x3x6	-0.375	0.375	negative
19	x1x2x5x6	0.294	0.29375	positive
20	x2x6	-0.281	0.28125	negative
21	x1x6	0.269	0.26875	positive
22	x3x6	-0.163	0.1625	negative
23	x2x3x6	-0.138	0.1375	negative
24	x2x5x6	0.131	0.13125	positive
25	x1x3x6	0.125	0.125	positive
26	x1x5x6	-0.106	0.10625	negative
27	x5x6	0.106	0.10625	positive
28	x3x5x6	-0.025	0.025	negative
29	x1x2x3x5x6	0.025	0.025	positive
30	x1x3x5x6	-0.013	0.0125	negative
31	x2x3x5x6	0.013	0.0125	positive
32	x1x4	0.000	1.27676E-15	negative
33	x2x4	0.000	1.05471E-15	negative
34	x3x4	0.000	1.05471E-15	negative
35	x4x5	0.000	1.05471E-15	negative
36	x4x6	0.000	1.05471E-15	negative
37	x2x4x6	0.000	1.05471E-15	negative
38	x3x4x5x6	0.000	1.05471E-15	negative
39	x4	0.000	7.21645E-16	positive
40	x4x5x6	0.000	7.21645E-16	positive
41	x2x3x4x5	0.000	6.10623E-16	negative
42	x2x3x4x6	0.000	6.10623E-16	negative
43	x1x4x5	0.000	4.996E-16	positive

Table 4-8 (continued)

44	x1x2x4x6	0.000	4.996E-16	positive
45	x1x2x3x4x6	0.000	4.996E-16	positive
46	x1x2x4	0.000	0	
47	x1x3x4	0.000	0	
48	x1x4x6	0.000	0	
49	x2x3x4	0.000	0	
50	x2x4x5	0.000	0	
51	x3x4x5	0.000	0	
52	x3x4x6	0.000	0	
53	x1x2x3x4	0.000	0	
54	x1x3x4x5	0.000	0	
55	x1x3x4x6	0.000	0	
56	x1x4x5x6	0.000	0	
57	x1x2x4x5	0.000	0	
58	x2x4x5x6	0.000	0	
59	x1x2x3x4x5	0.000	0	
60	x1x3x4x5x6	0.000	0	
61	x1x2x4x5x6	0.000	0	
62	x2x3x4x5x6	0.000	0	
63	x1x2x3x4x5x6	0.000	0	

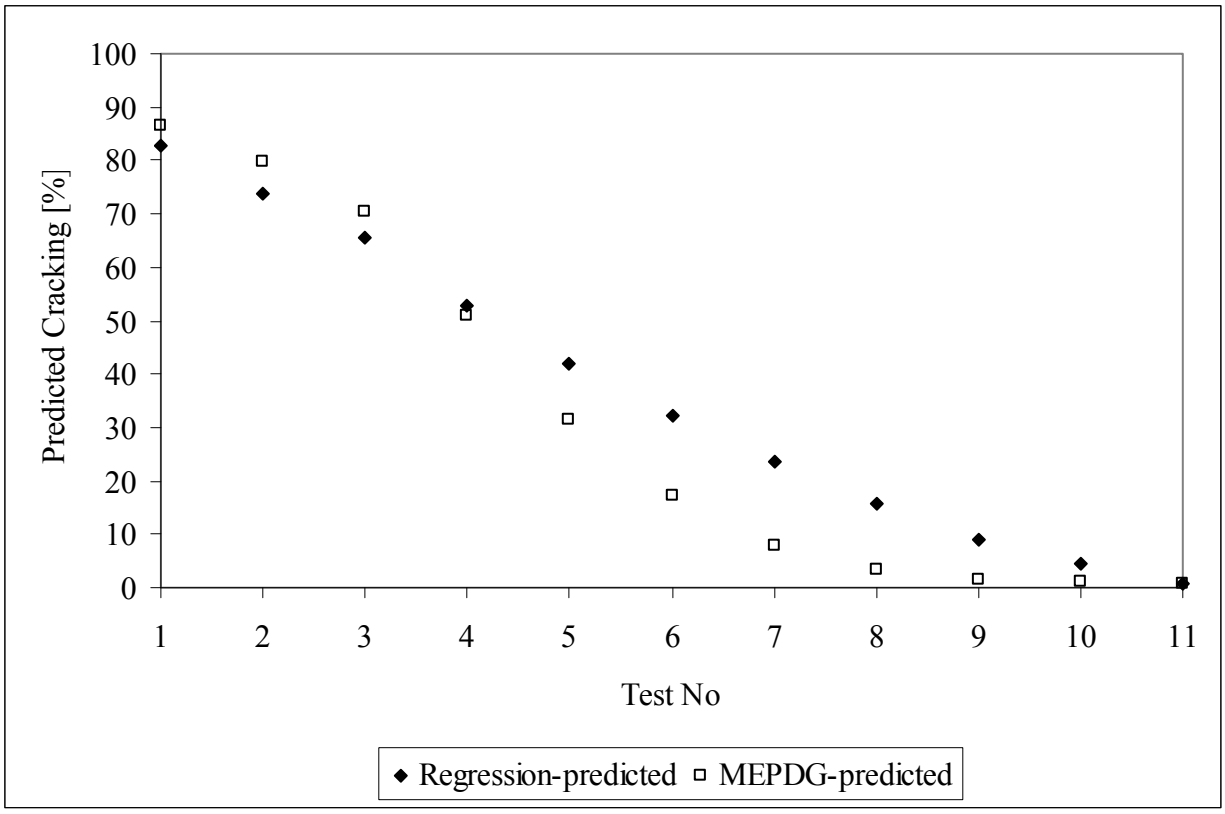

Figure 4.3 Results obtained from check design depicted in Table 4-9

Table 4-9 Design to check regression within (min, max) intervals

Test No.	Input magnitude (Coded input magnitude)					
	x1	x2	x3	x4	x5	x6
1	18	10.5	648	105	6	3789.5
	(1)	(-1)	(0)	(0)	(0)	(0)
2	17.9	10.6	648	105	6	3789.5
	(0.9)	(-0.8)	(0)	(0)	(0)	(0)
3	17.8	10.7	648	105	6	3789.5
	(0.8)	(-0.6)	(0)	(0)	(0)	(0)
4	17.5	10.8	648	105	6	3789.5
	(0.5)	(-0.4)	(0)	(0)	(0)	(0)
5	17.25	10.9	648	105	6	3789.5
	(0.25)	(-0.2)	(0)	(0)	(0)	(0)
6	17	11	648	105	6	3789.5
	(0)	(0)	(0)	(0)	(0)	(0)
7	16.75	11.1	648	105	6	3789.5
	(-0.25)	(0.2)	(0)	(0)	(0)	(0)
8	16.5	11.2	648	105	6	3789.5
	(-0.5)	(0.4)	(0)	(0)	(0)	(0)
9	16.25	11.3	648	105	6	3789.5
	(-0.75)	(0.6)	(0)	(0)	(0)	(0)
10	16.1	11.4	648	105	6	3789.5
	(-0.9)	(0.8)	(0)	(0)	(0)	(0)
11	16	11.5	648	105	6	3789.5
	(-1)	(1)	(0)	(0)	(0)	(0)

4.4 SECOND SCREENING 2^K EXPERIMENT

According to the results analyzed in the previous section, set temperature does not seem to be an influential input if compared to the other inputs, which suggests that it can be dismissed from the six-input approach for the cracking model. Instead of set temperature, the second screening experiment introduces the built-in effective temperature difference, which has been previously treated in the present research and whose influence on the model response is expected to be significant. Regarding the built-in effective temperature difference, it can be recalled (see Figure 3.12) that a singularity occurred at a value of -12, namely that for any given climate, the response of the MEPDG cracking model was at a minimum. In order to test this input, it was desired to have a negative and a positive value. This is why the mean was set at zero. It was estimated that an effective temperature difference in the range of -5 ^{o}F +5 ^{o}F was reasonable. Table 4-10 contains the design of experiment; Table 4-11 contains the actual runs; Table 4-12 presents the sensitivity ranking according to input and interaction coefficients. The built-in effective temperature difference turns out to be extremely influential as was expected. At this point, a very simple series of checks was undertaken in order to explore how well the regression model would describe the actual model outside the intervals used for fitting the first order model. These are illustrated in Figure 4.4 through Figure 4.11 and Table 4-13 through Table 4-20.

Table 4-10 2^k Design of experiment no.2

Input Number	Input	Units	Low value	Medium Value	High Value		Extremes ("Universal" range)	
1	Joint Spacing	ft	15	17	19		10	24
2	Slab Thickness	in	10.0	11	12.0		6.5	15
3	PCC Modulus of Rupture	psi	578	650	722		450	850
4	Built-in gradient	°F/in	-0.50		0.50			
5	PCC Coefficient of Thermal Expansion	in/in/°F ($x10^{-6}$)	5.3	6.0	6.7		4.1	7.3
6	Traffic	AADTT (Annual Average Daily Truck Traffic)	8000	9000	10000			
	Effective Temperature difference [°F]		-5.000		6.000			

Table 4-11 2^k inputs for experiment no.2

	Inputs							
	x1	x2	x3			x4	x5	x6
Run	Joint Spacing [ft]	Slab Thickness [in]	PCC MR	w/c	cem [lb/yd3]	Built-in temperature difference	CTE [F^{-1}]	AADTT
1	15	10	578	0.61	527	-5	5.30E-06	8000
2	19	10	578	0.61	527	-5	5.30E-06	8000
3	15	12	578	0.61	527	-5	5.30E-06	8000
4	19	12	578	0.61	527	-5	5.30E-06	8000
5	15	10	722	0.4	800	-5	5.30E-06	8000
6	19	10	722	0.4	800	-5	5.30E-06	8000
7	15	12	722	0.4	800	-5	5.30E-06	8000
8	19	12	722	0.4	800	-5	5.30E-06	8000
9	15	10	578	0.61	527	6	5.30E-06	8000
10	19	10	578	0.61	527	6	5.30E-06	8000
11	15	12	578	0.61	527	6	5.30E-06	8000
12	19	12	578	0.61	527	6	5.30E-06	8000
13	15	10	722	0.4	800	6	5.30E-06	8000
14	19	10	722	0.4	800	6	5.30E-06	8000
15	15	12	722	0.4	800	6	5.30E-06	8000
16	19	12	722	0.4	800	6	5.30E-06	8000
17	15	10	578	0.61	527	-5	6.70E-06	8000
18	19	10	578	0.61	527	-5	6.70E-06	8000
19	15	12	578	0.61	527	-5	6.70E-06	8000
20	19	12	578	0.61	527	-5	6.70E-06	8000
21	15	10	722	0.4	800	-5	6.70E-06	8000
22	19	10	722	0.4	800	-5	6.70E-06	8000
23	15	12	722	0.4	800	-5	6.70E-06	8000
24	19	12	722	0.4	800	-5	6.70E-06	8000
25	15	10	578	0.61	527	6	6.70E-06	8000
26	19	10	578	0.61	527	6	6.70E-06	8000
27	15	12	578	0.61	527	6	6.70E-06	8000
28	19	12	578	0.61	527	6	6.70E-06	8000
29	15	10	722	0.4	800	6	6.70E-06	8000
30	19	10	722	0.4	800	6	6.70E-06	8000
31	15	12	722	0.4	800	6	6.70E-06	8000
32	19	12	722	0.4	800	6	6.70E-06	8000
33	15	10	578	0.61	527	-5	5.30E-06	10000
34	19	10	578	0.61	527	-5	5.30E-06	10000
35	15	12	578	0.61	527	-5	5.30E-06	10000
36	19	12	578	0.61	527	-5	5.30E-06	10000
37	15	10	722	0.4	800	-5	5.30E-06	10000
38	19	10	722	0.4	800	-5	5.30E-06	10000
39	15	12	722	0.4	800	-5	5.30E-06	10000
40	19	12	722	0.4	800	-5	5.30E-06	10000

Table 4-11 (continued)

41	15	10	578	0.61	527	6	5.30E-06	10000
42	19	10	578	0.61	527	6	5.30E-06	10000
43	15	12	578	0.61	527	6	5.30E-06	10000
44	19	12	578	0.61	527	6	5.30E-06	10000
45	15	10	722	0.4	800	6	5.30E-06	10000
46	19	10	722	0.4	800	6	5.30E-06	10000
47	15	12	722	0.4	800	6	5.30E-06	10000
48	19	12	722	0.4	800	6	5.30E-06	10000
49	15	10	578	0.61	527	-5	6.70E-06	10000
50	19	10	578	0.61	527	-5	6.70E-06	10000
51	15	12	578	0.61	527	-5	6.70E-06	10000
52	19	12	578	0.61	527	-5	6.70E-06	10000
53	15	10	722	0.4	800	-5	6.70E-06	10000
54	19	10	722	0.4	800	-5	6.70E-06	10000
55	15	12	722	0.4	800	-5	6.70E-06	10000
56	19	12	722	0.4	800	-5	6.70E-06	10000
57	15	10	578	0.61	527	6	6.70E-06	10000
58	19	10	578	0.61	527	6	6.70E-06	10000
59	15	12	578	0.61	527	6	6.70E-06	10000
60	19	12	578	0.61	527	6	6.70E-06	10000
61	15	10	722	0.4	800	6	6.70E-06	10000
62	19	10	722	0.4	800	6	6.70E-06	10000
63	15	12	722	0.4	800	6	6.70E-06	10000
64	19	12	722	0.4	800	6	6.70E-06	10000

Table 4-12 2^k sensitivity analysis ranking for experiment no.2

Rank	Main Effect / Interaction	Coefficients	Absolute Value	SIGN (nature)
1	x2	-21.2515625	21.2515625	negative
2	x1	20.8515625	20.8515625	positive
3	x4	17.4015625	17.4015625	positive
4	x3	-12.5171875	12.5171875	negative
5	x1x2x4	9.7109375	9.7109375	positive
6	x5	8.4421875	8.4421875	positive
7	x1x2x3x4	-7.5140625	7.5140625	negative
8	x1x2x3	-6.0390625	6.0390625	negative
9	x1x2x3x4x5	6.0015625	6.0015625	positive
10	x1x2x4x5	4.7765625	4.7765625	positive
11	x1x4	4.2203125	4.2203125	positive
12	x2x3	3.6359375	3.6359375	positive
13	x2x4x5	3.3265625	3.3265625	positive
14	x2x3x4	-3.2515625	3.2515625	negative
15	x1x2	-3.2328125	3.2328125	negative
16	x1x3x4	3.0453125	3.0453125	positive
17	x1x5	2.9296875	2.9296875	positive
18	x1x2x5	2.9015625	2.9015625	positive
19	x3x5	2.6796875	2.6796875	positive
20	x1x3x5	2.6234375	2.6234375	positive
21	x2x4	-2.6078125	2.6078125	negative
22	x2x3x4x5	2.1203125	2.1203125	positive
23	x3x4	-2.0546875	2.0546875	negative
24	x1x4x5	-2.0328125	2.0328125	negative
25	x1x3	-1.9921875	1.9921875	negative
26	x2x5	-1.8984375	1.8984375	negative
27	x3x4x5	1.8359375	1.8359375	positive
28	x2x3x5	-1.6984375	1.6984375	negative
29	x1x3x4x5	-1.3703125	1.3703125	negative
30	x1x2x6	1.1109375	1.1109375	positive
31	x1x2x3x5	-0.9546875	0.9546875	negative
32	x6	0.9078125	0.9078125	positive
33	x3x4x6	0.8640625	0.8640625	positive
34	x5x6	0.6734375	0.6734375	positive
35	x3x5x6	0.5796875	0.5796875	positive
36	x2x3x5x6	-0.5296875	0.5296875	negative
37	x4x5x6	-0.5265625	0.5265625	negative
38	x1x3x5x6	0.4984375	0.4984375	positive
39	x2x3x4x5x6	0.4890625	0.4890625	positive
40	x4x6	0.4640625	0.4640625	positive
41	x2x3x4x6	-0.4515625	0.4515625	negative

Table 4-12 (continued)

42	x1x4x5x6	-0.4515625	0.4515625	negative
43	x3x6	-0.4484375	0.4484375	negative
44	x1x3x4x5x6	-0.4328125	0.4328125	negative
45	x2x4x5x6	0.3765625	0.3765625	positive
46	x1x2x3x4x6	0.3359375	0.3359375	positive
47	x2x5x6	-0.3234375	0.3234375	negative
48	x1x5x6	0.3234375	0.3234375	positive
49	x1x2x3x5x6	-0.2984375	0.2984375	negative
50	x1x6	-0.2984375	0.2984375	negative
51	x2x3x6	0.2609375	0.2609375	positive
52	x1x3x4x6	0.2515625	0.2515625	positive
53	x1x2x3x6	0.2234375	0.2234375	positive
54	x1x3x6	-0.2234375	0.2234375	negative
55	x1x2x4x5x6	0.1640625	0.1640625	positive
56	x1x4x6	0.1578125	0.1578125	positive
57	x1x2x5x6	-0.1234375	0.1234375	negative
58	x4x5	0.1171875	0.1171875	positive
59	x2x6	0.0921875	0.0921875	positive
60	x2x4x6	-0.0890625	0.0890625	negative
61	x1x2x4x6	0.0421875	0.0421875	positive
62	x3x4x5x6	0.0359375	0.0359375	positive
63	x1x2x3x4x5x6	0	0	

Table 4-13 through Table 4-20 and Figure 4.4 through Figure 4.11 illustrate how the regression model and the actual model diverge from each other outside the regression ranges. This provides further evidence that linear models do not describe the MEPDG cracking model for wide input ranges. In order to accomplish this, all inputs except one were kept at the low values. The one input was then varied throughout a range of values that covered regions inside and outside the regression intervals. It can be appreciated that the regression plots are always linear since it is basically the main effect of the given input that is being illustrated. In general, the estimated and actual response diverges dramatically outside the regression interval, while they only coincide, as expected, within it. Of particular illustrative significance is Figure 4.5, which shows the actual on/off behavior of the response in the variation of slab thickness.

Even though linear regression models should not be used for wide ranges, they seem to be a very versatile tool for small ranges, as can be appreciated in the above figures. This is especially advantageous for specific input ranges in the context of local agencies. If sensitivity needs to be evaluated for particular input ranges, a 2^k screening method is an excellent resource.

Table 4-13 Experiment design for AADTT variation (see Figure 4.4)

Run No	x1	x2	x3	x4	x5	x6	Coded x1	Coded x2	Coded x3	Coded x4	Coded x5	Coded x6
1	15	10	578	-5	5.3	500	-1.00	-1.00	-1.00	-1.00	-1.00	-8.50
2	15	10	578	-5	5.3	1000	-1.00	-1.00	-1.00	-1.00	-1.00	-8.00
3	15	10	578	-5	5.3	2000	-1.00	-1.00	-1.00	-1.00	-1.00	-7.00
4	15	10	578	-5	5.3	4000	-1.00	-1.00	-1.00	-1.00	-1.00	-5.00
5	15	10	578	-5	5.3	8000	-1.00	-1.00	-1.00	-1.00	-1.00	-1.00
6	15	10	578	-5	5.3	10000	-1.00	-1.00	-1.00	-1.00	-1.00	1.00
7	15	10	578	-5	5.3	12000	-1.00	-1.00	-1.00	-1.00	-1.00	3.00
8	15	10	578	-5	5.3	14000	-1.00	-1.00	-1.00	-1.00	-1.00	5.00
9	15	10	578	-5	5.3	16000	-1.00	-1.00	-1.00	-1.00	-1.00	7.00
10	15	10	578	-5	5.3	40000	-1.00	-1.00	-1.00	-1.00	-1.00	31.00

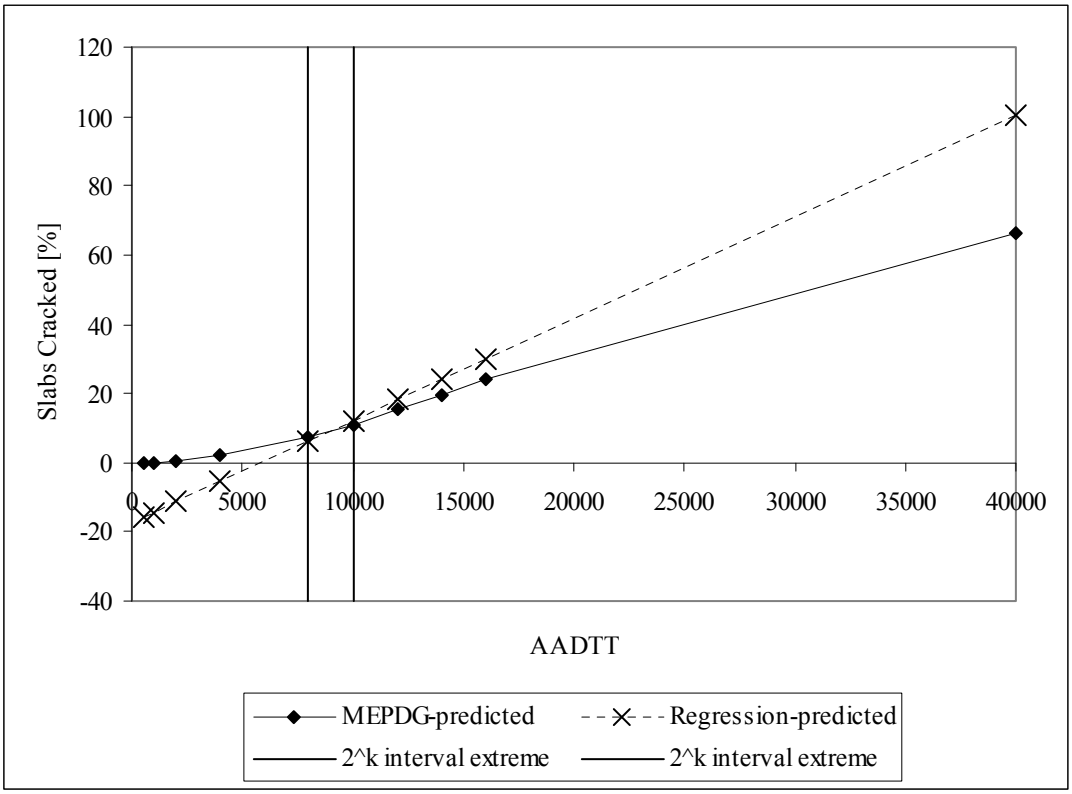

Figure 4.4 Variation in AADTT

Table 4-14 Experiment design for slab thickness variation (see Figure 4.5)

Run No	x1	x2	x3	x4	x5	x6	Coded x1	Coded x2	Coded x3	Coded x4	Coded x5	Coded x6
1	15	6	578	-5	5.3	8000	-1.00	-5.00	-1.00	-1.00	-1.00	-1.00
2	15	8	578	-5	5.3	8000	-1.00	-3.00	-1.00	-1.00	-1.00	-1.00
3	15	10	578	-5	5.3	8000	-1.00	-1.00	-1.00	-1.00	-1.00	-1.00
4	15	12	578	-5	5.3	8000	-1.00	1.00	-1.00	-1.00	-1.00	-1.00
5	15	14	578	-5	5.3	8000	-1.00	3.00	-1.00	-1.00	-1.00	-1.00
6	15	16	578	-5	5.3	8000	-1.00	5.00	-1.00	-1.00	-1.00	-1.00
7	15	18	578	-5	5.3	8000	-1.00	7.00	-1.00	-1.00	-1.00	-1.00
8	15	20	578	-5	5.3	8000	-1.00	9.00	-1.00	-1.00	-1.00	-1.00
9	15	22	578	-5	5.3	8000	-1.00	11.00	-1.00	-1.00	-1.00	-1.00
10	15	24	578	-5	5.3	8000	-1.00	13.00	-1.00	-1.00	-1.00	-1.00

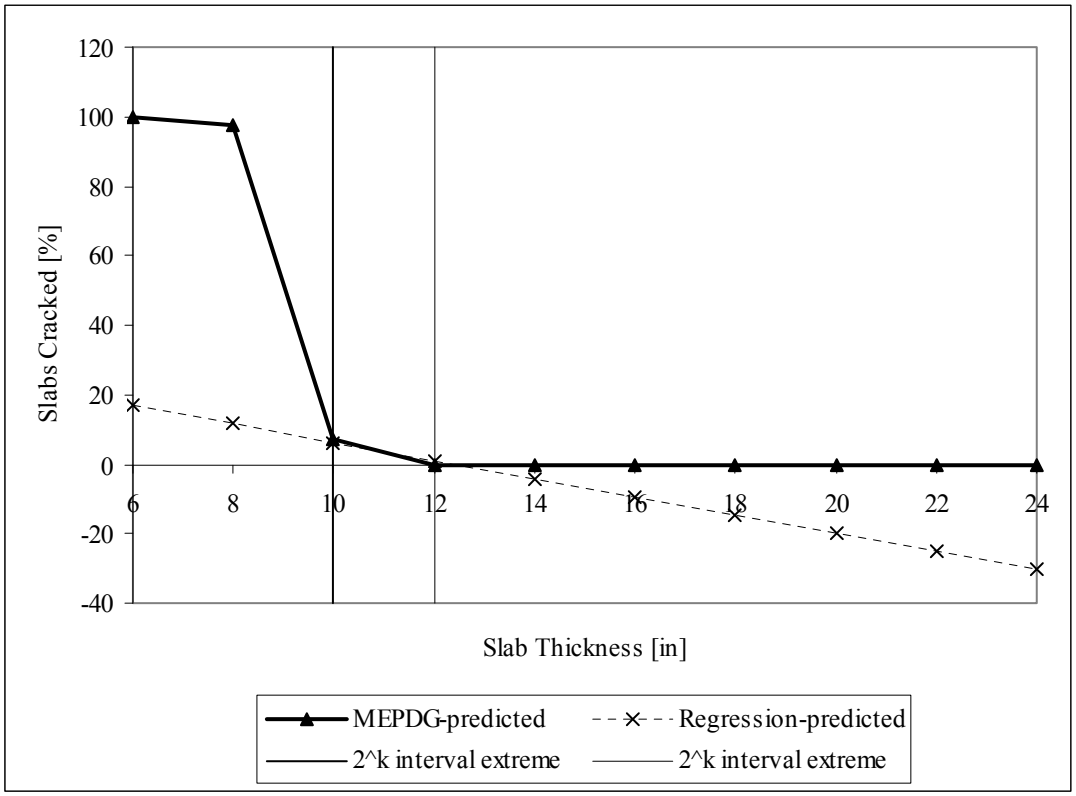

Figure 4.5 Variation in slab thickness

Figure 4.6 resembles the trend discussed in relation to Figure 3.12. It can be observed also here that -12 seems to be the built-in corresponding to least cracking. This is a good example of why first order sensitivity analyses should be avoided.

Table 4-15 Experiment design for built-in temperature difference (see Figure 4.6)

Run No	x1	x2	x3	x4	x5	x6	Coded x1	Coded x2	Coded x3	Coded x4	Coded x5	Coded x6
1	15	10	578	-30	5.3	8000	-1.00	-1.00	-1.00	-5.55	-1.00	-1.00
2	15	10	578	-25	5.3	8000	-1.00	-1.00	-1.00	-4.64	-1.00	-1.00
3	15	10	578	-20	5.3	8000	-1.00	-1.00	-1.00	-3.73	-1.00	-1.00
4	15	10	578	-15	5.3	8000	-1.00	-1.00	-1.00	-2.82	-1.00	-1.00
5	15	10	578	-10	5.3	8000	-1.00	-1.00	-1.00	-1.91	-1.00	-1.00
6	15	10	578	-5	5.3	8000	-1.00	-1.00	-1.00	-1.00	-1.00	-1.00
7	15	10	578	0	5.3	8000	-1.00	-1.00	-1.00	-0.09	-1.00	-1.00
8	15	10	578	6	5.3	8000	-1.00	-1.00	-1.00	1.00	-1.00	-1.00
9	15	10	578	10	5.3	8000	-1.00	-1.00	-1.00	1.73	-1.00	-1.00

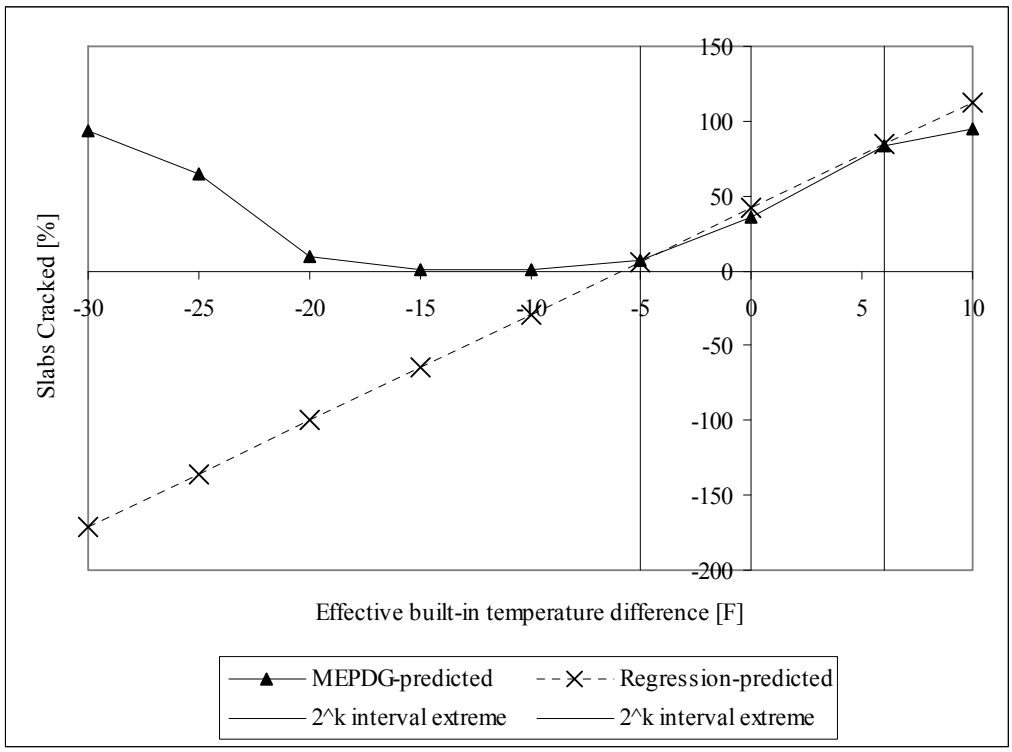

Figure 4.6 Variation in effective built-in temperature difference

Table 4-16 Experiment design for joint spacing (see Figure 4.7)

Run No	x1	x2	x3	x4	x5	x6	Coded x1	Coded x2	Coded x3	Coded x4	Coded x5	Coded x6
1	12	10	578	-5	5.3	8000	-2.50	-1.00	-1.00	-1.00	-1.00	-1.00
2	13	10	578	-5	5.3	8000	-2.00	-1.00	-1.00	-1.00	-1.00	-1.00
3	14	10	578	-5	5.3	8000	-1.50	-1.00	-1.00	-1.00	-1.00	-1.00
4	15	10	578	-5	5.3	8000	-1.00	-1.00	-1.00	-1.00	-1.00	-1.00
5	16	10	578	-5	5.3	8000	-0.50	-1.00	-1.00	-1.00	-1.00	-1.00
6	17	10	578	-5	5.3	8000	0.00	-1.00	-1.00	-1.00	-1.00	-1.00
7	18	10	578	-5	5.3	8000	0.50	-1.00	-1.00	-1.00	-1.00	-1.00
8	19	10	578	-5	5.3	8000	1.00	-1.00	-1.00	-1.00	-1.00	-1.00
9	20	10	578	-5	5.3	8000	1.50	-1.00	-1.00	-1.00	-1.00	-1.00
10	21	10	578	-5	5.3	8000	2.00	-1.00	-1.00	-1.00	-1.00	-1.00

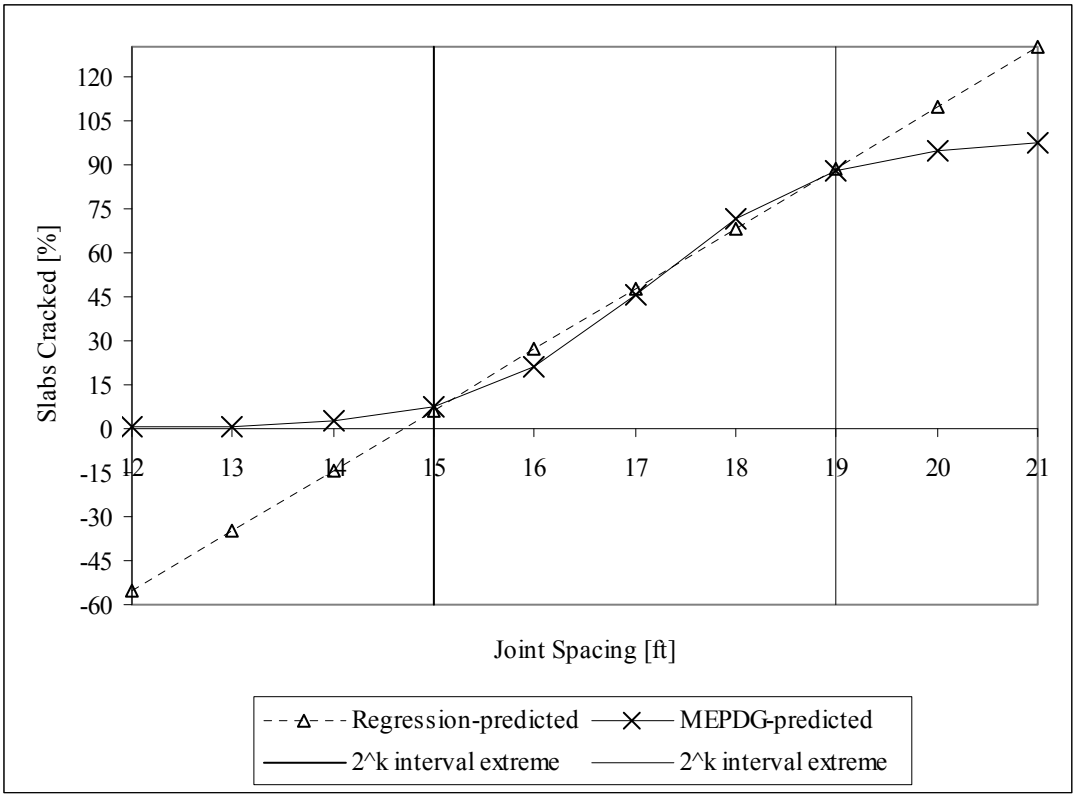

Figure 4.7 Variation in joint spacing

Table 4-17 Experiment design for modulus of rupture (see Figure 4.8)

Run No	x1	x2	x3	x4	x5	x6	Coded x1	Coded x2	Coded x3	Coded x4	Coded x5	Coded x6
1	15	10	400	-5	5.3	8000	-1.00	-1.00	-3.47	-1.00	-1.00	-1.00
2	15	10	450	-5	5.3	8000	-1.00	-1.00	-2.78	-1.00	-1.00	-1.00
3	15	10	500	-5	5.3	8000	-1.00	-1.00	-2.08	-1.00	-1.00	-1.00
4	15	10	550	-5	5.3	8000	-1.00	-1.00	-1.39	-1.00	-1.00	-1.00
5	15	10	578	-5	5.3	8000	-1.00	-1.00	-1.00	-1.00	-1.00	-1.00
6	15	10	600	-5	5.3	8000	-1.00	-1.00	-0.69	-1.00	-1.00	-1.00
7	15	10	650	-5	5.3	8000	-1.00	-1.00	0.00	-1.00	-1.00	-1.00
8	15	10	700	-5	5.3	8000	-1.00	-1.00	0.69	-1.00	-1.00	-1.00
9	15	10	722	-5	5.3	8000	-1.00	-1.00	1.00	-1.00	-1.00	-1.00
10	15	10	771	-5	5.3	8000	-1.00	-1.00	1.68	-1.00	-1.00	-1.00

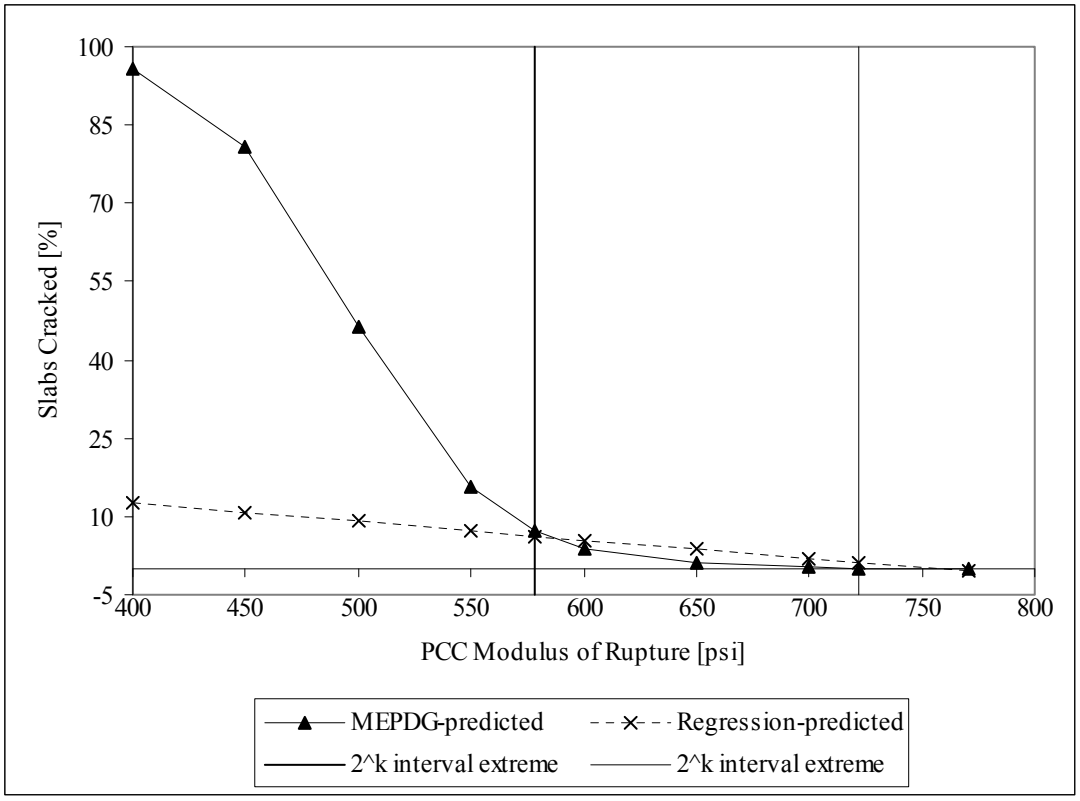

Figure 4.8 Variation in modulus of rupture

Table 4-18 Experiment design for coefficient of thermal expansion (see Figure 4.9)

Run No	x1	x2	x3	x4	x5	x6	Coded x1	Coded x2	Coded x3	Coded x4	Coded x5	Coded x6
1	15	10	578	-5	4	8000	-1.00	-1.00	-1.00	-1.00	-2.86	-1.00
2	15	10	578	-5	4.5	8000	-1.00	-1.00	-1.00	-1.00	-2.14	-1.00
3	15	10	578	-5	5	8000	-1.00	-1.00	-1.00	-1.00	-1.43	-1.00
4	15	10	578	-5	5.3	8000	-1.00	-1.00	-1.00	-1.00	-1.00	-1.00
5	15	10	578	-5	6	8000	-1.00	-1.00	-1.00	-1.00	0.00	-1.00
6	15	10	578	-5	6.7	8000	-1.00	-1.00	-1.00	-1.00	1.00	-1.00
7	15	10	578	-5	7	8000	-1.00	-1.00	-1.00	-1.00	1.43	-1.00
8	15	10	578	-5	7.5	8000	-1.00	-1.00	-1.00	-1.00	2.14	-1.00
9	15	10	578	-5	8	8000	-1.00	-1.00	-1.00	-1.00	2.86	-1.00
10	15	10	578	-5	8.5	8000	-1.00	-1.00	-1.00	-1.00	3.57	-1.00

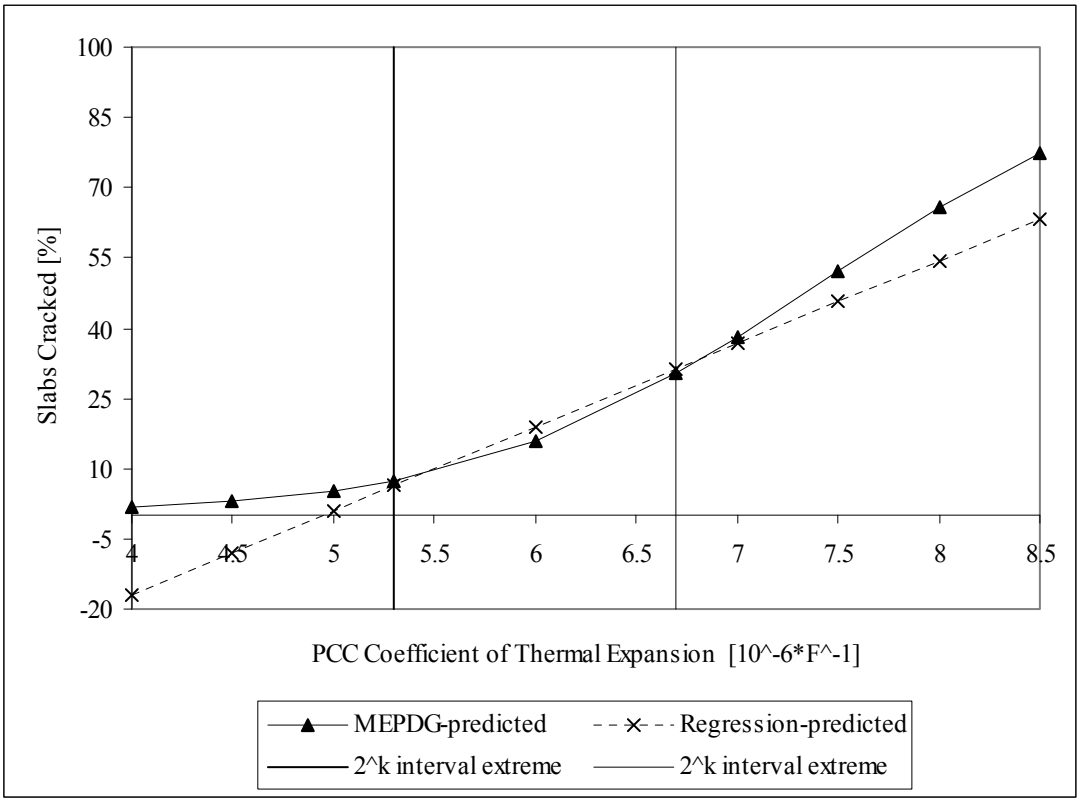

Figure 4.9 Variation in coefficient of thermal expansion

Two different tests were carried out for variation of the inputs within their regression intervals. As can be appreciated in Table 4-19 and Table 4-20, inputs were varied from low to high and high to low. In general, high discrepancies can be expected even within the ranges of regression. This result reinforces the fact that a first order model fails to describe the MEPDG cracking model even within small input intervals.

Table 4-19 Experiment No.1 varying inputs within (min, max) ranges (see Figure 4.10)

Run No	x1	x2	x3	x4	x5	x6	Coded x1	Coded x2	Coded x3	Coded x4	Coded x5	Coded x6
1	15	12	578	6	5.3	10000	-1.00	1.00	-1.00	1.00	-1.00	1.00
2	15.4	11.8	590	4.8	5.45	9800	-0.80	0.80	-0.83	0.78	-0.79	0.80
3	15.8	11.6	600	3.6	5.6	9600	-0.60	0.60	-0.69	0.56	-0.57	0.60
4	16.2	11.4	620	2.4	5.75	9400	-0.40	0.40	-0.42	0.35	-0.36	0.40
5	16.6	11.2	640	1.2	5.9	9200	-0.20	0.20	-0.14	0.13	-0.14	0.20
6	17	11	660	0	6.05	9000	0.00	0.00	0.14	-0.09	0.07	0.00
7	17.4	10.8	680	-1.2	6.2	8800	0.20	-0.20	0.42	-0.31	0.29	-0.20
8	17.8	10.6	700	-2.4	6.35	8600	0.40	-0.40	0.69	-0.53	0.50	-0.40
9	18.2	10.4	710	-3.6	6.5	8400	0.60	-0.60	0.83	-0.75	0.71	-0.60
10	19	10	722	-5	6.7	8000	1.00	-1.00	1.00	-1.00	1.00	-1.00

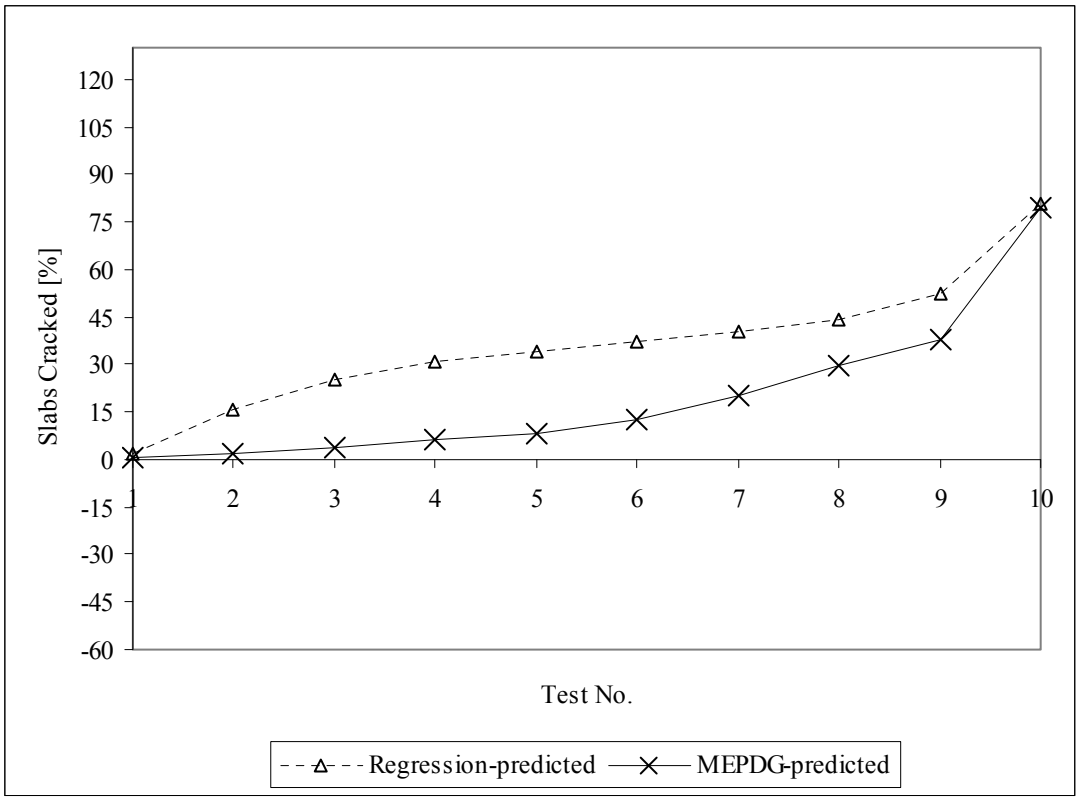

Figure 4.10 Test No. 1 within (min, max) ranges of 2^k screening

Table 4-20 Experiment No.2 varying inputs within (min, max) ranges (see Figure 4.11)

Run No	x1	x2	x3	x4	x5	x6	Coded x1	Coded x2	Coded x3	Coded x4	Coded x5	Coded x6
1	15	10	578	6	5.3	8000	-1.00	-1.00	-1.00	1.00	-1.00	-1.00
2	15.4	10.4	590	4.8	5.45	8400	-0.80	-0.60	-0.83	0.78	-0.79	-0.60
3	15.8	10.6	600	3.6	5.6	8600	-0.60	-0.40	-0.69	0.56	-0.57	-0.40
4	16.2	10.8	620	2.4	5.75	8800	-0.40	-0.20	-0.42	0.35	-0.36	-0.20
5	16.6	11	640	1.2	5.9	9000	-0.20	0.00	-0.14	0.13	-0.14	0.00
6	17	11.2	660	0	6.05	9200	0.00	0.20	0.14	-0.09	0.07	0.20
7	17.4	11.4	680	-1.2	6.2	9400	0.20	0.40	0.42	-0.31	0.29	0.40
8	17.8	11.6	700	-2.4	6.35	9600	0.40	0.60	0.69	-0.53	0.50	0.60
9	18.2	11.8	710	-3.6	6.5	9800	0.60	0.80	0.83	-0.75	0.71	0.80
10	19	12	722	-5	6.7	10000	1.00	1.00	1.00	-1.00	1.00	1.00

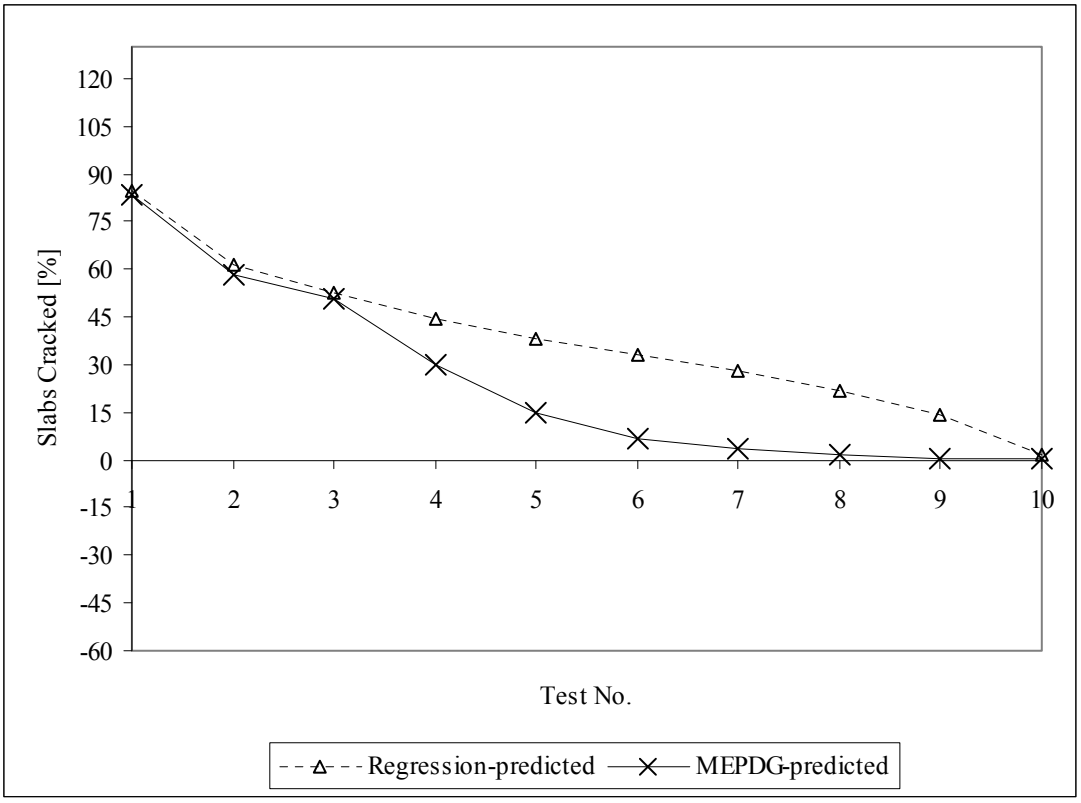

Figure 4.11 Test No. 2 within (min, max) ranges of 2^k screening

4.5 CONCLUSIONS (II)

Respecting the deterministic nature of the MEPDG, the best approach towards an exhaustive sensitivity analysis of this tool is to perform non-linear regression. Techniques required to achieve this are comprised in the area of Response Surface Methodology (RSM), which usually uses screening approaches in the earlier phases of the process. The screening experiments of the 2^k type used in this research demonstrate that first degree regression models can be very useful for narrow input ranges.

2^k approaches may be very useful in exploring specific regions of the model as it yields general information regarding the main effect and interactions between variables. 2^k screenings seem to be unavoidable in the process of improving regression models, for example in the process of including non-linear terms and interactions. This research facilitates the understanding of the mechanics of the process and introduces it as a potential analysis tool in the context of the MEPDG.

2^k approaches produce quantitative rankings. This research suggests that several different ranges of inputs of interest could be explored and a ranking obtained for a given design of experiment. Rankings and sensitivities could then be compared on a quantitative basis and regions of higher sensitivity could be established using this technique. Pertinent 2^k designs could yield valuable information in a very versatile way depending on the goal proposed, provided sufficient time and computer resources are available.

The second 2^k experiment presented in this work suggested that a difference between -5 ^oF, and +6 ^oF in permanent built-in equivalent temperature difference for the design of experiment proposed turned out to be influential, as was expected. This fact worsens the scenario depicted in regard to the permanent built-in equivalent temperature difference and the treatment it has received in the MEPDG. This is because it is an input with a high main effect and high interactions, thus contributing heavily to the final response of the model.

5.0 MEPDG PREDICTED VS MEASURED PERFORMANCE

5.1 MINNESOTA ROAD TEST - PROJECT DESCRIPTION

The last task of this research is to compare MEPDG-predicted performance with measured performance from a very well known test road. The Minnesota Road Research Test Road (Mn/ROAD) is an excellent choice due to the availability of accurate information regarding material properties and construction data. In order to evaluate the performance of the cracking model for JPCP, nine cells were chosen, as depicted in Table 5-1. Table 5-2 contains PCC properties and Table 5-3 contains the granular material gradation specifications according to the 1995 standards of Mn/ROAD.

The equivalent built-in temperature differences for the Mn/ROAD pavement cells are known and equal to zero in all cases but Cell 5, which has an equivalent built-in temperature difference of -0.16 ^{o}F. Knowledge of these parameters provides an opportunity to test the cracking model at values of built-in temperature difference other than -10 ^{o}F, and compare them to the predictions under a built-in temperature difference equal to -10 ^{o}F. The results of this analysis are contained in Table 5-4.

Table 5-1 Design of Mn/ROAD Test Sections used for Analysis (14)

Test Section	Cell	Slab Thickness mm (in)	Joint Spacing m (ft)	Lane Widths, Inside/Outside m (ft)	Dowel Diameter mm (in)	Base Type1, Thickness, mm (in)	Edge Drains	Comments
5-Year	5	190 (7.5)	6.1 (20)	4.0/4.3 (13/14)	25 (1)	cl4sp, 75 (3) over cl3sp (68)	No	
5-Year	6	190 (7.5)	4.6 (15)	4.0/4.3 (13/14)	25 (1)	cl4sp, 125 (5)	No	
5-Year	7	190 (7.5)	6.1 (20)	4.0/4.3 (13/14)	25 (1)	PASB2 100 (4) over cl4sp, 75 (3)	Yes	
5-Year	8	190 (7.5)	4.6 (15)	4.0/4.0/4.3 (13/13/14)	25 (1)	PASB2 100 (4) over cl4sp, 75	Yes	3 lanes, transverse steel
5-Year	9	190 (7.5)	4.6 (15)	4.0/4.0/4.3 (13/13/14)	25 (1)	PASB, 2 100 (4) over cl4sp, 75 (3)	Yes	3 lanes, no transverse steel
10-Year	10	240 (9.5)	6.1 (20)	3.7/3.7 (12/12)	32 (1.25)	PASB2, 100 (4) over cl4sp, (75)	Yes	
10-Year	11	240 (9.5)	7.3 (24)	3.7/3.7 (12/12)	32 (1.25)	cl5sp, 125 (5)	No	
10-Year	12	240 (9.5)	4.6 (15)	3.7/3.7 (12/12)	32 (1.25)	cl5sp, 125 (5)	Yes	
10-Year	13	240 (9.5)	6.1 (20)	3.7/3.7 (12/12)	32 (1.25)	cl5sp, 125 (5)	No	

Table 5-2 Basic concrete properties (14)

Test Section	Cell	Unit Weight	Compressive Strengths	Modulus of Elasticity	Poisson's Ratio	Thermal Coefficient
		kg/m^3 (psi/ft^3)	(28-day) MPa (psi)	(28-day) MPa (psi)		εμX° / (με/ °F)
5-Year	5	2390 (149)	36 (5215)	32900 (4800000)	0.19	8.1 (4.5)
5-Year	6	2390 (149)	37 (5405)	33900 (4900000)	0.19	8.1 (4.5)
5-Year	7	2395 (150)	36 (5205)	30000 (4400000)	0.19	8.1 (4.5)
5-Year	8	2400 (150)	33 (4790)	31800 (4600000)	0.19	8.4 (4.7)
5-Year	9	2385 (149)	37 (5430)	31900 (4600000)	0.19	9.8 (5.4)
10-Year	10	2370 (148)	35 (5110)	28800 (4200000)	0.19	8.1 (4.5)
10-Year	11	2405 (150)	39 (5590)	30100 (4400000)	0.19	6.7 (3.7)
10-Year	12	2380 (149)	36 (5270)	30100 (4400000)	0.21	8.8 (4.9)
10-Year	13	2370 (148)	34 (4885)	34400 (5000000)	0.22	8.8 (4.9)

Table 5-3 Mn/ROAD 1995 granular specifications (percent passing) (14)

	Base Material			
Sieve Size	cl3sp	Cl4sp	cl5sp	PASB
1-1/2-in	--	100	--	--
1-1/4-in	--	--	--	100
1-in	--	95-100	100	95-100
¾-in	--	90-100	90-100	85-98
½-in	100	--	--	--
3/8-in	95-100	80-95	70-85	50-80
No. 4	85-100	70-85	55-70	20-50
No. 10	65-90	55-70	35-55	0-20
No. 20	--	--	--	0-8
No. 40	30-50	15-30	15-30	0-5
No. 200	15-Aug	10-May	8-Mar	0-3

1 in = 25.4 mm

Special crushing requirements (sp):

cl3sp and cl4sp: crushed/fractured particles are not allowed

cl5sp: 10-15 percent crushed/fractured particles are required.

Table 5-4 MEPDG analysis of Mn/ROAD Cells 5 through 13

Cell	5	6	7	8	9	10	11	12	13
Surveyed Distress	16%	0%	0%	0%	0%	0%	9%	0%	0%
Predicted distress with known built-in temperature difference	100%	99%	89%	39%	38%	15%	97%	14%	100%
Predicted with built-in = -10	88.3%	67.2%	8.6%	2.6%	1.7%	0.1%	10.50%	0.3%	98.7%

5.2 ANALYSIS OF RESULTS

As shown in Table 5-4, the predictions of the MEPDG in the presence of actual built-in equivalent temperature differences are extremely divergent from the actual measured data. On the other hand, by letting the built-in equivalent temperature difference remain constant and equal to -10, the match between predicted and measured distress improves drastically with the exception of Cells 5, 6 and 13. Predictions in this analysis correspond to 15 years after construction.

In attempting to explain the divergence between predicted and measured performance for a built-in equivalent temperature difference of -10 ^{o}F, observations were made that are related to the sensitivity analysis. As can be seen from the input data, Cells 11 and 13 have similar designs. Even though the mix design used to construct each test section was the same, variations in the strength parameters can be assumed to be within reasonable ranges that are attributed to normal testing variation. However, the predicted performance seems to be extremely sensitive to variations in the strength and thermal properties of concrete. In order to demonstrate this, an additional test was carried out on Cell 13 by modifying the values of three parameters and bringing them to values equal to those of Cell 11, since the material properties of concrete for these two cells are assumed to be equal. Table 5-5 contains the prediction results for the replacement of the strength parameters of Cell 13 by those of Cell 11. Modification of modulus of elasticity, compressive strength, and coefficient of thermal expansion suggests that the main effects and interactions between these inputs are high. This is consistent with the results shown in Table 4-12. The shaded cells in Table 5-5 are replaced values.

An explanation for the persistent divergence in the performance predictions for Cells 5 and 6 does not seem to be similar to the situation of Cell 13 explained above. Rather than a high

sensitivity to material strength variation, the extremely high predictions for granular bases in conjunction with thin PCC slabs seems to be in connection with Figure 4.5, which depicts an abrupt on/off behavior in the variation of prediction with respect to slab thickness in the region of thin slab thickness. Even though a nonlinear variation in this behavior is expected, the one occurring here seems too pronounced.

Table 5-5 Replacement of PCC strength properties of Cell 13 by cell 11*

E [psi]	f'c [psi]	Coefficient of thermal expansion [10-6/°F]	Surveyed performance [% slabs cracked]	Predicted performance [% slabs cracked]
4400000	4885	4.9	0	84.5
5000000	5590	4.9	0	83.6
4400000	5590	4.9	0	39.2
5000000	4885	3.7	0	28.4
4400000	4885	3.7	0	9.4
5000000	5590	3.7	0	6.7
4400000	5590	3.7	0	1.9

* Gray cells correspond to replaced input values

5.3 CONCLUSIONS (III)

The results presented in Table 5-4 and discussed in section 5.2 support the discussion developed in section 3.2 and strongly suggest that the current state of the MEPDG should not allow the prediction of cracking in the presence of built-in temperature difference other than that equal to -10. The fatigue damage – cracking empirical relation depicted in Figure 2.3 was obtained through the fit of many different sites, all of which had a constant built-in temperature difference equal to -10. Therefore, it is not surprising to find out that the Mn/RROAD cells seem to be correctly predicted in the presence of this constant parameter.

The fact that the MEPDG seems to correctly predict distress in the presence of a built-in equivalent temperature difference of -10 ^{o}F suggests that the tool performs well as long as this parameter is kept constant and equal to that magnitude. This finding is discouraging however, because a substantial portion of the effect on distress is expected to be a function of this parameter, the nature of which has been conceived to be that of a random variable. The strongest expectations on the MEPDG have relied to a great extent on the nature and magnitude of the effects caused by the built-in equivalent temperature difference. The importance of this parameter can be illustrated by the fact that procedures to determine its actual numerical value have been and are a current matter of research. Therefore, it is not encouraging to find out that the MEPDG can only accept this parameter as a universal constant. A possible explanation to this limitation has been depicted in this work (section 3.2) and it has been suggested that an empirical model should be developed in which actual values of built-in temperature difference are included.

Analysis of divergences found in the comparison between observed and predicted performance are consistent with the sensitivity analysis results presented earlier. For example,

normal variations in the procedures of material testing prove to be influential in specific combinations of strength parameters, which is consistently explained by high main effects and interactions between inputs. The diverging results of Cells 5 and 6 can also be successfully explained through the sensitivity analysis results. This type of results suggests that the screening technique introduced in this research is promising in the sense that specific, localized analyses may be carried out at a very low computational cost and with great ease.

APPENDIX

EXPERIMENT DESIGNS

This appendix contains all experiment designs for which this work was based. For the sake of brevity, each table corresponds to a specific section and illustrates one single case among the various cases considered. The reader can refer to the various input values in order to determine a specific design out.

Table A 1. Experiment Design Data of Section 3.1

Project: JJG-Test-type13-20ft-S

General Information

Design Life	20 years
Pavement construction:	September, 2006
Traffic open:	October, 2006
Type of design	JPCP

Analysis Parameters

Performance Criteria	Limit	Reliability
Initial IRI (in/mi)	63	
Terminal IRI (in/mi)	172	90
Transverse Cracking (% slabs cracked)	15	90
Mean Joint Faulting (in)	0.12	90

Location:	
Project ID:	
Section ID:	
Date:	11/9/2007
Station/milepost format:	
Station/milepost begin:	
Station/milepost end:	
Traffic direction:	East bound

Default Input Level

Default input level	Level 3, Default and historical agency values.

Traffic

Initial two-way AADTT:	10000
Number of lanes in design direction:	2
Percent of trucks in design direction (%):	50
Percent of trucks in design lane (%):	100
Operational speed (mph):	60

Table A 1 (continued)

Traffic -- Volume Adjustment Factors

Monthly Adjustment Factors (Level 3, Default MAF)

Month	Vehicle Class									
	Class 4	**Class 5**	**Class 6**	**Class 7**	**Class 8**	**Class 9**	**Class 10**	**Class 11**	**Class 12**	**Class 13**
January	1.00	1.00	1.00	1.00	1.00	1.00	1.00	1.00	1.00	1.00
February	1.00	1.00	1.00	1.00	1.00	1.00	1.00	1.00	1.00	1.00
March	1.00	1.00	1.00	1.00	1.00	1.00	1.00	1.00	1.00	1.00
April	1.00	1.00	1.00	1.00	1.00	1.00	1.00	1.00	1.00	1.00
May	1.00	1.00	1.00	1.00	1.00	1.00	1.00	1.00	1.00	1.00
June	1.00	1.00	1.00	1.00	1.00	1.00	1.00	1.00	1.00	1.00
July	1.00	1.00	1.00	1.00	1.00	1.00	1.00	1.00	1.00	1.00
August	1.00	1.00	1.00	1.00	1.00	1.00	1.00	1.00	1.00	1.00
September	1.00	1.00	1.00	1.00	1.00	1.00	1.00	1.00	1.00	1.00
October	1.00	1.00	1.00	1.00	1.00	1.00	1.00	1.00	1.00	1.00
November	1.00	1.00	1.00	1.00	1.00	1.00	1.00	1.00	1.00	1.00
December	1.00	1.00	1.00	1.00	1.00	1.00	1.00	1.00	1.00	1.00

Vehicle Class Distribution
(Level 3, Default Distribution)

AADTT distribution by vehicle class

Class 4	0.0%
Class 5	0.0%
Class 6	0.0%
Class 7	0.0%
Class 8	0.0%
Class 9	0.0%
Class 10	0.0%
Class 11	0.0%
Class 12	0.0%
Class 13	100.0%

Hourly truck traffic distribution
by period beginning:

12:00 am	7.7%	Noon	0.0%
1:00 am	7.7%	1:00 pm	0.0%
2:00 am	7.7%	2:00 pm	0.0%
3:00 am	7.7%	3:00 pm	0.0%
4:00 am	7.7%	4:00 pm	0.0%
5:00 am	7.7%	5:00 pm	0.0%
6:00 am	7.7%	6:00 pm	0.0%
7:00 am	7.7%	7:00 pm	0.0%
8:00 am	7.6%	8:00 pm	7.7%
9:00 am	0.0%	9:00 pm	7.7%
10:00 am	0.0%	10:00 pm	7.7%
11:00 am	0.0%	11:00 pm	7.7%

Table A 1 (continued)

Traffic Growth Factor

Vehicle Class	Growth Rate	Growth Function
Class 4	6.0%	Compound
Class 5	6.0%	Compound
Class 6	6.0%	Compound
Class 7	6.0%	Compound
Class 8	6.0%	Compound
Class 9	6.0%	Compound
Class 10	6.0%	Compound
Class 11	6.0%	Compound
Class 12	6.0%	Compound
Class 13	6.0%	Compound

Traffic -- Axle Load Distribution Factors

Level 3: Default

Traffic -- General Traffic Inputs

Mean wheel location (inches from the lane marking):	18
Traffic wander standard deviation (in):	10
Design lane width (ft):	12

Number of Axles per Truck

Vehicle Class	Single Axle	Tandem Axle	Tridem Axle	Quad Axle
Class 4	1.62	0.39	0.00	0.00
Class 5	2.00	0.00	0.00	0.00
Class 6	1.02	0.99	0.00	0.00
Class 7	1.00	0.26	0.83	0.00
Class 8	2.38	0.67	0.00	0.00
Class 9	1.13	1.93	0.00	0.00
Class 10	1.19	1.09	0.89	0.00
Class 11	4.29	0.26	0.06	0.00
Class 12	3.52	1.14	0.06	0.00
Class 13	2.15	2.13	0.35	0.00

Table A 1 (continued)

Axle Configuration

Average axle width (edge-to-edge) outside dimensions,ft):	8.5
Dual tire spacing (in):	12

Axle Configuration

Tire Pressure (psi) :	120

Average Axle Spacing

Tandem axle(psi):	51.6
Tridem axle(psi):	49.2
Quad axle(psi):	49.2

Wheelbase Truck Tractor

	Short	Medium	Long
Average Axle Spacing (ft)	12	15	18
Percent of trucks	100%	0%	0%

Climate

icm file:	C:\Documents and Settings\Rania\My Documents\JUAN\allegheny.icm
Latitude (degrees.minutes)	40.21
Longitude (degrees.minutes)	-79.6
Elevation (ft)	1281
Depth of water table (ft)	10

Structure--Design Features

Permanent curl/warp effective temperature difference (°F):	-10

Joint Design

Joint spacing (ft):	20
Sealant type:	Liquid
Dowel diameter (in):	1
Dowel bar spacing (in):	12

Edge Support	Tied PCC shoulder
Long-term LTE(%):	40
Widened Slab (ft):	n/a

Table A 1 (continued)

Base Properties

Base type:	Asphalt treated
Erodibility index:	Erosion Resistant (3)
PCC-Base Interface	Full friction contact
Loss of full friction (age in months):	229

Structure--ICM Properties

Surface shortwave absorptivity:	0.85

Structure--Layers

Layer 1 -- JPCP

General Properties

PCC material	JPCP
Layer thickness (in):	8
Unit weight (pcf):	150
Poisson's ratio	0.2

Thermal Properties

Coefficient of thermal expansion (per F° x 10- 6):	5.5
Thermal conductivity (BTU/hr-ft-F°) :	1.25
Heat capacity (BTU/lb-F°):	0.28

Mix Properties

Cement type:	Type I
Cementitious material content (lb/yd^3):	600
Water/cement ratio:	0.42
Aggregate type:	Limestone
PCC zero-stress temperature (F°)	100
Ultimate shrinkage at 40% R.H (microstrain)	Derived
Reversible shrinkage (% of ultimate shrinkage):	50
Time to develop 50% of ultimate shrinkage (days):	35
Curing method:	Curing compound

Strength Properties

Input level:	Level 3
28-day PCC modulus of rupture (psi):	600
28-day PCC compressive strength (psi):	n/a

Table A 1 (continued)

Layer 2 -- Asphalt permeable base

Material type:	Asphalt permeable base
Layer thickness (in):	5

General Properties

General

Reference temperature (F°):	70

Volumetric Properties as Built

Effective binder content (%):	11
Air voids (%):	8.5
Total unit weight (pcf):	148

Poisson's ratio:	0.35 (user entered)

Thermal Properties

Thermal conductivity asphalt (BTU/hr-ft-F°):	0.67
Heat capacity asphalt (BTU/lb-F°):	0.23

Asphalt Mix

Cumulative % Retained 3/4 inch sieve:	25
Cumulative % Retained 3/8 inch sieve:	67
Cumulative % Retained #4 sieve:	84
% Passing #200 sieve:	3

Asphalt Binder

Option:	Superpave binder grading
A	10.9800 (correlated)
VTS:	-3.6800 (correlated)

High temp.	**Low temperature, °C**						
°C	**-10**	**-16**	**-22**	**-28**	**-34**	**-40**	**-46**
46							
52							
58							
64							
70							
76							
82							

Table A 1 (continued)

Layer 3 -- Crushed stone

Unbound Material:	Crushed stone
Thickness(in):	10

Strength Properties

Input Level:	Level 3
Analysis Type:	ICM inputs (ICM Calculated Modulus)
Poisson's ratio:	0.35
Coefficient of lateral pressure,Ko:	0.5
Modulus (input) (psi):	30000

ICM Inputs

Gradation and Plasticity Index

Plasticity Index, PI:	1
Liquid Limit (LL)	6
Compacted Layer	No
Passing #200 sieve (%):	8.7
Passing #40	20
Passing #4 sieve (%):	44.7
D10(mm)	0.1035
D20(mm)	0.425
D30(mm)	1.306
D60(mm)	10.82
D90(mm)	46.19

Sieve	Percent Passing
0.001mm	
0.002mm	
0.020mm	
#200	8.7
#100	
#80	12.9
#60	
#50	
#40	20
#30	
#20	
#16	

Table A 1 (continued)

#10	33.8
#8	
#4	44.7
3/8"	57.2
1/2"	63.1
3/4"	72.7
1"	78.8
1 1/2"	85.8
2"	91.6
2 1/2"	
3"	
3 1/2"	97.6
4"	97.6

Calculated/Derived Parameters

Maximum dry unit weight (pcf):	127.2 (derived)
Specific gravity of solids, Gs:	2.70 (derived)
Saturated hydraulic conductivity (ft/hr):	0.05054 (derived)
Optimum gravimetric water content (%):	7.4 (derived)
Calculated degree of saturation (%):	61.2 (calculated)

Soil water characteristic curve parameters: Default values

Parameters	**Value**
a	7.2555
b	1.3328
c	0.82422
Hr.	117.4

Table A 1 (continued)

Layer 4 -- A-6

Unbound Material:	A-6
Thickness(in):	Semi-infinite

Strength Properties

Input Level:	Level 3
Analysis Type:	ICM inputs (ICM Calculated Modulus)
Poisson's ratio:	0.35
Coefficient of lateral pressure,Ko:	0.5
Modulus (input) (psi):	14000

ICM Inputs

Gradation and Plasticity Index

Plasticity Index, PI:	16
Liquid Limit (LL)	33
Compacted Layer	No
Passing #200 sieve (%):	63.2
Passing #40	82.4
Passing #4 sieve (%):	93.5
D10(mm)	0.000285
D20(mm)	0.0008125
D30(mm)	0.002316
D60(mm)	0.05364
D90(mm)	1.922

Sieve	Percent Passing
0.001mm	
0.002mm	
0.020mm	
#200	63.2
#100	
#80	73.5
#60	
#50	
#40	82.4
#30	
#20	
#16	

Table A 1 (continued)

#10	90.2
#8	
#4	93.5
3/8"	96.4
1/2"	97.4
3/4"	98.4
1"	99
1 1/2"	99.5
2"	99.8
2 1/2"	
3"	
3 1/2"	100
4"	100

Calculated/Derived Parameters

Maximum dry unit weight (pcf):	107.9 (derived)
Specific gravity of solids, Gs:	2.70 (derived)
Saturated hydraulic conductivity (ft/hr):	1.95e-005 (derived)
Optimum gravimetric water content (%):	17.1 (derived)
Calculated degree of saturation (%):	82.1 (calculated)

Soil water characteristic curve parameters: Default values

Parameters	**Value**
a	108.41
b	0.68007
c	0.21612
Hr.	500

Table A 1 (continued)

Distress Model Calibration Settings - Rigid (new)

Faulting

Faulting Coefficients

C1	1.018
C2	0.917
C3	0.002
C4	9E-04
C5	250
C6	0.4
C7	1.833
C8	400

Reliability (FAULT)

Std. Dev.	POWER(0.0097*FAULT,0.5178)+0.014

Cracking

Fatigue Coefficients

C1	2
C2	1.22

Cracking Coefficients

C4	1
C5	-1.98

Reliability (CRACK)

Std. Dev.	POWER(5.3116*CRACK,0.3903) + 2.99

IRI(jpcp)

C1	0.82
C2	0.442
C3	20.37
C4	1.493
C5	25.24
Standard deviation in initial IRI (in/mile):	5.4

Table A 2. Experiment Design Data of Section 3.2

Project: -15_Pittsburgh

General Information

Description:

Design Life	20 years
Pavement construction:	September, 2006
Traffic open:	October, 2006
Type of design	JPCP

Analysis Parameters

Performance Criteria

	Limit	Reliability
Initial IRI (in/mi)	63	
Terminal IRI (in/mi)	172	50
Transverse Cracking (% slabs cracked)	15	50
Mean Joint Faulting (in)	0.12	50

Location:	
Project ID:	
Section ID:	
Date:	11/27/2007
Station/milepost format:	
Station/milepost begin:	
Station/milepost end:	
Traffic direction:	East bound

Default Input Level

Default input level	Level 3, Default and historical agency values.

Traffic

Initial two-way AADTT:	2000
Number of lanes in design direction:	2
Percent of trucks in design direction (%):	50
Percent of trucks in design lane (%):	95
Operational speed (mph):	60

Table A 2 (continued)

Traffic -- Volume Adjustment Factors

Monthly Adjustment Factors (Level 3, Default MAF)

	Vehicle Class									
Month	**Class 4**	**Class 5**	**Class 6**	**Class 7**	**Class 8**	**Class 9**	**Class 10**	**Class 11**	**Class 12**	**Class 13**
January	1.00	1.00	1.00	1.00	1.00	1.00	1.00	1.00	1.00	1.00
February	1.00	1.00	1.00	1.00	1.00	1.00	1.00	1.00	1.00	1.00
March	1.00	1.00	1.00	1.00	1.00	1.00	1.00	1.00	1.00	1.00
April	1.00	1.00	1.00	1.00	1.00	1.00	1.00	1.00	1.00	1.00
May	1.00	1.00	1.00	1.00	1.00	1.00	1.00	1.00	1.00	1.00
June	1.00	1.00	1.00	1.00	1.00	1.00	1.00	1.00	1.00	1.00
July	1.00	1.00	1.00	1.00	1.00	1.00	1.00	1.00	1.00	1.00
August	1.00	1.00	1.00	1.00	1.00	1.00	1.00	1.00	1.00	1.00
September	1.00	1.00	1.00	1.00	1.00	1.00	1.00	1.00	1.00	1.00
October	1.00	1.00	1.00	1.00	1.00	1.00	1.00	1.00	1.00	1.00
November	1.00	1.00	1.00	1.00	1.00	1.00	1.00	1.00	1.00	1.00
December	1.00	1.00	1.00	1.00	1.00	1.00	1.00	1.00	1.00	1.00

Vehicle Class Distribution

(Level 3, Default Distribution)

AADTT distribution by vehicle class

Class 4	0.0%
Class 5	0.0%
Class 6	0.0%
Class 7	0.0%
Class 8	0.0%
Class 9	####
Class 10	0.0%
Class 11	0.0%
Class 12	0.0%
Class 13	0.0%

Hourly truck traffic distribution

by period beginning:

Midnight	2.3%	Noon	5.9%
1:00 am	2.3%	1:00 pm	5.9%
2:00 am	2.3%	2:00 pm	5.9%
3:00 am	2.3%	3:00 pm	5.9%
4:00 am	2.3%	4:00 pm	4.6%
5:00 am	2.3%	5:00 pm	4.6%
6:00 am	5.0%	6:00 pm	4.6%
7:00 am	5.0%	7:00 pm	4.6%
8:00 am	5.0%	8:00 pm	3.1%
9:00 am	5.0%	9:00 pm	3.1%
10:00 am	5.9%	10:00 pm	3.1%
11:00 am	5.9%	11:00 pm	3.1%

Table A 2 (continued)

Traffic Growth Factor

Vehicle Class	Growth Rate	Growth Function
Class 4	4.0%	No Growth
Class 5	4.0%	No Growth
Class 6	4.0%	No Growth
Class 7	4.0%	No Growth
Class 8	4.0%	No Growth
Class 9	4.0%	No Growth
Class 10	4.0%	No Growth
Class 11	4.0%	No Growth
Class 12	4.0%	No Growth
Class 13	4.0%	No Growth

Traffic -- Axle Load Distribution Factors

Level 3: Default

Traffic -- General Traffic Inputs

Mean wheel location (inches from the lane marking):	18
Traffic wander standard deviation (in):	10
Design lane width (ft):	12

Number of Axles per Truck

Vehicle Class	Single Axle	Tandem Axle	Tridem Axle	Quad Axle
Class 4	1.62	0.39	0.00	0.00
Class 5	2.00	0.00	0.00	0.00
Class 6	1.02	0.99	0.00	0.00
Class 7	1.00	0.26	0.83	0.00
Class 8	2.38	0.67	0.00	0.00
Class 9	1.13	1.93	0.00	0.00
Class 10	1.19	1.09	0.89	0.00
Class 11	4.29	0.26	0.06	0.00
Class 12	3.52	1.14	0.06	0.00
Class 13	2.15	2.13	0.35	0.00

Table A 2 (continued)

Axle Configuration

Average axle width (edge-to-edge) outside dimensions,ft):	8.5
Dual tire spacing (in):	12

Axle Configuration

Tire Pressure (psi) :	120

Average Axle Spacing

Tandem axle(psi):	51.6
Tridem axle(psi):	49.2
Quad axle(psi):	49.2

Wheelbase Truck Tractor

	Short	Medium	Long
Average Axle Spacing (ft)	12	15	18
Percent of trucks	50%	0%	50%

Climate

icm file:	C:\DG2002\Projects\Pittsburgh.icm
Latitude (degrees.minutes)	40.21
Longitude (degrees.minutes)	-79.6
Elevation (ft)	1281
Depth of water table (ft)	10

Structure--Design Features

Permanent curl/warp effective temperature difference (°F):	-15

Joint Design

Joint spacing (ft):	15
Sealant type:	Liquid
Dowel diameter (in):	None
Dowel bar spacing (in):	None

Edge Support None

Long-term LTE(%):	n/a
Widened Slab (ft):	n/a

Table A 2 (continued)

Base Properties

Base type:	Granular
Erodibility index:	Erosion Resistant (3)
PCC-Base Interface	Full friction contact
Loss of full friction (age in months):	245

Structure--ICM Properties

Surface shortwave absorptivity:	0.85

Structure--Layers

Layer 1 -- JPCP

General Properties

PCC material	JPCP
Layer thickness (in):	10
Unit weight (pcf):	150
Poisson's ratio	0.2

Thermal Properties

Coefficient of thermal expansion (per F° x 10- 6):	5.06
Thermal conductivity (BTU/hr-ft-F°) :	1.54
Heat capacity (BTU/lb-F°):	0.23

Mix Properties

Cement type:	Type I
Cementitious material content (lb/yd^3):	600
Water/cement ratio:	0.5
Aggregate type:	Limestone
PCC zero-stress temperature (F°)	100
Ultimate shrinkage at 40% R.H (microstrain)	Derived
Reversible shrinkage (% of ultimate shrinkage):	50
Time to develop 50% of ultimate shrinkage (days):	35
Curing method:	Curing compound

Strength Properties

Input level:	Level 3
28-day PCC modulus of rupture (psi):	600
28-day PCC compressive strength (psi):	n/a

Table A 2 (continued)

Layer 2 -- A-3

Unbound Material:	A-3
Thickness(in):	5

Strength Properties

Input Level:	Level 3
Analysis Type:	ICM inputs (ICM Calculated Modulus)
Poisson's ratio:	0.35
Coefficient of lateral pressure,Ko:	0.5
Modulus (input) (psi):	29000

ICM Inputs

Gradation and Plasticity Index

Plasticity Index, PI:	0
Liquid Limit (LL)	11
Compacted Layer	Yes
Passing #200 sieve (%):	5.2
Passing #40	76.8
Passing #4 sieve (%):	95.3
D10(mm)	0.08974
D20(mm)	0.1304
D30(mm)	0.1895
D60(mm)	0.3255
D90(mm)	1.456

Sieve	Percent Passing
0.001mm	
0.002mm	
0.020mm	
#200	5.2
#100	
#80	33
#60	
#50	
#40	76.8
#30	
#20	
#16	
#10	93.4
#8	

Table A 2 (continued)

#4	95.3
3/8"	96.6
1/2"	97.1
3/4"	98
1"	98.6
1 1/2"	99.2
2"	99.7
2 1/2"	
3"	
3 1/2"	99.9
4"	99.9

Calculated/Derived Parameters

Maximum dry unit weight (pcf):	120.0 (user input)
Specific gravity of solids, Gs:	2.70 (derived)
Saturated hydraulic conductivity (ft/hr):	0.003777 (derived)
Optimum gravimetric water content (%):	7.3 (derived)
Calculated degree of saturation (%):	49.1 (calculated)
Soil water characteristic curve parameters:	Default values

Parameters	Value
a	4.757
b	2.881
c	0.869
Hr.	100

Layer 3 -- A-3

Unbound Material:	A-3
Thickness(in):	Semi-infinite

Strength Properties

Input Level:	Level 3
Analysis Type:	ICM inputs (ICM Calculated Modulus)
Poisson's ratio:	0.35
Coefficient of lateral pressure,Ko:	0.5
Modulus (input) (psi):	16000

Table A 2 (continued)

ICM Inputs

Gradation and Plasticity Index

Plasticity Index, PI:	0
Liquid Limit (LL)	11
Compacted Layer	Yes
Passing #200 sieve (%):	5.2
Passing #40	76.8
Passing #4 sieve (%):	95.3
D10(mm)	0.08974
D20(mm)	0.1304
D30(mm)	0.1895
D60(mm)	0.3255
D90(mm)	1.456

Sieve	Percent Passing
0.001mm	
0.002mm	
0.020mm	
#200	5.2
#100	
#80	33
#60	
#50	
#40	76.8
#30	
#20	
#16	
#10	93.4
#8	
#4	95.3
3/8"	96.6
1/2"	97.1
3/4"	98
1"	98.6
1 1/2"	99.2
2"	99.7
2 1/2"	
3"	
3 1/2"	99.9
4"	99.9

Table A 2 (continued)

Calculated/Derived Parameters

Maximum dry unit weight (pcf):	120.0 (user input)
Specific gravity of solids, Gs:	2.70 (derived)
Saturated hydraulic conductivity (ft/hr):	0.003777 (derived)
Optimum gravimetric water content (%):	7.3 (derived)
Calculated degree of saturation (%):	49.1 (calculated)
Soil water characteristic curve parameters:	Default values

Parameters	Value
a	4.757
b	2.881
c	0.869
Hr.	100

Distress Model Calibration Settings - Rigid (new)

Faulting

Faulting Coefficients

C1	1.018
C2	0.917
C3	0.002
C4	9E-04
C5	250
C6	0.4
C7	1.833
C8	400

Reliability (FAULT)

Std. Dev.	POWER(0.0097*FAULT,0.5178)+0.014

Table A 2 (continued)

Cracking	
Fatigue Coefficients	
C1	2
C2	1.22
Cracking Coefficients	
C4	1
C5	-1.98
Reliability (CRACK)	
Std. Dev.	POWER(5.3116*CRACK,0.3903) + 2.99
IRI(jpcp)	
C1	0.82
C2	0.442
C3	20.37
C4	1.493
C5	25.24
Standard deviation in initial IRI (in/mile):	5.4

Table A 3. Experiment Design Data of Section 4.3

Project: 1

General Information

Design Life	20 years
Pavement construction:	September, 2006
Traffic open:	October, 2006
Type of design	JPCP

Description:

Analysis Parameters

Performance Criteria

	Limit	Reliability
Initial IRI (in/mi)	63	
Terminal IRI (in/mi)	172	50
Transverse Cracking (% slabs cracked)	15	50
Mean Joint Faulting (in)	0.12	50

Location:
Project ID:
Section ID:

Date:

Station/milepost format:
Station/milepost begin:
Station/milepost end:
Traffic direction:

Default Input Level

Default input level: Level 3, Default and historical agency values.

Traffic

Initial two-way AADTT:	3613
Number of lanes in design direction:	2
Percent of trucks in design direction (%):	50
Percent of trucks in design lane (%):	95
Operational speed (mph):	60

Table A 3 (continued)

Traffic -- Volume Adjustment Factors

Monthly Adjustment Factors (Level 3, Default MAF)

	Vehicle Class									
Month	**Class 4**	**Class 5**	**Class 6**	**Class 7**	**Class 8**	**Class 9**	**Class 10**	**Class 11**	**Class 12**	**Class 13**
January	1.00	1.00	1.00	1.00	1.00	1.00	1.00	1.00	1.00	1.00
February	1.00	1.00	1.00	1.00	1.00	1.00	1.00	1.00	1.00	1.00
March	1.00	1.00	1.00	1.00	1.00	1.00	1.00	1.00	1.00	1.00
April	1.00	1.00	1.00	1.00	1.00	1.00	1.00	1.00	1.00	1.00
May	1.00	1.00	1.00	1.00	1.00	1.00	1.00	1.00	1.00	1.00
June	1.00	1.00	1.00	1.00	1.00	1.00	1.00	1.00	1.00	1.00
July	1.00	1.00	1.00	1.00	1.00	1.00	1.00	1.00	1.00	1.00
August	1.00	1.00	1.00	1.00	1.00	1.00	1.00	1.00	1.00	1.00
September	1.00	1.00	1.00	1.00	1.00	1.00	1.00	1.00	1.00	1.00
October	1.00	1.00	1.00	1.00	1.00	1.00	1.00	1.00	1.00	1.00
November	1.00	1.00	1.00	1.00	1.00	1.00	1.00	1.00	1.00	1.00
December	1.00	1.00	1.00	1.00	1.00	1.00	1.00	1.00	1.00	1.00

Vehicle Class Distribution

(Level 3, Default Distribution)

AADTT distribution by vehicle class

Class 4	0.0%
Class 5	0.0%
Class 6	0.0%
Class 7	0.0%
Class 8	0.0%
Class 9	100.0%
Class 10	0.0%
Class 11	0.0%
Class 12	0.0%
Class 13	0.0%

Hourly truck traffic distribution

by period beginning:

Midnight	2.3%	Noon	5.9%
1:00 am	2.3%	1:00 pm	5.9%
2:00 am	2.3%	2:00 pm	5.9%
3:00 am	2.3%	3:00 pm	5.9%
4:00 am	2.3%	4:00 pm	4.6%
5:00 am	2.3%	5:00 pm	4.6%
6:00 am	5.0%	6:00 pm	4.6%
7:00 am	5.0%	7:00 pm	4.6%
8:00 am	5.0%	8:00 pm	3.1%
9:00 am	5.0%	9:00 pm	3.1%
10:00 am	5.9%	10:00 pm	3.1%
11:00 am	5.9%	11:00 pm	3.1%

Table A 3 (continued)

Traffic Growth Factor

Vehicle Class	Growth Rate	Growth Function
Class 4	4.0%	No Growth
Class 5	4.0%	No Growth
Class 6	4.0%	No Growth
Class 7	4.0%	No Growth
Class 8	4.0%	No Growth
Class 9	4.0%	No Growth
Class 10	4.0%	No Growth
Class 11	4.0%	No Growth
Class 12	4.0%	No Growth
Class 13	4.0%	No Growth

Traffic -- Axle Load Distribution Factors

Level 3: Default

Traffic -- General Traffic Inputs

Mean wheel location (inches from the lane marking):	18
Traffic wander standard deviation (in):	10
Design lane width (ft):	12

Number of Axles per Truck

Vehicle Class	Single Axle	Tandem Axle	Tridem Axle	Quad Axle
Class 4	1.62	0.39	0.00	0.00
Class 5	2.00	0.00	0.00	0.00
Class 6	1.02	0.99	0.00	0.00
Class 7	1.00	0.26	0.83	0.00
Class 8	2.38	0.67	0.00	0.00
Class 9	1.13	1.93	0.00	0.00
Class 10	1.19	1.09	0.89	0.00
Class 11	4.29	0.26	0.06	0.00
Class 12	3.52	1.14	0.06	0.00
Class 13	2.15	2.13	0.35	0.00

Table A 3 (continued)

Axle Configuration

Average axle width (edge-to-edge) outside dimensions,ft):	8.5
Dual tire spacing (in):	12

Axle Configuration

Tire Pressure (psi) :	120

Average Axle Spacing

Tandem axle(psi):	51.6
Tridem axle(psi):	49.2
Quad axle(psi):	49.2

Wheelbase Truck Tractor

	Short	Medium	Long
Average Axle Spacing (ft)	12	15	18
Percent of trucks	33%	33%	34%

Climate

icm file:	C:\DG2002\Projects\Pittsburgh.icm
Latitude (degrees.minutes)	40.21
Longitude (degrees.minutes)	-79.55
Elevation (ft)	1281
Depth of water table (ft)	10

Structure--Design Features

Permanent curl/warp effective temperature difference (°F):	-2.625

Joint Design

Joint spacing (ft):	16
Sealant type:	Liquid
Dowel diameter (in):	1.5
Dowel bar spacing (in):	12

Edge Support	None
Long-term LTE(%):	n/a
Widened Slab (ft):	n/a

Table A 3 (continued)

Base Properties

Base type:	Granular
Erodibility index:	Erosion Resistant (3)
PCC-Base Interface	Full friction contact
Loss of full friction (age in months):	245

Structure--ICM Properties

Surface shortwave absorptivity:	0.85

Structure--Layers

Layer 1 -- JPCP

General Properties

PCC material	JPCP
Layer thickness (in):	10.5
Unit weight (pcf):	150
Poisson's ratio	0.2

Thermal Properties

Coefficient of thermal expansion (per F° x 10- 6):	5.7
Thermal conductivity (BTU/hr-ft-F°) :	1.25
Heat capacity (BTU/lb-F°):	0.28

Mix Properties

Cement type:	Type I
Cementitious material content (lb/yd^3):	577
Water/cement ratio:	0.56
Aggregate type:	Limestone
PCC zero-stress temperature (F°)	100
Ultimate shrinkage at 40% R.H (microstrain)	Derived
Reversible shrinkage (% of ultimate shrinkage):	50
Time to develop 50% of ultimate shrinkage (days):	35
Curing method:	Curing compound

Strength Properties

Input level:	Level 3
28-day PCC modulus of rupture (psi):	618
28-day PCC compressive strength (psi):	n/a

Table A 3 (continued)

Layer 2 -- Crushed stone

Unbound Material:	Crushed stone
Thickness(in):	10

Strength Properties

Input Level:	Level 3
Analysis Type:	ICM inputs (ICM Calculated Modulus)
Poisson's ratio:	0.35
Coefficient of lateral pressure,Ko:	0.5
Modulus (input) (psi):	30000

ICM Inputs

Gradation and Plasticity Index

Plasticity Index, PI:	1
Liquid Limit (LL)	6
Compacted Layer	No
Passing #200 sieve (%):	8.7
Passing #40	20
Passing #4 sieve (%):	44.7
D10(mm)	0.1035
D20(mm)	0.425
D30(mm)	1.306
D60(mm)	10.82
D90(mm)	46.19

Sieve	Percent Passing
0.001mm	
0.002mm	
0.020mm	
#200	8.7
#100	
#80	12.9
#60	
#50	
#40	20
#30	
#20	
#16	

Table A 3 (continued)

#10	33.8
#8	
#4	44.7
3/8"	57.2
1/2"	63.1
3/4"	72.7
1"	78.8
1 1/2"	85.8
2"	91.6
2 1/2"	
3"	
3 1/2"	97.6
4"	97.6

Calculated/Derived Parameters

Maximum dry unit weight (pcf):	127.2 (derived)
Specific gravity of solids, Gs:	2.70 (derived)
Saturated hydraulic conductivity (ft/hr):	0.05054 (derived)
Optimum gravimetric water content (%):	7.4 (derived)
Calculated degree of saturation (%):	61.2 (calculated)

Soil water characteristic curve parameters: Default values

Parameters	Value
a	7.2555
b	1.3328
c	0.8242
Hr.	117.4

Layer 3 -- A-1-a

Unbound Material:	A-1-a
Thickness(in):	12

Table A 3 (continued)

Strength Properties

Input Level:	Level 3
Analysis Type:	ICM inputs (ICM Calculated Modulus)
Poisson's ratio:	0.35
Coefficient of lateral pressure,Ko:	0.5
Modulus (input) (psi):	18000

ICM Inputs

Gradation and Plasticity Index

Plasticity Index, PI:	1
Liquid Limit (LL)	6
Compacted Layer	No
Passing #200 sieve (%):	8.7
Passing #40	20
Passing #4 sieve (%):	44.7
D10(mm)	0.1035
D20(mm)	0.425
D30(mm)	1.306
D60(mm)	10.82
D90(mm)	46.19

Sieve	Percent Passing
0.001mm	
0.002mm	
0.020mm	
#200	8.7
#100	
#80	12.9
#60	
#50	
#40	20
#30	
#20	
#16	
#10	33.8
#8	
#4	44.7
3/8"	57.2

Table A 3 (continued)

1/2"	63.1
3/4"	72.7
1"	78.8
1 1/2"	85.8
2"	91.6
2 1/2"	
3"	
3 1/2"	97.6
4"	97.6

Calculated/Derived Parameters

Maximum dry unit weight (pcf):	127.2 (derived)
Specific gravity of solids, Gs:	2.70 (derived)
Saturated hydraulic conductivity (ft/hr):	0.05054 (derived)
Optimum gravimetric water content (%):	7.4 (derived)
Calculated degree of saturation (%):	61.2 (calculated)

Soil water characteristic curve parameters: Default values

Parameters	Value
a	7.2555
b	1.3328
c	0.8242
Hr.	117.4

Layer 4 -- A-1-a

Unbound Material:	A-1-a
Thickness(in):	Semi-infinite

Strength Properties

Input Level:	Level 3
Analysis Type:	ICM inputs (ICM Calculated Modulus)
Poisson's ratio:	0.35
Coefficient of lateral pressure,Ko:	0.5
Modulus (input) (psi):	18000

Table A 3 (continued)

ICM Inputs

Gradation and Plasticity Index

Plasticity Index, PI:	1
Liquid Limit (LL)	6
Compacted Layer	No
Passing #200 sieve (%):	8.7
Passing #40	20
Passing #4 sieve (%):	44.7
D10(mm)	0.1035
D20(mm)	0.425
D30(mm)	1.306
D60(mm)	10.82
D90(mm)	46.19

Sieve	Percent Passing
0.001mm	
0.002mm	
0.020mm	
#200	8.7
#100	
#80	12.9
#60	
#50	
#40	20
#30	
#20	
#16	
#10	33.8
#8	
#4	44.7
3/8"	57.2
1/2"	63.1
3/4"	72.7
1"	78.8
1 1/2"	85.8
2"	91.6
2 1/2"	
3"	
3 1/2"	97.6
4"	97.6

Table A 3 (continued)

Calculated/Derived Parameters

Maximum dry unit weight (pcf):	127.2 (derived)
Specific gravity of solids, Gs:	2.70 (derived)
Saturated hydraulic conductivity (ft/hr):	0.05054 (derived)
Optimum gravimetric water content (%):	7.4 (derived)
Calculated degree of saturation (%):	61.2 (calculated)
Soil water characteristic curve parameters:	Default values

Parameters	Value
a	7.2555
b	1.3328
c	0.8242
Hr.	117.4

Distress Model Calibration Settings - Rigid (new)

Faulting

Faulting Coefficients

C1	1.0184
C2	0.9166
C3	0.0022
C4	0.0009
C5	250
C6	0.4
C7	1.8331
C8	400

Reliability (FAULT)

Std. Dev.	POWER(0.0097*FAULT,0.5178)+0.014

Cracking

Fatigue Coefficients

C1	2
C2	1.22

Cracking Coefficients

C4	1
C5	-1.98

Table A 3 (continued)

Reliability (CRACK)	
Std. Dev.	POWER(5.3116*CRACK,0.3903) + 2.99
IRI(jpcp)	
C1	0.8203
C2	0.4417
C3	20.37
C4	1.4929
C5	25.24
Standard deviation in initial IRI (in/mile):	5.4

Table A 4. Experiment Design Data of Section 4.4

Project: 1-1.dgp

General Information

Description:

Design Life	20 years
Pavement construction:	August, 2004
Traffic open:	September, 2004
Type of design	JPCP

Analysis Parameters

Performance Criteria

	Limit	Reliability
Initial IRI (in/mi)	63	
Terminal IRI (in/mi)	172	95
Transverse Cracking (% slabs cracked)	15	95
Mean Joint Faulting (in)	0.12	95

Location:	Smart Pavement
Project ID:	SR 22 B02
Section ID:	
Date:	12/12/2007
Station/milepost format:	
Station/milepost begin:	
Station/milepost end:	
Traffic direction:	East bound

Default Input Level

Default input level	Level 3, Default and historical agency values.

Traffic

Initial two-way AADTT:	8000
Number of lanes in design direction:	2
Percent of trucks in design direction (%):	50
Percent of trucks in design lane (%):	95
Operational speed (mph):	35

Table A 4 (continued)

Traffic -- Volume Adjustment Factors

Monthly Adjustment Factors (Level 1, Site Specific - MAF)

	Vehicle Class									
Month	**Class 4**	**Class 5**	**Class 6**	**Class 7**	**Class 8**	**Class 9**	**Class 10**	**Class 11**	**Class 12**	**Class 13**
January	0.80	0.80	0.80	0.80	0.80	0.80	0.80	0.80	0.80	0.80
February	0.80	0.80	0.80	0.80	0.80	0.80	0.80	0.80	0.80	0.80
March	1.02	1.02	1.02	1.02	1.02	1.02	1.02	1.02	1.02	1.02
April	1.06	1.06	1.06	1.06	1.06	1.06	1.06	1.06	1.06	1.06
May	1.07	1.07	1.07	1.07	1.07	1.07	1.07	1.07	1.07	1.07
June	1.09	1.09	1.09	1.09	1.09	1.09	1.09	1.09	1.09	1.09
July	1.06	1.06	1.06	1.06	1.06	1.06	1.06	1.06	1.06	1.06
August	1.05	1.05	1.05	1.05	1.05	1.05	1.05	1.05	1.05	1.05
September	0.96	0.96	0.96	0.96	0.96	0.96	0.96	0.96	0.96	0.96
October	1.02	1.02	1.02	1.02	1.02	1.02	1.02	1.02	1.02	1.02
November	1.03	1.03	1.03	1.03	1.03	1.03	1.03	1.03	1.03	1.03
December	1.05	1.05	1.05	1.05	1.05	1.05	1.05	1.05	1.05	1.05

Vehicle Class Distribution

(Level 1, Site Specific Distribution)

AADTT distribution by vehicle class

Class 4	2.0%
Class 5	39.0%
Class 6	3.0%
Class 7	1.0%
Class 8	7.0%
Class 9	48.0%
Class 10	0.0%
Class 11	0.0%
Class 12	0.0%
Class 13	0.0%

Hourly truck traffic distribution

by period beginning:

Midnight	0.7%	Noon	5.6%
1:00 am	0.4%	1:00 pm	5.5%
2:00 am	0.4%	2:00 pm	5.5%
3:00 am	0.5%	3:00 pm	5.6%
4:00 am	1.1%	4:00 pm	5.6%
5:00 am	4.1%	5:00 pm	6.2%
6:00 am	7.3%	6:00 pm	5.4%
7:00 am	7.9%	7:00 pm	4.2%
8:00 am	6.9%	8:00 pm	3.4%
9:00 am	6.0%	9:00 pm	3.0%
10:00 am	5.8%	10:00 pm	1.9%
11:00 am	5.8%	11:00 pm	1.2%

Table A 4 (continued)

Traffic Growth Factor

Vehicle Class	Growth Rate	Growth Function
Class 4	1.6%	No Growth
Class 5	1.6%	No Growth
Class 6	1.6%	No Growth
Class 7	1.6%	No Growth
Class 8	1.6%	No Growth
Class 9	1.6%	No Growth
Class 10	1.6%	No Growth
Class 11	1.6%	No Growth
Class 12	1.6%	No Growth
Class 13	1.6%	No Growth

Traffic -- Axle Load Distribution Factors

Level 3: Default

Traffic -- General Traffic Inputs

Mean wheel location (inches from the lane marking):	18
Traffic wander standard deviation (in):	10
Design lane width (ft):	12

Number of Axles per Truck

Vehicle Class	Single Axle	Tandem Axle	Tridem Axle	Quad Axle
Class 4	1.62	0.39	0.00	0.00
Class 5	2.00	0.00	0.00	0.00
Class 6	1.02	0.99	0.00	0.00
Class 7	1.00	0.26	0.83	0.00
Class 8	2.38	0.67	0.00	0.00
Class 9	1.13	1.93	0.00	0.00
Class 10	1.19	1.09	0.89	0.00
Class 11	4.29	0.26	0.06	0.00
Class 12	3.52	1.14	0.06	0.00
Class 13	2.15	2.13	0.35	0.00

Table A 4 (continued)

Axle Configuration

Average axle width (edge-to-edge) outside dimensions,ft):	8.5
Dual tire spacing (in):	12

Axle Configuration

Tire Pressure (psi) :	120

Average Axle Spacing

Tandem axle(psi):	51.6
Tridem axle(psi):	49.2
Quad axle(psi):	49.2

Wheelbase Truck Tractor

	Short	Medium	Long
Average Axle Spacing (ft)	12	15	18
Percent of trucks	33%	33%	34%

Climate

icm file:	C:\JUAN\01-26-08_one-phase-approach\Pittsburgh.icm
Latitude (degrees.minutes)	40.21
Longitude (degrees.minutes)	-79.55
Elevation (ft)	1281
Depth of water table (ft)	9

Structure--Design Features

Permanent curl/warp effective temperature difference (°F):	-5

Joint Design

Joint spacing (ft):	15
Sealant type:	Liquid
Dowel diameter (in):	1.5
Dowel bar spacing (in):	12

Edge Support	Tied PCC shoulder
Long-term LTE(%):	40
Widened Slab (ft):	n/a

Table A 4 (continued)

Base Properties

Base type:	Granular
Erodibility index:	Very Erosion Resistant (2)
PCC-Base Interface	Full friction contact
Loss of full friction (age in months):	229

Structure--ICM Properties

Surface shortwave absorptivity:	0.85

Structure--Layers

Layer 1 -- JPCP

General Properties

PCC material	JPCP
Layer thickness (in):	10
Unit weight (pcf):	143.4
Poisson's ratio	0.17

Thermal Properties

Coefficient of thermal expansion (per F° x 10- 6):	5.3
Thermal conductivity (BTU/hr-ft-F°) :	1.25
Heat capacity (BTU/lb-F°):	0.24

Mix Properties

Cement type:	Type I
Cementitious material content (lb/yd^3):	527
Water/cement ratio:	0.61
Aggregate type:	Limestone
PCC zero-stress temperature (F°)	104
Ultimate shrinkage at 40% R.H (microstrain)	945
Reversible shrinkage (% of ultimate shrinkage):	50
Time to develop 50% of ultimate shrinkage (days):	30
Curing method:	Curing compound

Strength Properties

Input level:	Level 3
28-day PCC modulus of rupture (psi):	578
28-day PCC compressive strength (psi):	n/a

Table A 4 (continued)

Layer 2 -- A-3

Unbound Material:	A-3
Thickness(in):	5

Strength Properties

Input Level:	Level 3
Analysis Type:	ICM inputs (ICM Calculated Modulus)
Poisson's ratio:	0.35
Coefficient of lateral pressure,Ko:	0.5
Modulus (input) (psi):	29000

ICM Inputs

Gradation and Plasticity Index

Plasticity Index, PI:	0
Liquid Limit (LL)	11
Compacted Layer	Yes
Passing #200 sieve (%):	5.2
Passing #40	76.8
Passing #4 sieve (%):	95.3
D10(mm)	0.08974
D20(mm)	0.1304
D30(mm)	0.1895
D60(mm)	0.3255
D90(mm)	1.456

Sieve	Percent Passing
0.001mm	
0.002mm	
0.020mm	
#200	5.2
#100	
#80	33
#60	
#50	
#40	76.8
#30	
#20	
#16	

Table A 4 (continued)

#10	93.4
#8	
#4	95.3
3/8"	96.6
1/2"	97.1
3/4"	98
1"	98.6
1 1/2"	99.2
2"	99.7
2 1/2"	
3"	
3 1/2"	99.9
4"	99.9

Calculated/Derived Parameters

Maximum dry unit weight (pcf):	120.0 (user input)
Specific gravity of solids, Gs:	2.70 (derived)
Saturated hydraulic conductivity (ft/hr):	0.003777 (derived)
Optimum gravimetric water content (%):	7.3 (derived)
Calculated degree of saturation (%):	49.1 (calculated)
Soil water characteristic curve parameters:	Default values

Parameters	Value
a	4.7572
b	2.8814
c	0.8694
Hr.	100

Layer 3 -- Crushed stone

Unbound Material:	Crushed stone
Thickness(in):	5

Table A 4 (continued)

Strength Properties

Input Level:	Level 2
Analysis Type:	ICM inputs (ICM Calculated Modulus)
Poisson's ratio:	0.4
Coefficient of lateral pressure,Ko:	0.5
Modulus (input) (psi):	19500

ICM Inputs

Gradation and Plasticity Index

Plasticity Index, PI:	10
Liquid Limit (LL)	10
Compacted Layer	Yes
Passing #200 sieve (%):	5
Passing #40	14.4
Passing #4 sieve (%):	37
D10(mm)	0.1879
D20(mm)	1.18
D30(mm)	2.911
D60(mm)	10.33
D90(mm)	28.06

Sieve	Minimum Percent Passing	Maximum Percent Passing
0.001mm		
0.002mm		
0.020mm		
#200	0	10
#100		
#80		
#60		
#50		
#40		
#30		
#20		
#16	10	30
#10		
#8	16	38
#4	24	50
3/8"	36	70

Table A 4 (continued)

1/2"	52	100
3/4"		
1"		
1 1/2"		
2"	100	100
2 1/2"		
3"		
3 1/2"		
4"		

Calculated/Derived Parameters

Maximum dry unit weight (pcf):	121.6 (user input)
Specific gravity of solids, Gs:	2.68 (user input)
Saturated hydraulic conductivity (ft/hr):	0.6 (user input)
Optimum gravimetric water content (%):	11.8 (user input)
Calculated degree of saturation (%):	84.3 (calculated)
Soil water characteristic curve parameters:	Default values

Parameters	Value
a	3.6169
b	2.0362
c	0.7899
Hr.	200

Layer 4 -- Crushed stone

Unbound Material:	Crushed stone
Thickness(in):	24

Strength Properties

Input Level:	Level 2 ICM inputs (ICM Calculated
Analysis Type:	Modulus)
Poisson's ratio:	0.4
Coefficient of lateral pressure,Ko:	0.5
Modulus (input) (psi):	19500

Table A 4 (continued)

ICM Inputs

Gradation and Plasticity Index

Plasticity Index, PI:	6
Liquid Limit (LL)	6
Compacted Layer	Yes
Passing #200 sieve (%):	7.5
Passing #40	15
Passing #4 sieve (%):	36.6
D10(mm)	0.1337
D20(mm)	0.922
D30(mm)	2.906
D60(mm)	27.35
D90(mm)	64.78

Sieve	Minimum Percent Passing	Maximum Percent Passing
0.001mm		
0.002mm		
0.020mm		
#200	0	15
#100		
#80		
#60		
#50		
#40	0	30
#30		
#20		
#16		
#10	0	50
#8		
#4		
3/8"		
1/2"		
3/4"		
1"		
1 1/2"		
2"		
2 1/2"		
3"	65	82
3 1/2"		
4"		

Table A 4 (continued)

Calculated/Derived Parameters

Maximum dry unit weight (pcf):	121.0 (user input)
Specific gravity of solids, Gs:	2.69 (user input)
Saturated hydraulic conductivity (ft/hr):	3 (user input)
Optimum gravimetric water content (%):	12.2 (user input)
Calculated degree of saturation (%):	84.7 (calculated)
Soil water characteristic curve parameters:	Default values

Parameters	Value
a	5.8073
b	1.5602
c	0.7787
Hr.	190

Layer 5 -- A-6

Unbound Material:	A-6
Thickness(in):	Semi-infinite

Strength Properties

Input Level:	Level 2
Analysis Type:	ICM inputs (ICM Calculated Modulus)
Poisson's ratio:	0.4
Coefficient of lateral pressure,Ko:	0.5
Modulus (input) (psi):	4500

ICM Inputs

Gradation and Plasticity Index

Plasticity Index, PI:	11
Liquid Limit (LL)	11
Compacted Layer	Yes
Passing #200 sieve (%):	77
Passing #40	98
Passing #4 sieve (%):	100
D10(mm)	0.0002212
D20(mm)	0.0004894
D30(mm)	0.001189
D60(mm)	0.01849
D90(mm)	0.1789

Table A 4 (continued)

Sieve	Percent Passing
0.001mm	29
0.002mm	33
0.020mm	
#200	77
#100	
#80	
#60	95
#50	
#40	98
#30	
#20	99
#16	
#10	
#8	
#4	100
3/8"	
1/2"	
3/4"	
1"	
1 1/2"	
2"	
2 1/2"	
3"	
3 1/2"	
4"	

Calculated/Derived Parameters

Maximum dry unit weight (pcf):	110.7 (user input)
Specific gravity of solids, Gs:	2.73 (user input)
Saturated hydraulic conductivity (ft/hr):	5.7e-006 (user input)
Optimum gravimetric water content (%):	17.2 (user input)
Calculated degree of saturation (%):	87.1 (calculated)
Soil water characteristic curve parameters:	Default values

Table A 4 (continued)

Parameters	Value
a	102.59
b	0.7196
c	0.2543
Hr.	500

Distress Model Calibration Settings - Rigid (new)

Faulting

Faulting Coefficients

C1	1.0184
C2	0.9166
C3	0.0022
C4	0.0009
C5	250
C6	0.4
C7	1.8331
C8	400

Reliability (FAULT)

Std. Dev.	POWER(0.0097*FAULT,0.5178)+0.014

Cracking

Fatigue Coefficients

C1	2
C2	1.22

Cracking Coefficients

C4	1
C5	-1.98

Reliability (CRACK)

Std. Dev.	POWER(5.3116*CRACK,0.3903) + 2.99

Table A 4 (continued)

IRI(jpcp)	
C1	0.8203
C2	0.4417
C3	20.37
C4	1.4929
C5	25.24
Standard deviation in initial IRI (in/mile):	5.4

Table A 5. Experiment Design Data of Section 5.1

Project: Min_Road_cell7-10

General Information

Description:

Design Life	20 years
Pavement construction:	September, 1992
Traffic open:	October, 1992
Type of design	JPCP

Analysis Parameters

Performance Criteria

	Limit	Reliability
Initial IRI (in/mi)	63	
Terminal IRI (in/mi)	172	50
Transverse Cracking (% slabs cracked)	15	50
Mean Joint Faulting (in)	0.12	50

Location:
Project ID:
Section ID:
Principal Arterials - Interstate and Defense Routes
Date:

Station/milepost format:
Station/milepost begin:
Station/milepost end:
Traffic direction:

Default Input Level

Default input level: Level 3, Default and historical agency values.

Traffic

Initial two-way AADTT:	2573
Number of lanes in design direction:	2
Percent of trucks in design direction (%):	50
Percent of trucks in design lane (%):	75
Operational speed (mph):	60

Table A 5 (continued)

Traffic -- Volume Adjustment Factors

Monthly Adjustment Factors (Level 3, Default MAF)

Month	Vehicle Class									
	Class 4	Class 5	Class 6	Class 7	Class 8	Class 9	Class 10	Class 11	Class 12	Class 13
January	1.00	1.00	1.00	1.00	1.00	1.00	1.00	1.00	1.00	1.00
February	1.00	1.00	1.00	1.00	1.00	1.00	1.00	1.00	1.00	1.00
March	1.00	1.00	1.00	1.00	1.00	1.00	1.00	1.00	1.00	1.00
April	1.00	1.00	1.00	1.00	1.00	1.00	1.00	1.00	1.00	1.00
May	1.00	1.00	1.00	1.00	1.00	1.00	1.00	1.00	1.00	1.00
June	1.00	1.00	1.00	1.00	1.00	1.00	1.00	1.00	1.00	1.00
July	1.00	1.00	1.00	1.00	1.00	1.00	1.00	1.00	1.00	1.00
August	1.00	1.00	1.00	1.00	1.00	1.00	1.00	1.00	1.00	1.00
September	1.00	1.00	1.00	1.00	1.00	1.00	1.00	1.00	1.00	1.00
October	1.00	1.00	1.00	1.00	1.00	1.00	1.00	1.00	1.00	1.00
November	1.00	1.00	1.00	1.00	1.00	1.00	1.00	1.00	1.00	1.00
December	1.00	1.00	1.00	1.00	1.00	1.00	1.00	1.00	1.00	1.00

Vehicle Class Distribution
(Level 3, Default Distribution)

AADTT distribution by vehicle class

Class 4	0.9%
Class 5	14.5%
Class 6	4.0%
Class 7	0.5%
Class 8	4.4%
Class 9	69.2%
Class 10	3.7%
Class 11	2.0%
Class 12	0.7%
Class 13	0.1%

Hourly truck traffic distribution
by period beginning:

Midnight	1.0%	Noon	6.8%
1:00 am	1.0%	1:00 pm	6.9%
2:00 am	0.9%	2:00 pm	7.0%
3:00 am	1.1%	3:00 pm	6.8%
4:00 am	1.5%	4:00 pm	6.3%
5:00 am	2.6%	5:00 pm	5.4%
6:00 am	4.2%	6:00 pm	4.2%
7:00 am	5.6%	7:00 pm	3.3%
8:00 am	6.5%	8:00 pm	2.7%
9:00 am	6.7%	9:00 pm	2.3%
10:00 am	6.9%	10:00 pm	1.8%
11:00 am	7.0%	11:00 pm	1.5%

Table A 5 (continued)

Traffic Growth Factor

Vehicle Class	Growth Rate	Growth Function
Class 4	10.0%	Compound
Class 5	10.0%	Compound
Class 6	10.0%	Compound
Class 7	10.0%	Compound
Class 8	10.0%	Compound
Class 9	10.0%	Compound
Class 10	10.0%	Compound
Class 11	10.0%	Compound
Class 12	10.0%	Compound
Class 13	10.0%	Compound

Traffic -- Axle Load Distribution Factors

Level 1: Site Specific

Traffic -- General Traffic Inputs

Mean wheel location (inches from the lane marking):	18.6
Traffic wander standard deviation (in):	6.8
Design lane width (ft):	14

Number of Axles per Truck

Vehicle Class	Single Axle	Tandem Axle	Tridem Axle	Quad Axle
Class 4	1.62	0.39	0.00	0.00
Class 5	2.00	0.00	0.00	0.00
Class 6	1.02	0.99	0.00	0.00
Class 7	1.00	0.26	0.83	0.00
Class 8	2.38	0.67	0.00	0.00
Class 9	1.13	1.93	0.00	0.00
Class 10	1.19	1.09	0.89	0.00
Class 11	4.29	0.26	0.06	0.00
Class 12	3.52	1.14	0.06	0.00
Class 13	2.15	2.13	0.35	0.00

Table A 5 (continued)

Axle Configuration

Average axle width (edge-to-edge) outside dimensions,ft):	8.5
Dual tire spacing (in):	12

Axle Configuration

Tire Pressure (psi) :	120

Average Axle Spacing

Tandem axle(psi):	51.6
Tridem axle(psi):	49.2
Quad axle(psi):	49.2

Wheelbase Truck Tractor

	Short	Medium	Long
Average Axle Spacing (ft)	12	15	18
Percent of trucks	33%	33%	34%

Climate

icm file:	C:\DG2002\Projects\interp_minnesota.icm
Latitude (degrees.minutes)	45.32
Longitude (degrees.minutes)	-94.03
Elevation (ft)	1021
Depth of water table (ft)	5

Structure--Design Features

Permanent curl/warp effective temperature difference (°F):	-10

Joint Design

Joint spacing (ft):	20
Sealant type:	Liquid
Dowel diameter (in):	1
Dowel bar spacing (in):	12

Edge Support	None
Long-term LTE(%):	n/a
Widened Slab (ft):	n/a

Table A 5 (continued)

Base Properties

Base type:	Asphalt treated
Erodibility index:	Erosion Resistant (3)
PCC-Base Interface	Full friction contact
Loss of full friction (age in months):	245

Structure--ICM Properties

Surface shortwave absorptivity:	0.85

Structure--Layers

Layer 1 -- JPCP

General Properties

PCC material	JPCP
Layer thickness (in):	7.5
Unit weight (pcf):	150
Poisson's ratio	0.19

Thermal Properties

Coefficient of thermal expansion (per F° x 10- 6):	4.5
Thermal conductivity (BTU/hr-ft-F°) :	1.25
Heat capacity (BTU/lb-F°):	0.28

Mix Properties

Cement type:	Type I
Cementitious material content (lb/yd^3):	600
Water/cement ratio:	0.42
Aggregate type:	Limestone
PCC zero-stress temperature (F°)	Derived
Ultimate shrinkage at 40% R.H (microstrain)	Derived
Reversible shrinkage (% of ultimate shrinkage):	50
Time to develop 50% of ultimate shrinkage (days):	35
Curing method:	Curing compound

Strength Properties

Input level:	Level 3
28-day PCC modulus of rupture (psi):	n/a
28-day PCC compressive strength (psi):	5205

Table A 5 (continued)

Layer 2 -- Asphalt permeable base

Material type:	Asphalt permeable base
Layer thickness (in):	4

General Properties

General

Reference temperature (F°):	70

Volumetric Properties as Built

Effective binder content (%):	11
Air voids (%):	8.5
Total unit weight (pcf):	148

Poisson's ratio:	0.35 (user entered)

Thermal Properties

Thermal conductivity asphalt (BTU/hr-ft-F°):	0.67
Heat capacity asphalt (BTU/lb-F°):	0.23

Asphalt Mix

Cumulative % Retained 3/4 inch sieve:	8.5
Cumulative % Retained 3/8 inch sieve:	35
Cumulative % Retained #4 sieve:	65
% Passing #200 sieve:	1.5

Asphalt Binder

Option:	Superpave binder grading
A	10.9800 (correlated)
VTS:	-3.6800 (correlated)

High temp. °C	Low temperature, °C						
	-10	-16	-22	-28	-34	-40	-46
46							
52							
58							
64							
70							
76							
82							

Table A 5 (continued)

Layer 3 -- A-1-b

Unbound Material:	A-1-b
Thickness(in):	3

Strength Properties

Input Level:	Level 3
Analysis Type:	ICM inputs (ICM Calculated Modulus)
Poisson's ratio:	0.35
Coefficient of lateral pressure,Ko:	0.5
Modulus (input) (psi):	29500

ICM Inputs

Gradation and Plasticity Index

Plasticity Index, PI:	1
Liquid Limit (LL)	6
Compacted Layer	No
Passing #200 sieve (%):	7.5
Passing #40	22.5
Passing #4 sieve (%):	77.5
D10(mm)	0.1001
D20(mm)	0.3183
D30(mm)	0.5682
D60(mm)	1.815
D90(mm)	11.97

Sieve	Minimum Percent Passing	Maximum Percent Passing
0.001mm		
0.002mm		
0.020mm		
#200	7.5	7.5
#100		
#80		
#60		
#50		
#40	22.5	22.5
#30		
#20		
#16		

Table A 5 (continued)

#10	62.5	62.5
#8		
#4	77.5	77.5
3/8"	87.5	87.5
1/2"		
3/4"	95	95
1"	97.5	97.5
1 1/2"	100	100
2"		
2 1/2"		
3"		
3 1/2"		
4"		

Calculated/Derived Parameters

Maximum dry unit weight (pcf):	108.7 (user input)
Specific gravity of solids, Gs:	2.70 (derived)
Saturated hydraulic conductivity (ft/hr):	0.003794 (derived)
Optimum gravimetric water content (%):	9.7 (derived)
Calculated degree of saturation (%):	47.6 (calculated)
Soil water characteristic curve parameters:	Default values

Parameters	Value
a	3.7719
b	1.8132
c	0.7996
Hr.	115

Table A 5 (continued)

Layer 4 -- A-6

Unbound Material:	A-6
Thickness(in):	Semi-infinite

Strength Properties

Input Level:	Level 2
Analysis Type:	ICM inputs (ICM Calculated Modulus)
Poisson's ratio:	0.35
Coefficient of lateral pressure,Ko:	0.5
R - Value:	12
Modulus (calculated) (psi):	7815

ICM Inputs

Gradation and Plasticity Index

Plasticity Index, PI:	16
Liquid Limit (LL)	33
Compacted Layer	No
Passing #200 sieve (%):	63.2
Passing #40	82.4
Passing #4 sieve (%):	93.5
D10(mm)	0.000285
D20(mm)	0.0008125
D30(mm)	0.002316
D60(mm)	0.05364
D90(mm)	1.922

Sieve	Percent Passing
0.001mm	
0.002mm	
0.020mm	
#200	63.2
#100	
#80	73.5
#60	
#50	
#40	82.4
#30	
#20	

Table A 5 (continued)

#16	
#10	90.2
#8	
#4	93.5
3/8"	96.4
1/2"	97.4
3/4"	98.4
1"	99
1 1/2"	99.5
2"	99.8
2 1/2"	
3"	
3 1/2"	100
4"	100

Calculated/Derived Parameters

Maximum dry unit weight (pcf):	107.9 (derived)
Specific gravity of solids, Gs:	2.70 (derived)
Saturated hydraulic conductivity (ft/hr):	3.2e-005 (user input)
Optimum gravimetric water content (%):	17.1 (derived)
Calculated degree of saturation (%):	82.1 (calculated)
Soil water characteristic curve parameters:	User input

Parameters	Value
a	130.8
b	0.5473
c	0.0692
Hr.	500

Table A 5 (continued)

Distress Model Calibration Settings - Rigid (new)	
Faulting	
Faulting Coefficients	
C1	1.0184
C2	0.9166
C3	0.0022
C4	0.0009
C5	250
C6	0.4
C7	1.8331
C8	400
Reliability (FAULT)	
Std. Dev.	POWER(0.0097*FAULT,0.5178)+0.014
Cracking	
Fatigue Coefficients	
C1	2
C2	1.22
Cracking Coefficients	
C4	1
C5	-1.98
Reliability (CRACK)	
Std. Dev.	POWER(5.3116*CRACK,0.3903) + 2.99
IRI(jpcp)	
C1	0.8203
C2	0.4417
C3	20.37
C4	1.4929
C5	25.24
Standard deviation in initial IRI (in/mile):	5.4

BIBLIOGRAPHY

1. Sudjianto, A., Du, X., Chen, W. (2005), Probabilistic Sensitivity Analysis in Engineering Design using Uniform Sampling and Saddlepoint Approximation, SAE International.

2. Liu, H., Chen, W., Sudjianto, A. (2006), Relative Entropy Based Method for Probabilistic Sensitivity Analysis in Engineering Design, ASME.

3. Liu, H., Chen, W. (2005), Probabilistic Sensitivity Analysis Methods for Design under Uncertainty, American Institute of Aeronautics and Astronautics.

4. Haldar, A., Mahadevan, S. (2004), Probability, Reliability and Statistical Methods in Engineering Design, John Wiley & Sons, Inc.

5. Hogg, R.V., Ledolter, J. (1992), Applied Statistics for Engineers and Physical Scientists, Macmillan Publishing Company.

6. Saltelli, A., Chan, K., Scott, E.M. (Edited by) (2000), Sensitivity Analysis, John Wiley and Sons, Ltd.

7. Saltelli, A., Tarantola, S., Campolongo, F., Ratto, M. (2004), Sensitivity Analysis in Practice, John Wiley & Sons, Ltd.

8. Kannekanti, V., Harvey, J. (2005), Sensitivity Analysis of 2002 Design Guide Distress Prediction Models for Jointed Plain Concrete Pavement. Pavement Research Center, University of California, Davis and Berkeley.

9. Hall, K.D., Beam, S. (2005) Estimating the Sensitivity of Design Inputs for Rigid Pavement Analysis using Mechanistic-Empirical Design Guide, Journal of the Transportation Research Board No. 1919, Washington D.C. (PP. 65-73)

10. Literature of the Guide for Mechanistic-Empirical Design of New and Rehabilitated Pavement Structures. ARA, Inc., ERES Division. http://www.trb.org/mepdg/guide.htm

11. Myers, R.H., Montgomery, D.C. (2002), Response Surface Methodology, Wiley Series in Probability and Statistics, Second Edition.

12. NOAA website: www.noaa.gov. (2007)

13. Mehta, P.K., Monteiro, P.J.M. (2005), Concrete Microstructure, Properties, and Materials, Third Edition, McGraw-Hill.

14. Vandenbossche, J.M. (2003), Interpreting Falling Weight Deflectometer Results for Curled and Warped Portland Cement Concrete Pavements, Thesis for the Degree Doctor of Philosophy in Civil Engineering, University of Minnesota.

15. Vandenbossche, J.M., Koubaa, A., Wells, S.A., Rettner, D.L., Snyder, M.B. (2004), A Proposal for Evaluation of the R1-37A Rigid Pavement Design Procedure, submitted to Federal Highway Administration.

16. MEPDG 1.0. version, developed by Applied Research Associates, Inc. (2007).